The Role of the Human Amygdala and Insular Cortex in Emotional Processing: Investigations using Functional MRI combined with Probabilistic Anatomical Maps

Dissertation

der Fakultät für Informations- und Kognitionswissenschaften
der Eberhard-Karls-Universität Tübingen
zur Erlangung des Grades eines
Doktors der Naturwissenschaften
(Dr. rer. nat.)

vorgelegt von
Dipl.-Psych. Isabella Mutschler
aus Freiburg

Tübingen
2007

Tag der mündlichen Qualifikation:	18.07.2007
Dekan:	Prof. Dr. Michael Diehl
1. Berichterstatter:	Prof. Dr. Martin Hautzinger
2. Berichterstatter:	Prof. Dr. Niels Birbaumer

1 Abstract

Background: Activation of the human amygdala and the insular cortex has been reported in many neuroimaging studies that investigated emotions and its underlying brain network. The human amygdala is thought to play a pivotal role in the processing of emotionally sensory information and the insular cortex has been proposed as being involved in different functions including peripheral autonomic change and somatovisceral perception, which has been assumed to play an important role in emotion. There is anatomical evidence both for the amygdala and the insular cortex that they are not homogenous structures but are composed of multiple subregions. Very little is known, however, how these subregions behave functionally.

Methods: (1) In this thesis functional MRI has been combined with cyto-architectonically defined probabilistic maps to analyze the response characteristics of the amygdala and its subregions (the laterobasal group = LB, the superficial group = SF, and the centromedial group = CM) in subjects during the processing of emotionally significant auditory stimuli. (2) Insular cortex subregions were investigated by conducting an activation likelihood estimate (ALE) meta-analysis mapping coordinates of activation foci obtained from different insula-neuroimaging studies. (3) In addition, based on a further coordinate-based meta-analysis of previous neuroimaging studies reporting amygdala-activation a co-activation likelihood estimation was carried out in order to delineate the brain areas consistently co-activated with the amygdala. (4) Finally, the impact of the degree to which the individual subjects experience the strength of their positive and negative emotions, a personally trait known as affect intensity, on brain activation patterns was studied using a correlation analysis. Based on previous studies it was expected that participants with high affect intensity scores activate more a network of brain areas that has been described to play a crucial role in emotion recognition, including the right somatosensory cortex, the supramarginal gyrus, and the right insular cortex. For interpretation of the results obtained, the usefulness of the functional map of the insular cortex that was established in this thesis was assessed.

Results: (1) In the fMRI experiment, differential, subregional amygdala response patterns could be demonstrated. Amygdala activity with positive auditory stimulation-related signal changes

predominated in probabilistically defined LB, and negative responses predominated in SF and CM. In the left amygdala, mean response magnitude in the core area of LB with 90-100% assignment probability was significantly larger than in the core areas of SF and CM. These differences were observed for pleasant and unpleasant stimuli. (2) Subregional functional specialization in the anterior insular cortex was found based on the conducted ALE meta-analysis, showing different subregions consistently activated during motor tasks (located in the mid-insular cortex), language/auditory tasks (located in the rostral part of the anterior insula), and in respect to peripheral physiological changes (in the anteroventral insula), respectively. (3) The results of the amygdala meta-analysis revealed that probabilistically defined amygdala-activations co-activate with a restricted zone at the border of anterior insula and the frontal opercular cortex. (4) Correlation analysis with the affect intensity measure (AIM) revealed that subjects with high affect intensity demonstrated, as predicted, a stronger activity in the right somatosensory cortex, the supramarginal gyrus, and in the anteroventral insula region. The later brain region could be assigned, using the functional map of the insula established in part (3) of the thesis, to the part of the insula consistently showing peripheral autonomic change related activation, suggesting a stronger physiological response in the individuals scoring high in affect intensity as a possible cause for the AIM related differences in brain activation.

Conclusions: The results of this thesis suggest that the combination of functional MRI and of meta-analyses of functional imaging studies with probabilistic anatomical maps may make an important contribution in improving functional localization and in investigating internal functional organization of emotion related brain areas.

2 Introduction

2.1 *Studies of emotion*

Interest in the study of emotions based on psychological concepts and using neuroimaging methods has increased dramatically in the last years. Research has addressed a wide variety of issues including investigating the functional neuroanatomy of human affective processes using positron emission tomography (PET) or functional magnetic resonance imaging (fMRI) [1], and examinating the relationship between personality traits and the experience of emotions [2–4]. Figure 1 shows the key structures of the 'emotional brain', including the amygdala, the insula, the cingulate cortex, and the orbitofrontal cortex [1,5]. In the present thesis attention is particularly paid to two of those key structures: the human amygdala and the insular cortex. Both of these brain regions have been reported in many neuroimaging studies that investigated emotional processing and its underlying brain network [1,5]. The human amygdala is thought to play a pivotal role in the processing of emotionally significant sensory information [6–10] and the insular cortex has been reported being involved in different functions including somatovisceral perception [11] and peripheral autonomic change [12–15], which has been claimed to play an important role in emotion [16,17].

In the present work functional MRI has been combined with cyto-architectonically defined probabilistic maps to analyze the response characteristics of the amygdala and its subregions in eighteen subjects presented with emotionally significant auditory stimuli. Further, brain activation correlating with individual differences in affect intensity, a personality trait that refers to the degree to which individuals experience the strength of their emotion during the exposure of the same affect-evoking stimuli [18], has been investigated. In addition, a coordinate-based meta-analysis of previous fMRI and PET studies reporting amygdala-activation was carried out. The principle aim of this amygdala meta-analysis was to determine brain area(s) that are consistently co-activated with the amygdala. To realize this analysis only published amygdala-coordinates which were probabilistically located in the amygdala entered the (co-)activation

likelihood estimation (ALE) [19]. A second coordinate based ALE [20,21] meta-analysis of previous PET and fMRI studies reporting insula activation was conducted to investigate the question whether different previously assumed insula-functions are consistently processed in specific subregions of the anterior insula. As a result, this meta-analysis provided a first functional map of the anterior insula that was found to be useful for interpreting functional data of this work. The two meta-analyses were also motivated by the more global question whether neuroimaging studies investigating similar functions show consistent responses across different experiments, subjects, and stimuli, because it has been argued that functional measurements have a low reliability [22,23]. In this work functional localization was carried out – if available – by using probabilistic maps which will be addressed in chapter 4.5 [24,25]. The use of these maps was mainly motivated by the fact that they enable anatomical assignments with considering interindividual anatomical variability. In addition, they enable anatomical assignments of brain areas, particularly the amygdala and its subregions, which cannot be distinguished on current structural brain images [24,25].

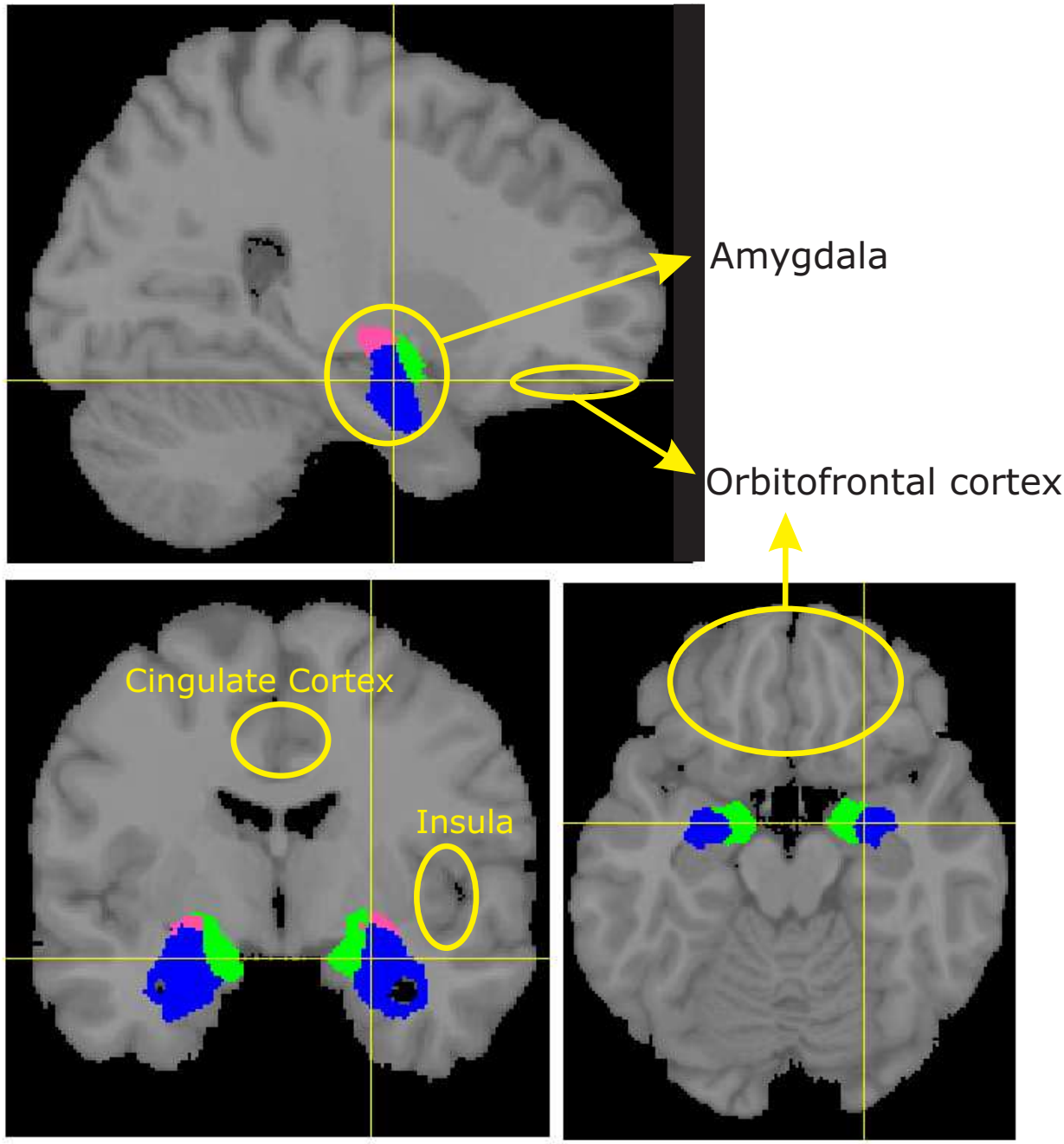

Figure 1: **Key structures of the 'emotional brain'**, including the amygdala, the insula, the cingulate cortex, and the orbitofronal cortex. The figure shows also the probabilistically defined amygdala and its subregions (the subregions are marked in blue, green and magenta, see chapter 4.5 for further details).

2.2 *The Role of the Amygdala in emotional processing*

The challenge of unraveling the function of the human amygdala is attracting great interest [6–10]. This is reflected in a broad range of neuroimaging studies that includes investigations of emotional processing of chemosensory information [26–28], visual stimuli such as facial emotional expression [29–31], and auditory stimuli including communication sounds [32,33] and music [34,35]. In addition, to the desire to understand the neuronal basis of human emotion, an important motivation behind these studies is to understand the role of the amygdala in psychological disorders such as depression, anxiety disorders, and antisocial personality disorder [36–39]. Birbaumer and co-workers found that psychopaths show less activation in the limbic-prefrontal circuit including the amygdala than healthy controls during fear conditioning [37]. Individuals suffering on social phobia on the other hand tend to show stronger amygdala activation during the presentation of potentially fear-relevant stimuli [36].

Anatomically, the human amygdala is located in the medial temporal lobe (see figure 1). Studies in many mammalian species [7,40–45] including humans [24] have firmly established that the amygdala is not a single homogenous structure but that it is composed of several anatomical groups of subnuclei. In animal research, investigation of the intrinsic amygdaloid network and information flow plays a crucial role and is generally thought to be a key issue for elucidating amygdala function [46]. Similarly, greater understanding of amygdala function in humans may be achieved by differentiating response properties of human amygdala subregions. There is however a lack of such data in humans, the major reason for which is that current structural brain scans do not enable the differentiation of individual subregions of the human amygdala [24]. This problem is compounded by the fact that the exact location of the amygdala subregions varies between individuals and that standard atlas systems do not provide information about this inter-individual anatomical variability. Therefore, in this study functional magnetic resonance imaging (fMRI) with probabilistic anatomical maps [24] based on histological analysis of ten human post-mortem brains were combined. The advantage of such probabilistic maps is that they provide information about the location and inter-individual variability of brain areas in standard reference space. This allows assignment of activation sites

to micro-anatomically defined brain regions in a probabilistic fashion [25], even if these brain regions are not discernible in structural brain images.

The major amygdala subdivisions and their assumed function as established in animal research are as follows: There is evidence in mammalian species including monkeys that the majority of subcortical and cortical inputs converge in the laterobasal group [7,40–45]. This structure is believed to play a crucial role in assigning emotional value to sensory stimuli [47]. The superficial (cortical) part of the amygdala is a neighboring structure of the laterobasal group. Its function has been investigated less thoroughly. The acquisition of a conditioned defensive response in normal rats has however been shown to be associated with increased metabolic activity in the area of the superficial group, suggesting an involvement of this subregion in affective processing [48]. The centromedial group receives convergent information from several other amygdaloid regions and sends efferents to various subcortical structures, generating behavioural responses such as modulation of autonomic activity [41,46]. According to the model by LeDoux and co-workers [41] (see figure 2) an acoustic stimulus reaches the lateral part of the laterobasal amygdaloid group from auditory processing areas in medial division of the medial geniculate body of the thalamus (MGm) and the auditory cortex. The lateral part of the laterobasal amygdaloid group itself, projects to the centromedial group (CM). The centromedial group is connected with the brainstem, the hypothalamic nuclei [49], and with the anterior insular cortex [50]. It is assumed that the central amygdala is involved in a network that controls behavior (e.g. peripheral autonomic arousal for defense responses) via projections to the brainstem, and hypothalamic nuclei [51,52]. Similarly, the human amygdala is believed to be not a homogeneous anatomical structure [24]: Based on differences in cyto-, myelo-, and chemoarchitecture, it can be differentiated into the laterobasal amygdaloid group (LB), the centromedial group (CM), and the superficial group (SF) [24,53]. LB comprises the lateral, basolateral, basomedial and paralaminar nuclei, CM the central and the medial nuclei, and SF includes the anterior amygdaloid area, the ventral and posterior cortical nuclei [24]. Results from previous neuroimaging studies [29–31] suggest functional differences in the human amygdala region similar to those of the animal amygdala, but response differences between LB,

SF, and CM, were not directly assessed in these studies. The specific functional response properties of these major subdivisions of the human amygdala are therefore unclear. On this background, the principle aim of this study was to determine the response properties of probabilistically defined LB, SF, and CM of the human amygdala during processing of emotionally significant sensory information. To investigate this, piano melodies were presented to eighteen healthy subjects during acquisition of blood oxygenation level dependent (BOLD) contrast sensitive functional MR images in a 3 Tesla scanner. The distribution of BOLD signal changes was then analyzed using probabilistic maps of the three anatomical amygdala subregions [24].

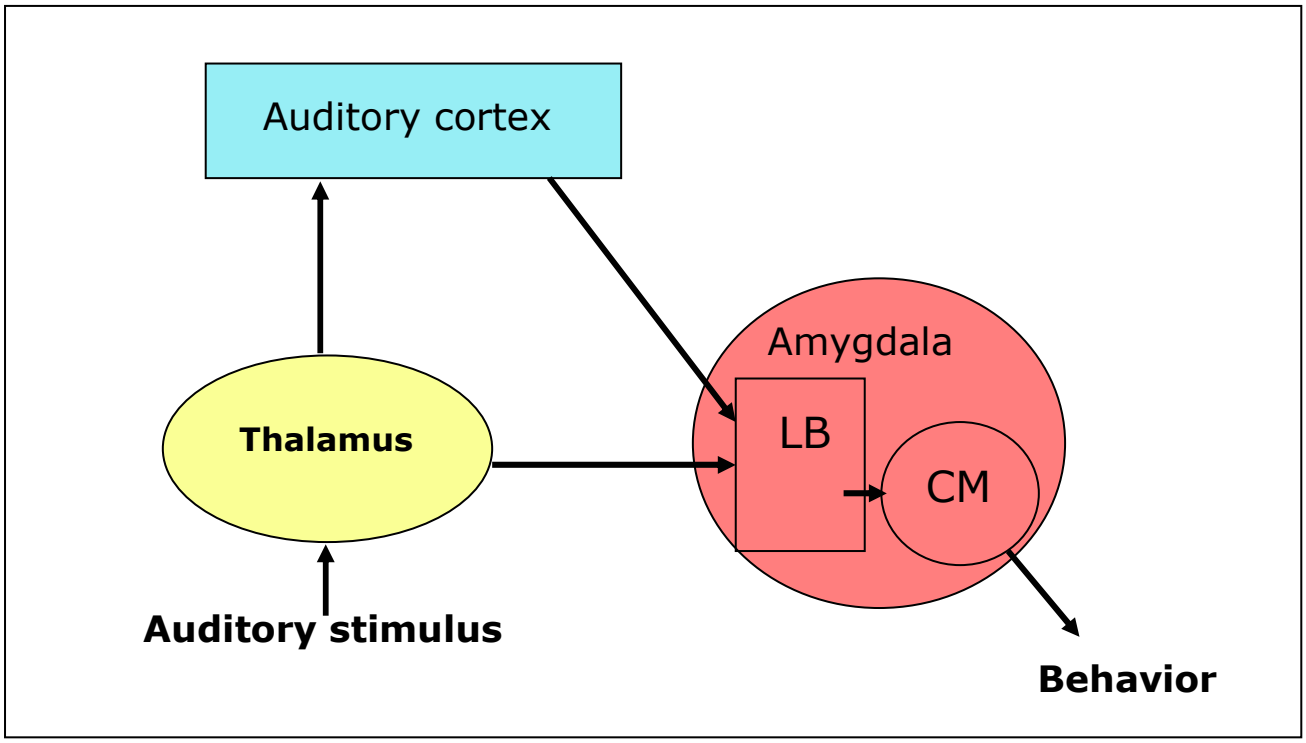

Figure 2: **The auditory pathways to the amygdala** (modified after LeDoux, 2000 [41]). Information about acoustic stimulus reaches the lateral part of the laterobasal amygdala from auditory processing areas in medial division of the medial geniculate body of the thalamus (MGm) and the auditory cortex. The lateral part of the laterobasal amygdala itself, projects to the centromedial group (CM). CM is connected with the brainstem, the hypothalamic nuclei [49], and with the anterior insular cortex [50]. It is assumed that CM is involved in a network that controls behavior (e.g. peripheral autonomic arousal, defense response) via projections to the brainstem, and hypothalamic nuclei [51,52].

2.2.1 Hypotheses of the functional MRI study

This study had the aim to determine the distribution of BOLD signal changes of the three anatomical amygdala subregions LB, SF, and CM during processing of emotionally significant auditory information using probabilistic maps [24]. Based on available evidence from animal research [41] it was expected that auditory stimulation should activate the laterobasal part of the amygdala, because the majority of auditory inputs enter there into the amygdala, and it was expected that there might be reciprocal changes in the laterobasal and centromedial groups.

2.2.2 Hypothesis of the meta-analysis of amygdala co-activations

Are there brain areas that are consistently co-activated with the amygdala? This question was investigated in an explorative way by conducting a coordinate-based meta-analysis of neuroimaging studies reporting amygdala-activation.

2.3 *Functional anatomy of the insular cortex*

Studies have repeatedly shown that the human insular cortex is involved in diverse functions including language, auditory processing, peripheral autonomic change, somatovisceral perception, sensorimotor processing, and taste [54–60], and there is an increasing interest in unravelling the function of the human insula in psychological disturbances such as anxiety disorders [61], drug addiction [62], and emotion dysregulation [63]. Anatomically, in humans the insula lies in the depth of the sylvian fissure. The central insular sulcus ('sulcus centralis insulae') divides the insula into two parts, the larger anterior insula and in the smaller posterior insula [50,64]. The localization of the insular cortex is shown in figure 1.

The insular cortex in primates including humans has connections with the frontal (operculum, premotor area), temporal (auditory cortex, temporal pole), olfactory, and parietal cortex (primary and secondary somatosensory areas) [50,55], and to the basal nuclei [65]. Further, the insula is reciprocally connected to the brainstem, hypothalamic nuclei, and amygdala [49]. Because of this widespread connectivity to sensory areas, it has been speculated whether the insula serves as an integration cortex where multimodal information converge [50]. Most recently, Dossenbach and co-workers suggested based on a cross-studies analysis that the anterior insula and the adjacent frontal operculum is involved in a brain network that forms a more general task-set processing system [66].

Little attention, however, is paid to the question whether different functions that are assumed in the insular cortex are processed in specific sub-regions of the anterior insula. In order to investigate this question, an activation likelihood estimate (ALE) meta-analysis [21] by mapping

coordinates of 112 activation foci obtained in 50 different studies selected through a search of functional magnetic resonance imaging (fMRI) and positron emission tomography (PET) literature was carried out. Studies investigating language, auditory processing, sensorimotor tasks, or change in the peripheral autonomic nervous system (mostly investigated by measuring cardiovascular or electrodermal activity) were selected because they have repeatedly reported to find activation in the anterior insula.

Auditory and language functions

A number of brain imaging studies demonstrate the involvement of the anterior insular cortex and the adjacent deep frontal operculum in auditory processing like perception of vocalization (e.g. parents listening to infant crying) and music processing [33,35,56,67,68]. In addition, Habib and colleagues reported that ischemic infarcts involving the bilateral insular cortex resulted in persistent auditory agnosia [69]. Bamiou and co-workers found auditory temporal processing deficits in patients with insular stroke [70], suggesting that the insula is a crucial component in auditory processing. This assumption is in line with the fact that the insular cortex is connected with the auditory cortex [50,55]. In addition, a lesion study [71] reported impaired speech in a patient with a left anterior insular infarction. Further, several functional neuroimaging studies suggest that the human insula and the adjacent deep frontal operculum is also involved in language processing [55,72]. It has therefore been suggested that the insula is involved in a functional network that mediates speech [54,73,74]. The exact subregion within the insula serving auditory and language functions, however, has not be systematically delineated.

Sensorimotor functions

There is increasing evidence that the insular cortex might play a role in sensorimotor processing. Stimulation of the insular cortex of the monkey has been reported to have sensorimotor effects [55]. Further, motor responses in the anterior insular has been also reported by stimulation of the human insular cortex [75] and it has been claimed that the insular cortex is a motor association area [55]. Colebatch and co-workers measured regional

cerebral blood flow (rCBF) using PET in six healthy subjects while they were performing different repetitive movements of the right arm [76]. Both finger opposition and shoulder movements were associated with activation in the left insular cortex. In contrast, it has also been claimed that the insular cortex is not an area that is typically activated during motor tasks in neuroimaging experiments [77]. Similar to the auditory and language functions, it is not clear whether there is a subregion within the insular cortex which shows reproducibly activation during sensorimotor tasks.

Peripheral autonomic functions

The insular cortex has also been implicated as an important brain area being involved in peripheral autonomic functions. Electrical stimulation of the insular region has shown to produce changes in heart rate in both primates [78,79] and in humans [80]. This finding is in agreement with the fact that, the insular cortex has reciprocal connectivity with other brain areas such as the amygdala and hypothalamus which are involved in autonomic functions [52,81]. Neuroimaging studies demonstrate that activity in the insular cortex correlate with evoked peripheral responses [12–15]. Moreover, these studies have reported association between insula activity and cardiovascular responses [14,15], electrodermal activity [12,13], pupil responses [82], or the administration of procaine (a drug evoking physiological arousal) [83]. More recently, a lesion study reported that subjects with damage to the insular cortex were more likely to disrupt addiction to cigarette smoking than smokers without a damage in the insular cortex, suggesting that the insula mediates physiological addiction to smoking [62]. Critchley and co-workers suggested that studies investigating brain activity related to peripheral autonomic change will find activation in the anteroventral insula [82]. This assumption, however, has not been systematically investigated yet.

2.3.1 Hypothesis

This meta-analysis aimed to investigate the hypothesis that different functions are processed in specific regions of the anterior insula. Studies investigating language, auditory processing, sensorimotor tasks, or change in the peripheral autonomic nervous system (mostly investigated

by measuring cardiovascular or electrodermal activity) were selected because they have repeatedly reported to find activation in the anterior insula.

2.4 *The impact of the personality trait 'Affect Intensity' on emotional processing*

There is a current growth of interest in exploring the role of affect intensity, a personality trait that refers to the degree to which individuals experience the strength of their positive and negative emotions. The impact of affect intensity on people's social life and health-related consequences has been investigated [84]. What is currently less clear, however, is whether there are emotional-cognitive benefits to be derived from being emotionally sensitive in personal life and social life. According to Larsen and Diener, individuals scoring high on the affect intensity dimension will, given the same level of emotional stimulation and regardless of the specific emotion evoked, exhibit stronger emotional responses. Larsen and co-workers discussed different mechanisms that could cause these individual differences in affect intensity (see figure 3) [18]: It might be that people with high in comparison to low affect intensity are more attentive to emotional stimuli in the environment and/or have the tendency to interpret stimuli as more emotion-relevant. Additional or alternatively, it might be that subjects with high affect intensity have a stronger physiological reaction to the perception of emotional stimuli. Furthermore, it could be that high affect intensity individuals are more perceptive of their bodily reactions which accompanies emotional states such as physiological (e.g. change in heart rate) and motoric (e.g. facial expressions) responses and/or interpret those responses more likely as emotion.

Flett and colleagues asked subjects to describe occasions when they felt happiness, pride, anxiety, and hate [85]. Subjects with high affect intensity scores rated their emotional events as more intense, and reported experiencing emotions more frequently and being better able to recall their emotional experiences. The last finding is consistent with research showing a positive relationship between the intensity of affect and the ability to recall emotional events of

personal importance [86]. Haddock and colleagues investigated affect intensity as a potential moderator variable in social judgments [87]. The authors reported that affect intensity influenced subjects attitudes, stereotypes, and feelings towards different social groups. Further, health-related consequences of high affect intensity is evident in the number of significantly associated somatic symptoms (e.g. nervousness, headaches, shortness of breath), suggesting that affect intensity is related to somatic distress [84]. But are there also advantages associated with high affect intensity?

Recently, a behavioral study demonstrated, that high affect intensity is also associated with emotional-cognitive benefits [88]: In this behavioral experiment the authors investigated the hypothesis whether high scores on the affect intensity dimension, as assessed by the Affect Intensity Measurement (AIM) [84,89], have an impact on the recognition of the emotional content of piano music performances. To test this hypothesis, 40 subjects without a professional music education were asked to recognize the emotional expression of piano melodies of four basic emotions: Happiness, sadness, anger, or fear. The piano melodies were independently played by three professional pianists. The experiment followed a similar procedure described by Juslin [90]. The behavioral results show that subjects with high affect intensity demonstrate a significantly better performance in this emotion recognition task. Adolphs and colleagues [91] conducted a lesion mapping study of 108 Patients with focal damage and aimed to identify brain areas which are associated with emotional recognition. Particularly damage of right somatosensory areas was found to correlate with impairments in naming basic emotions from facial expressions. In addition, also the right insula and the supramarginal gyrus have been found to play an important role in this task.

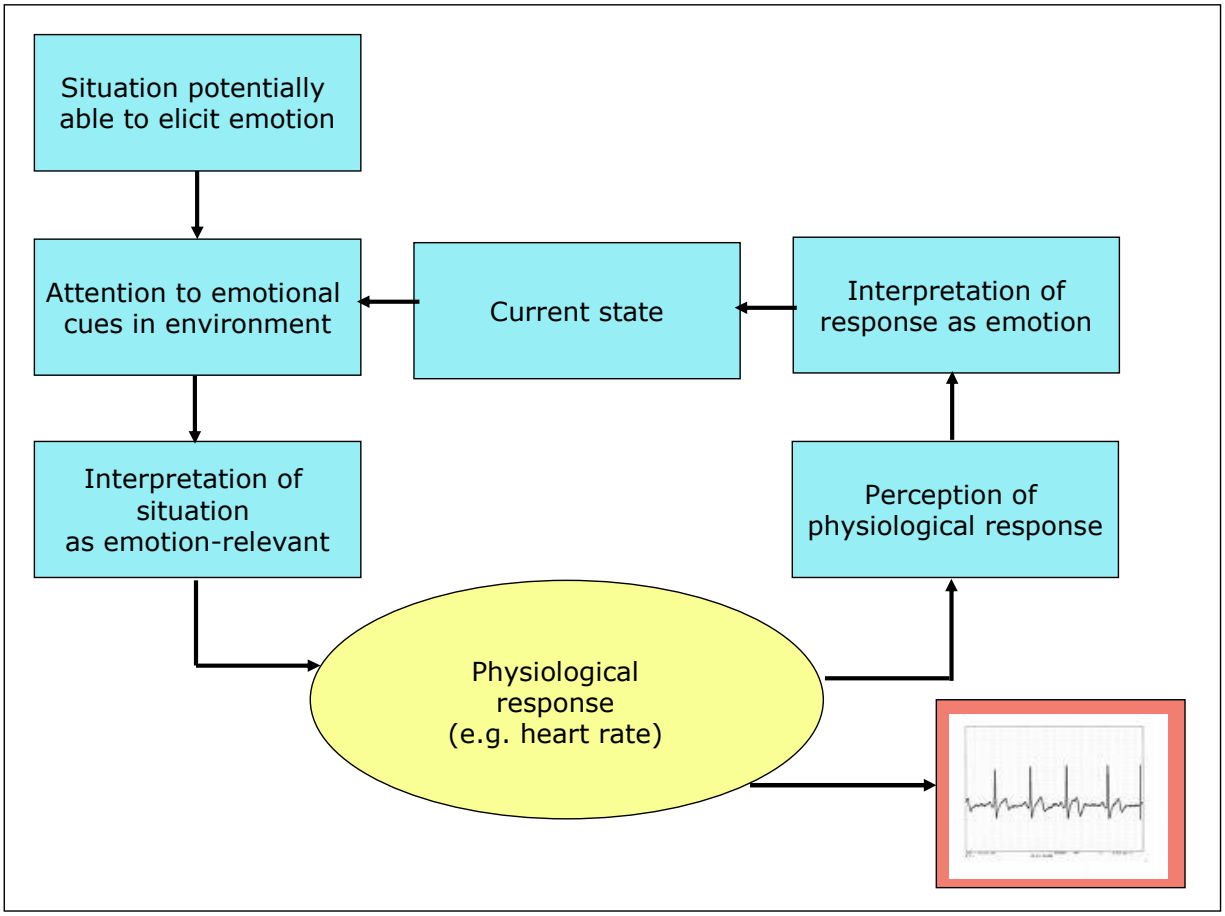

Figure 3: **Mechanisms hypothesized to contribute to individual differences in affect intensity** (modified according to Larsen and co-workers [18]). It might be that people with high in comparison to low affect intensity are more attentive to emotional stimuli in the environment or have the tendency to interpret stimuli as more emotion-relevant. Additional or alternatively, it might be that subjects with high affect intensity have a stronger physiological reaction to the perception of emotional stimuli. Furthermore, it could be that high affect intensity individuals are more perceptive of their bodily reactions which accompanies emotional states such as physiological (change in heart rate) and motoric (facial expressions) responses and/or interpret those responses more likely as emotion.

2.4.1 Hypothesis

The aim of the study was to investigate the neural network associated with high affect intensity during the exposure of piano music using functional magnetic resonance imaging (fMRI). Based on a previous behavioral study showing that subjects with high scores on the affect intensity dimension (as assessed by the Affect Intensity Measurement (AIM) [84,89]) demonstrate better performance in an emotion recognition task [88] it was expected that participants with high

scores activate more a network of brain areas described by Adolphs and co-workers [91] being involved in emotion recognition, i.e. in particular, the right somatosensory cortex and also the right insular cortex and the right supramarginal gyrus that have been described to play a crucial role in emotion recognition.

3 Material and Methods of the functional MRI study

3.1 *Subjects*

Eighteen subjects (11 females, 7 males, mean age = 22.72 years, range = 19-34 years) without professional musical education took part in this study after giving written informed consent. The study was approved by the ethics committee of the University of Freiburg, Germany. All participants were healthy, with no past history of psychiatric or neurological diseases or hearing problems. Subjects were right-handed according to the Edinburgh Handedness Inventory [92]: Mean = 84.11 %, range = 75–100 %.

3.2 *Stimuli*

For auditory stimulation, 10 piano pieces, each of 24 second duration, were presented. The musical stimuli were selected in cooperation with a professional musician and chosen from the romantic period. All pieces were examples of major-minor tonal music. The tempo and harmony of the 10 selected piano melodies (see Table 1) were varied, creating four versions of each tune: consonant-fast (CF), consonant-slow (CS), dissonant-fast (DF), and dissonant-slow (DS). Tempi for the fast and slow versions were 156 and 84 beats per minute, respectively. These values were selected because they represented the fastest/slowest tempi that still sounded natural to one professional musician and five non-musicians. The consonant stimuli were the original tunes, whereas the dissonant stimuli were electronically manipulated counterparts of the original tunes, created by shifting the melody of the original excerpt, but not the accompanying chords, by a half tone below the original pitch. Thus, the dissonant and consonant, and the fast and slow versions of a tune had the same rhythmic structure. All stimuli were processed using Cubase VST/32 R.5 (Steinberg) as software. Finally, all sound files were transformed into wave files for stimulation in the scanner using WaveLab (Steinberg).

The aim was to select stimuli that elicit significant emotional reactions (see results section). In view of the ongoing controversy about whether the human amygdala responds to pleasant and

unpleasant stimuli in a similar [93,94] or rather in a different manner [35] a further goal was to select stimuli that evoke either pleasant or unpleasant emotional reactions. A further aim was to use relatively unknown piano melodies, because several studies indicate that the response of the human amygdala to emotional stimuli diminishes with repeated presentations [95–98], that is, with increasing familiarity. Consequently, relatively unknown musical excerpts were chosen. Familiarity was immediately after scanning assessed.

Composer	**Opus**	**Interpreter**
Schubert	Four Impromptus, D.935, Op.posth.142; No.1 in F	J.E. Dery
Mendelssohn	Book 5, Op.62; 6.Frühlingslied in A	C. Meesangnin
Tchaikovsky	Album pour enfants, Op.39; 5.March of the Wooden Soldiers	M. Knezevic
Chopin	Waltz in Db, Op.69, No.1 ('L'adieu')	P.M.P. Blondel
Mozart	Piano Sonata in C, K.330; 2. Andante cantabile	R. Ungar
Liszt	Valse Impromptue	G. Giulimondi
Chopin	Mazurka in A-, Op.67, No.4	R. Lubetsky
Haydn	Keyboard Sonata in G, Hob.XVI:27, Op.14, No.1 (No.42)	T. Leen
Tchaikovsky	12 morceaux, difficulté moyen, Op.40; 6.Song Without Words	M. Knezevic
Schumann	Kinderszenen, Op.15; 2.Kuriose Geschichte	G. Giulimondi

Table 1**:** Composer, opus, and interpreter of the 24 second **piano music excerpts** used in the fMRI experiment.

3.3 *Experimental design*

The image acquisition started with localizing the brain, a reference scan for the distortion correction, and the anatomical scans of the brain which were obtained using a MPRAGE sequence of 7 minutes duration (T1, see chapter 3.5 for further details). The Experimental (see Figure 4) started with the German version of the State Anxiety Inventory by Spielberger and co-workers [99]. Subjects were asked to complete the German Version of the State Anxiety Inventory by using a magnetic resonance-compatible mouse. This mouse allowed subjects to move a white box to the left or right along a visually presented scale by pressing the corresponding mouse buttons with the right hand. This evaluation was conducted to assess and to control subjects' state anxiety level in the scanner for the later affect intensity analysis. Subsequently, the fMRI experiment was conducted using a Block design.

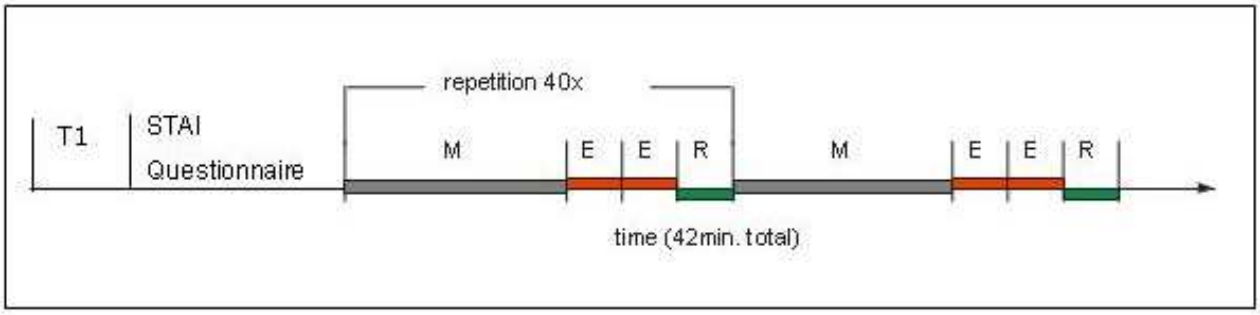

Figure 4: This figure shows **the experimental design**. The measurement started with localizing the brain, a reference scan for the distortion correction, and the anatomical scans of the brain which were obtained using a MPRAGE sequence of 7 minutes duration (T1, see chapter 3.5 for further details). The STAI questionnaire was conducted during fMRI measurement with 4 minutes duration. Subsequently, the fMRI experiment was conducted using a block design. Each block consisted of music presentation with 24 seconds duration (M), and the evaluation of the perceived valence (ranging from very pleasant to very unpleasant) and arousal (ranging from very calming to very arousing). Each evaluation (E) had a duration of 6 seconds. Each block finished with 'rest' (R) of 11 seconds duration during which subjects had only to attend a fixation cross. Each block was repeated 40 times and the fMRI experiment had a total duration of 42 minutes.

The 4 variations of the 10 piano tunes were presented during the fMRI experiment in a random order, using in-house developed presentation software, via magnetic resonance compatible

headphones (NordicNeuroLab, Norway). Subjects viewed a fixation cross during the experiment and were instructed to listen attentively to the music and to avoid any overt movement. Each melody was preceded by a written instruction presented on the screen ('music starts'), and each melody lasted 24 seconds. Each melody was followed by a period of evaluation. Within this period, participants were asked to rate the tune on a 7-point self-assessment scale along the dimensions valence (ranging from -3 = very unpleasant to 3 = very pleasant) and arousal (ranging from -3 = very calming to 3 = very arousing). Each of the two rating periods lasted 6 seconds. Subject conveyed their decision by using a magnetic resonance compatible mouse which allowed them to move a white box on the visually presented scale leftwards or rightwards by pressing the corresponding mouse button with their right hand. The evaluation was followed by a resting time of 11 seconds duration. There were 40 runs (each consisting of melody presentation, evaluation, and rest). Total scanning time for the experiment was 42 minutes. After scanning subjects were asked to rate the familiarity (ranging from 0 = not familiar; to 3 = familiar). Subjects gave two global familiarity ratings, one for the pleasant and one for the unpleasant melodies.

After the fMRI measurements subjects completed the German translation of the Affect Intensity Measurement (AIM) [84,89]. The AIM is a 40-item questionnaire that inquires about the strengths of affective reactions to typical life situations and measures a total score for the affect intensity as well as separate scores for positive and negative affect intensity. In addition, lifetime musical education (cumulated in years) was assessed using a questionnaire translated and modified from Litle and Zuckerman [100]. This questionnaire also included ratings for enjoying listening to classical music (ranging from 0 = not at all, to 4 = frequently).

3.4 *Functional and structural MRI*

3.4.1 Functional MRI and BOLD signal

Functional magnet-resonance-imaging (fMRI) is a non-invasive method to measure brain activity. In 1990, Ogawa and colleagues [101] described that changes in cerebral blood oxygenation (Blood oxygenation level dependent signal = BOLD signal) can be measured using MRT. The local vascular network of the active region is flooded with fresh oxygenated blood and leads to characteristic changes in the concentrations of oxyhemoglobin (Hb) and deoxyhemoglobin (dHb). Due to the different magnetic attributes of dHb and Hb (dHb is paramagnetic, Hb is not) these alterations in concentration result in local magnetic field changes and can be measured in the MR-scanner (using T2* weighted imaging technique). These signal changes can be described by the hemodynamic response function (HRF, see Figure 5). The exact mechanisms that lead to these changes in the cerebral blood flow (CBF) are still not exactly known. Recently, studies using simultaneous fMRI and intracortical electrical recordings in monkeys have started to characterize the relationship between BOLD signal and neuronal activity: Logothetis and co-workers demonstrated that the positive BOLD signal is closely related to neuronal activity (that is to local field potentials, LFPs) [102]. Shmuel and colleagues reported that the negative BOLD signal was associated with local decreases in neuronal activity (that is with decreases in LFPs) [103]. More recently, also in humans a relationship between neuronal activity (LFPs) and BOLD signal has been demonstrated by comparing the neuronal activity in epilepsy patients with intracranial depths electrodes with the fMRI signal of healthy subjects during the presentation of a movie [104]. Increases or decreases in BOLD-signal were therefore interpreted in this work as evidence of local neuronal activation or deactivation, respectively.

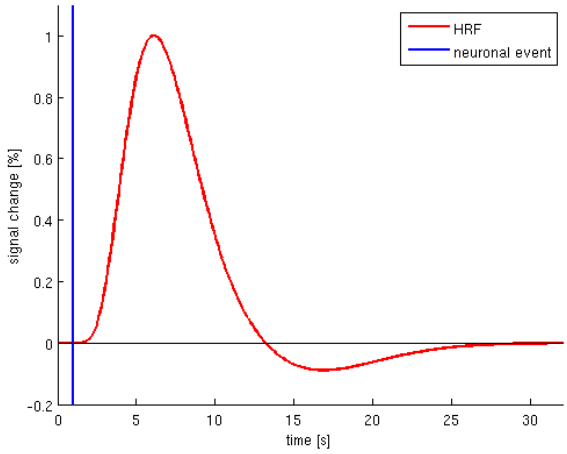

Figure 5: **The shape of the Hemodynamic Response Function** (HRF, red curve) describes the Blood oxigenation level dependent signal (BOLD signal) after a short 'event' like a flash. The maximum signal change is delayed and is reached after approximately six seconds and is followed by an undershoot.

3.4.2 Methodological issues regarding imaging the human amygdala: Signal drop out, image distortions, draining vein, and spatial resolution

Amygdala fMRI studies do mostly not show the echo planar imaging (EPI) raw data. But the raw data quality can be problematic in the amygdala region. By detecting amygdala activation or deactivation using functional MRI there can emerge several methodological problems which will be discussed in the following chapter, including signal dropout, image distortions, and the 'drawing vein' problem. An additional methodological problem relates to the amygdala`s small volume. Anatomically, the human amygdala is located in the medial temporal lobe (see figure 1). In the amygdala-area there is typically a high level of inhomogeneity in the magnetic field caused by the presence of tissues with different magnetic properties. This inhomogeneity can lead to loss of signal in the amygdala region during echo planar imaging [105], or to distortions that can lead to signal mislocalization [10]. In this study the possibility of **signal dropout** in the amygdala region has been analyzed. As illustrated in Figure 11 good EPI quality in the region of interest was achieved in all subjects investigated. Further, in this study a correction for geometric distortion correction developed by Zaitsev and co-workers [106] has been applied in

order to handle **image distortions** arising in the amygdala region. The distortion correction technique is a recently developed method based on the point-spread-function (PSF) measurement of the echo planar imaging signal (see also next chapter). The applicability of this technique to the amygdala region critically rests on sufficient signal strength in this area. In this study the signal strength was sufficient in the amygdala area for application the PSF-technique in all subjects investigated (see Figure 11). Based on the shift and broadening of the point spread function in phase encoding direction, the original signal location and intensity in phase encoding direction is being recovered to result in an undistorted image. This correction has been shown to yield subvoxel accuracy [106]. **Draining veins** can lead to signal mislocalization. While the previously discussed point (image distortions) is more severe in the amygdala region as compared with other commonly examined brain regions, the draining vein problem can be assumed to be less pronounced in the amygdala for the following reasons: (1) the draining vein problem is more severe for large areas of activated neuronal tissue [107]. The amygdala, and especially its subnuclei, is/are relatively small. Also, the activated volume in this study is relatively small (see table 4). The volume is approx. 100 mm^3. (2) Contamination by apparent activation along a draining vein will be most pronounced if a single vein drains the activated area [107]. The amygdala is however drained by a large number of veins [108], again reducing the draining vein problem; and, (3) these general considerations are confirmed by experimental data from BOLD venography. Venograms indicated that there are no sizable draining vein artifacts in the amygdala region likely to cause mislocated activation in functional studies [109]. An additional methodological factor is related to the small volume of the human amygdala. It is poorly systematically investigated whether functional MRI techniques possess sufficient **spatial resolution** to detect activation and deactivation in the amygdala and its subregions. Addressing this issue, further analyses were carried out and are presented in chapter 6.3.2.

3.5 *Functional and structural image-acquisition*

Functional and structural images were acquired on a 3 Tesla scanner (Siemens Magnetom Trio, Erlangen, Germany). Structural T1-weighted images were obtained using a MPRAGE sequence

(resolution: 1mm isotropic, matrix: 256*256*160, TR: 2200ms, TI: 1000ms, 12° flip angle). Functional images were acquired using a multislice gradient echo planar imaging method (EPI). Each volume consisted of 44 sagittal slices (resolution: 3 mm isotropic, matrix: 64*64, FOV 192 mm*192 mm, TR 3000 ms, TE 30 ms, 90º flip angle). The sagittal slice orientation resulted in significantly lower acoustic noise generated by the imaging gradients, enabling a better stimulus perception. In addition, this orientation in combination with the thin slice thickness reduced the signal loss in the amygdala region to give more reliable detection of activation.

An accurate registration of the functional and structural images was enabled by correction of the EPI data for geometric distortions [106]. The distortion field was derived from the local point spread function (PSF) in each voxel as determined in a one minute reference scan. Prior to distortion correction, the data were motion corrected by image realignment with the reference scan. Motion and distortion correction were performed online during the reconstruction process. The applicability of the PSF-based image correction to the amygdala region critically rests on a sufficiently strong signal that might be compromised by local signal drop out (see also chapter before). It has been therefore verified that the whole analyzed extent of the amygdala had good EPI signal quality and that distortion correction was possible in this region (see results section).

4 Preprocessing, statistical analysis, and anatomical assignment

Both, preprocessing and statistical analyses of the fMRI data were preformed with SPM5 (Wellcome Department of Cognitive Neurology, London, UK), and by using an in-house developed software (MTV). Figure 6 illustrates the different preprocessing steps and the statistical analyses of the functional MR data which will be explained in the following chapter. The anatomical location of activation was determined using probabilistic anatomical maps.

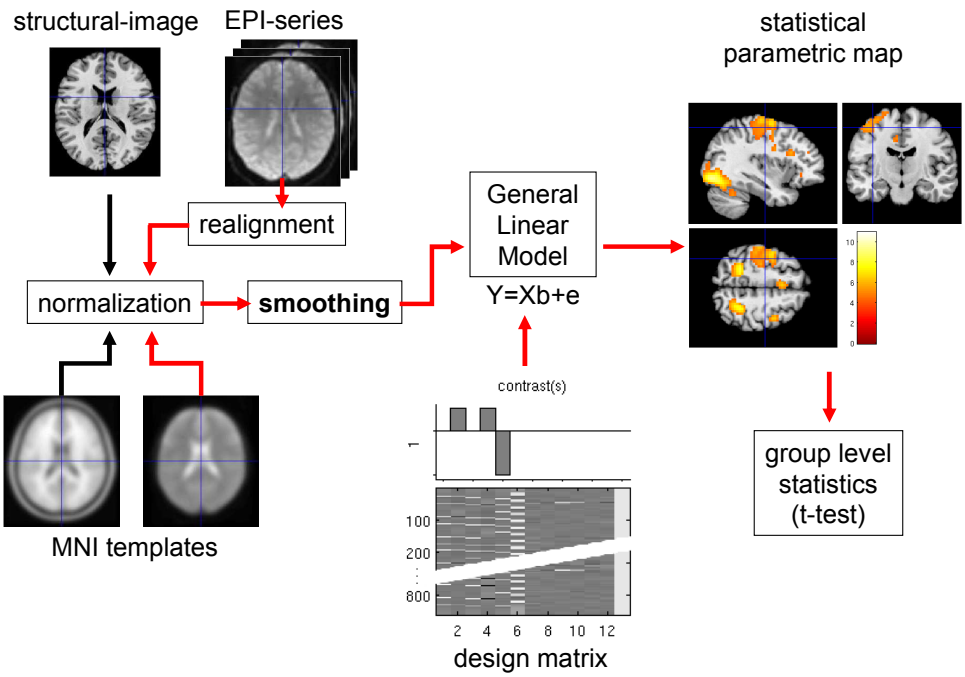

Figure 6: **Stages of image processing (modified according to Friston)**: Preprocessing and statistical analyses of the functional MRI data were preformed with SPM5 (Wellcome Department of Cognitive Neurology, London, UK), and by using an in-house developed software (MTV). Motion correction (realignment) and distortion correction were performed online during the reconstruction process. The preprocessing (see next chapter) consisted of normalisation into standard stereotaxic space of the Montreal Neurological Institute (MNI) template into the MNI space and spatial smoothing. The Generral Linear Model (GLM) and the statistical analysis in explained in chapter 4.2 and 4.3.

4.1 *Preprocessing*

Motion correction (realignment) and distortion correction were performed online during the reconstruction process. Preprocessing consisted of normalisation, and smoothing (see figure 6). All functional images were normalized into standard stereotaxic space of the Montreal Neurological Institute (MNI) template. Subsequently, the images were smoothed using for the amygdala analysis a 6 mm and for the other analyses (music presentation > implicit baseline, and correlation with the affect intensity scores) a 10 mm full-width-at-half-maximum (FWHM) Gaussian kernel to minimize the effects of individual variations in anatomy and to improve the signal to noise ratio.

4.2 *General linear model and statistical analysis*

The timing information of the four music conditions (consonant-fast (CF), consonant-slow (CS), dissonant-fast (DF), and dissonant-slow (DS)) and of the evaluation periods were each modeled with a box-car function convolved with a canonical hemodynamic response function. A high-pass filter with a cut-off of 1/128 Hz was applied before the parameter estimation according to the general linear model (GLM) used by SPM5. Contrast images of music presentation > implicit baseline (i.e. time periods during which subjects passively viewed the fixation cross without stimulus presentation) were calculated for all subjects.

The GLM expresses the observed response Y of each voxel in terms of a linear combination of the regressors each weighed by a voxel-specific parameter β which has to be estimated: $Y = X*\beta + \varepsilon$, where ε describes not explainable variance such as error or noise.

With the five experimental conditions (consonant-fast (1), consonant-slow (2), dissonant-fast (3), and dissonant-slow (4) evaluation1 and evaluation2 (5)), the measured time series of each voxel can be expressed as:

$$Y_1 = X1 * \beta1_1 + X2 * \beta2_1 + X3 * \beta3_1 + X4 * \beta4_1 + X5 * \beta5_1 + \varepsilon_1$$

$$Y_2 = X1 * \beta1_2 + X2 * \beta2_2 + X3 * \beta3_2 + X4 * \beta4_2 + X5 * \beta5_2 + \varepsilon_2$$

...

$$Y_N = X1 * \beta1_N + X2 * \beta2_N + X3 * \beta3_N + X4 * \beta4_N + X5 * \beta5_N + \varepsilon_N$$

With N being the number of voxels.

According to the standard procedure in SPM, the calculation of the β values was done voxelwise. To compare the significance of the BOLD effects of the four music conditions and the resting condition in individual subjects, the difference between the estimated βs of both condition types was calculated. T-statistic was then used to test the null hypothesis that this contrast of the estimates is zero. In this way, the contrast strength and significance of each subject was calculated. Then group level statistics were used to reveal significant activations over the total group of the eighteen subjects.

Two group statistics were calculated:

1. The T-contrast images of music presentation > implicit baseline from the individual level were used to calculate a T-test on group level. For that, a voxelwise T-test over the individual contrast strengths was calculated, with the variance of the contrast strengths over subjects as denominator (results at $p < 0.05$, FDR corrected are reported).

2. The T-contrast images of music presentation > implicit baseline from the individual level were used for the correlation on second-level. The individual aim-scores were used as linear regressors (results at $p < 0.005$, uncorrected, in the a priori regions of interest are reported). A priori regions of interest were brain areas involved in emotion recognition, i.e. the right somatosensory cortices, the right supramarginal gyrus, and the right insula, as described in [91].

4.3 *Statistical analysis of the amygdala and its subregions*

After calculating contrast images of music presentation > implicit baseline (i.e. time periods during which subjects passively viewed the fixation cross without music presentation) for all subjects, for each music condition, the BOLD percentage signal change (PSC) was then extracted (using an in-house developed software) for all voxels which were assigned with a probability of least 50% to one of the amygdala subregions LB, CM, or SF (separately for right and left amygdala), using the probabilistic amygdala maps of Amunts and colleagues [24]. The probabilistic anatomical maps can be freely accessed through: www.fz-juelich.de/ime/spm_anatomy_toolbox.

Voxels (having 3 mm isotropic size in the functional data) were assigned according to the probability at the voxel center. Voxelwise between-subjects random effects were statistically evaluated in two ways: (1) based on the mean responses across all four music conditions, and (2) for consonant and dissonant music conditions (collapsing slow and fast conditions), separately. In many of the analyzed voxels, the null hypothesis that the PSC data (both for the mean and consonant/dissonant case) were normally distributed with unspecified mean and variance had to be rejected ($p<0.001$, 2-sided Bera-Jarque test of composite normality).

Therefore nonparametric tests were used for further analysis. For the random effect analysis, a sign test was used to evaluate the hypothesis that the PSC data (i.e. all 18 values per voxel) came from a distribution with zero median. The significance level for this analysis was $p<0.0026$, corresponding to a significance of $p<0.05$ for the whole amygdala (corrected for multiple comparisons based on the number of analyzed resolution elements). To determine the activated/deactivated volume in the amygdala subregions, the voxels with significant effects were up-sampled to 1 mm isotropic resolution and the number of resulting voxels within LB, SF, and CM was determined.

Further, histograms with 30 equally spaced bins across the whole range of the voxelwise PSC data were computed, separately for LB, SF, and CM, the lateralization index (LI), defined as (Rn-Ln)/(Rn+Ln))*100, with Rn and Ln being the number of voxels in the right and left amygdala for a given PSC bin was determined. In addition to the voxelwise analysis, also region of interest (ROI) analyses for six areas of interest (right and left LB, SF, and CM) were performed. In order to increase the robustness of the results against spatial errors, the ROI to the core of the amygdala subregions had >=90% assignment probability. As illustrated in Figure 12, in this way the localisatory assignment is made more robust against spatial localization errors as compared to less strictly defined ROI (e.g. the area with >=50% assignment probability).

For each of the LB, SF, and CM ROIs, the mean PSC of all voxels (i.e. all voxels with at least 90% probability to belong to a given area) was determined for each of the subjects. The resulting data were normally distributed ($p>0.2$, Bera-Jarque test). Differences in ROI data between amygdala subdivisions were assessed using a Students t-test for all combinations of the 3 areas of interest, both for the right and left amygdala. As with the voxelwise analysis, the ROI analysis was carried out both for the mean effect across the four music conditions and for the consonant and dissonant music conditions, individually.

4.4 *Statistical analysis of the behavioral data*

The results of the subjects' valence and arousal ratings were analyzed by two-way repeated measurements ANOVA, using Matlab (Version 7.0.4, the Mathworks, USA). Normal distribution of the questionnaire data were tested with the Kolmogorov-Smirnov test (KS-test), and analysed using SPSS (14.0). Subjects' ratings regarding familiarity was also analysed using SPSS (14.0).

4.5 *Anatomical assignment using probabilistic anatomical maps*

Several concepts can be applied for the anatomical assignment of functional activations [110]. The brain atlas of Brodman [111] was a first achievements in labelling different brain areas. It is based on macroanatomical landmarks, such as sulci and gyri. But two aspects are critical: first, anatomical demarcation of areas was made based on the subjective impression gained by visual inspection of the histological brain structure, not by objective criteria. Second, only a single brain was analyzed and therefore information about the inter-subject variability of the represented brain areas is lacking.

An approach which overcomes these limitations are probabilistic anatomical maps of the brain [112,113]. Each probability map is based on computerized, objective analysis of the cytoarchitecture of a sample of several post mortem brains. These maps have been published for different brain regions, including the motor, somatosensory, visual, auditory and language related areas [25]. In conjunction with normalisation to a standard reference space these probability maps provide anatomical assignments with considering interindividual variability. In addition, the amygdala and particularly its subregions cannot be distinguished on current structural brain scans, that means on macroanatomical landmarks [24]. Recently, also for the human amygdala a probabilistic-anatomical map has been published [24]. This map is based on observer-independent analysis of the cytoarchitecture in a sample of ten human post-mortem brains. The advantage of that probabilistic map is that functional activity can be anatomically

assignment, even when borders between distinct regions are not visible on structural images (macroanatomical landmarks) or when the borders of microstructural areas do not show a reliable relationship to macroanatomical landmarks. Eickhoff and colleagues [25] used the data of those probabilistic anatomical maps to develop maximum probability maps (MPMs) and implemented it in an anatomy toolbox in the SPM software package. In the MPMs, for each voxel coordinate in MNI-space the most probable assignment to a probabilistically defined region of the brain is calculated (an example is shown in figure 7).

In this thesis, the maximum probability maps (MPMs) method was used to assign active voxels to brain regions. For example for the insular cortex and the cerebellum there is no probabilistic map available yet. Activations that could not be assigned by these maps were localized according the T1 template provided by SPM5.

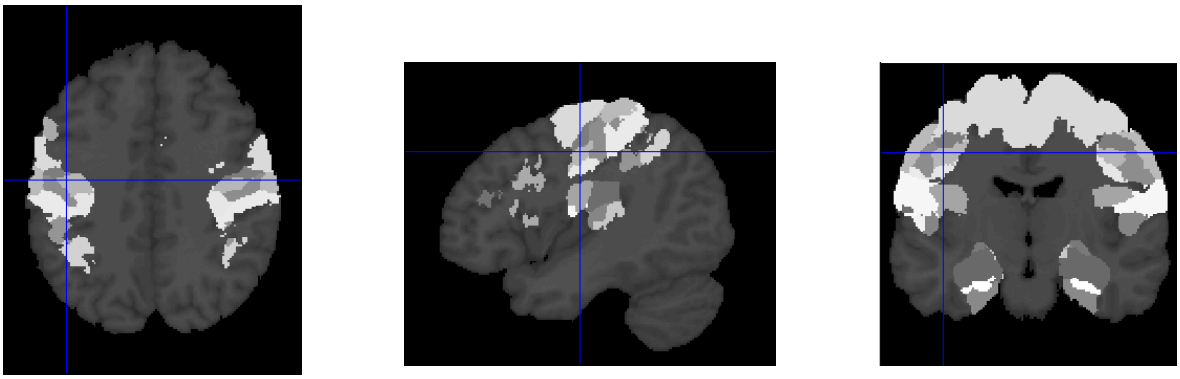

Figure 7: **The maximum probability maps (MPMs, Eickhoff and co-workers [25]).** The images with axial, sagittal and coronal view were taken from the SPM implemented anatomy toolbox. They are normalized to Montreal Neurological Institute (MNI) space. The grey fields show different MPMs for areas for which probabilistic anatomical maps are already available. For example, the crosshair's position (-43/-13/+40) is with a probability of 60% at A4p, with a probability of 40% at A4a and with a probability of 30% at A3b. The MPMs would assign this position and its corresponding voxel to A4p, because it has the highest probability.

5 Material and methods of the meta-analyses

5.1 *Meta-analysis of amygdala-studies using functional imaging*

A coordinate-based meta-analysis of previous fMRI and PET studies reporting amygdala-activation was carried out. Studies included in the meta-analysis had to fulfill the following criteria: (1) they had to use fMRI or PET as neuroimaging method, (2) and to report amygdala-activation (3). In addition they had to investigate healthy adult subjects, (2) and they had to measure whole brain and not only regions of interest. (3) Further, the coordinates had to be given either in Talairach [114] or in MNI (Montreal Neurological Institute) space, and (4) the studies had to investigate emotional processing. (6) Only coordinates reflecting activation (not deactivation) data were included in the analysis. A total of 120 articles reporting 288 amygdala-coordinates were identified through the literature search in Medline (see table IV in the supplement). [115–164] [27,165–213] [214–230] [138,219,231].

The principle aim of this amygdala meta-analysis was to determine brain area(s) that are consistently co-activated with the amygdala. To realize this analysis only published amygdala-coordinates which were probabilistically defined located in the amygdala entered the (co-) activation likelihood estimation (ALE) [19]. For this step the maximum probability maps has been applied [24,25].

5.2 *Meta-analysis of insula-investigations using functional imaging*

The meta-analysis of insula-studies included investigations exploring sensorimotor functions, language and the processing of music and vocalization, and studies examining peripheral autonomic change. Studies included in the meta-analysis had to fulfill the following criteria: (1) they had to use fMRI or PET as neuroimaging method, (2) they had to investigate healthy adult subjects, (2) and the coordinates had to be given either in Talairach [114] or in MNI (Montreal Neurological Institute) space.

The following 50 studies meeting these criteria were surveyed:

1. 20 studies investigating **language or auditory processing** were analysed:
    a.) 10 language studies, 5 studies reporting speech perception-induced [232–237], and 5 studies demonstrating speech production-induced [238–242] insula activity were included. In total, 26 stereotaxic coordinates (16 on the left, 8 on the right hemisphere) were analysed.
    b.) 2 study investigating the perception of vocalization (mothers and parents listening to infant crying) with 8 stereotaxic coordinates (3 on the left, 5 on the right hemisphere) were analyzed [33,67].
    c.) 8 studies exploring music perception and reporting insula activity were analyzed [35,68,243–247]. 11 stereotaxic coordinates (6 on the left, 5 on the right hemisphere) were analysed.
2. 20 studies investigating **hand or leg movement** [248–267], in total, 49 stereotaxic coordinates (27 on the left, 22 on the right hemisphere) were analyzed.
3. 10 studies reporting **peripheral autonomic change** and activity in the insula were analysed. 4 Studies investigating cardiovascular activity [14,268–270] 4 studies simultaneously measuring sympathetic skin responses [12,13,37,39] one study exploring pupil responses [82], and one study investigating the administration of drug evoking peripheral arousal [83] were included in the meta-analysis. In total, 21 stereotaxic coordinates (7 on the left, 14 on the right hemisphere) were analyzed.

In total, 112 stereotaxic coordinates taken from 50 fMRI or PET studies were analyzed. Talairach coordinates were translated to match the MNI space. The reported foci were treated as localization probability distributions centered at the given Y and Z peak coordinates [21]. The probability distribution was modeled by two dimensional Gaussian functions with 8 mm full with at half maximum (FWHM) both in the Y and Z direction. Since the included functional imaging data was preprocessed by spatial filtering using Gaussian kernels, this use of Gaussian functions yields an approximation of the volumes underlying the published peak data. The FWHM of 8 mm used for this analysis is within the range of the smoothing filters used in the

original studies included in the meta-analysis (from 4 mm to 20 mm). Subsequently an 'activation likelihood estimate' (ALE) [21], given by the union of the probabilities associated with the different foci, was calculated for an area comprising the whole Y and Z extent of the insular cortex. The later was determined by manual segmentation from the T1-multi-subject template provided with SPM5. If the size of the smoothing kernel was missing in the publication the most representative value of the group was taken.

6 Results

6.1 *Behavioural results*

Mean values (+/-standard error of the mean) for valence ratings of consonant-slow (CS) consonant-fast (CF), dissonant-slow (DS), and dissonant-fast (DF) stimuli were -1.05 (+/-0.12), -0.92 (+/-0.12), 0.87 (+/-0.12), and 1.06 (+/-0.12). The corresponding results for arousal ratings were -0.86 (+/-0.12), 0.01 (+/-0.13), -0.27 (+/-0.12), and 1.04 (+/-0.12). A two-way repeated measurements ANOVA of the effects of harmony and tempo on valence and arousal ratings showed a significant main effect of harmony on valence ratings and of both harmony and tempo on arousal ratings ($p<0.0001$). The results are shown in figure 8.

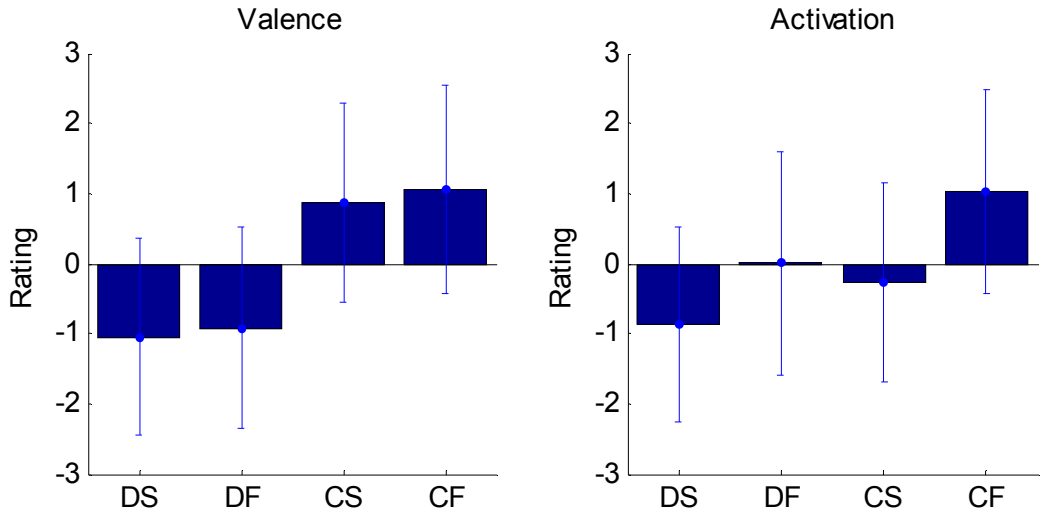

Figure 8: The bars show **subjects valence and arousal ratings** of the consonant-slow (CS) consonant-fast (CF), dissonant-slow (DS), and dissonant-fast (DF) piano melodies (mean with the standard deviation). The two bipolar dimensions valence (ranging from -3 = very unpleasant, to 3 = very pleasant) and arousal (ranging from -3 = very calming to 3 = very arousing) were given during the fMRI experiment always after the stimuli presentation.

After scanning, subjects were asked to rate globally the familiarity (ranging from 0 = not familiar; to 3 = familiar) of the pleasant and unpleasant stimuli. Familiarity ratings for the pleasant and unpleasant melodies were identical in all cases. The mean familiarity ratings both were 0.72 (SD = 0.87), indicating that musical pieces were on average only slightly familiar to the subjects. Normal distribution of the questionnaire data were tested with the Kolmogorov-Smirnov test (KS-test). All questionnaire scores were Gaussian distributed. Total scores for the AIM ranged from 1 to 68, with a mean of 32.43 and a standard deviation of 18.94. Women tended to have higher scores than man (M = 36.71, SD = 16.32 vs. M = 25.80 SD = 18.36), but the difference did not reach significance, P > 0.303. STAI state scores ranged from 29.00 to 61.00, with a mean of 41.07 and a standard deviation of 8.58. Music education (cumulated in years) ranged from 0.5 to 17 years, with a mean of 8.6 years and a standard deviation of 5.22 years. There were no significant correlations between musical education, AIM-scores, and STAI (state version) scores ($p > 0.05$). The results are summarized in table 2:

Questionnaires/Ratings	**Mean , range or standard deviation (SD) of the 18 Subjects**
Edinburgh Handedness Inventory [92]	Mean = 84.11 %, Range = 75 - 100 %
STAI-S (State-Trait Anxiety Inventory, State) [99]	Mean = 39.06 Range = 29 - 61
AIM (Affect Intensity Measurement) [84,89]	Mean = 30.44 Range = 2 - 68
Music Education [100] (cumulated in years)	Mean = 8 years (SD = 4.80)
Ratings for enjoying listening to classical music (ranging from 0 = not at all, to 4 = frequently)	Mean = 2.28 (SD = 1.27)
Familiarity ratings for the pleasant melodies (ranging from 0 = not familiar; to 3 = familiar)	Mean = 0.72 (SD = 0.87)
Familiarity ratings for the unpleasant melodies (ranging from 0 = not familiar; to 3 = familiar)	Mean = 0.72 (SD = 0.87)

6.2 *Brain areas activated during the exposure of piano music*

Figures 9 and 10 show the brain areas activated in 18 right-handed subjects with no professional musical education during the exposure to piano excerpts. Significant activation of clusters at the $p < 0.05$ (FDR corrected) level for music perception minus rest contrast was demonstrated in the right and left auditory cortex, in the right and left inferior frontal cortex (including Broca`s area), in the supplementary motor area (SMA), and in the left and right cerebellum. The cerebral activation showed greater spatial extent to the left side. Activation was also shown in the left and right amygdala. The amygdala activation has been analysed more detailed (see chapter 6.3). The activated brain areas are summarized in table 3.

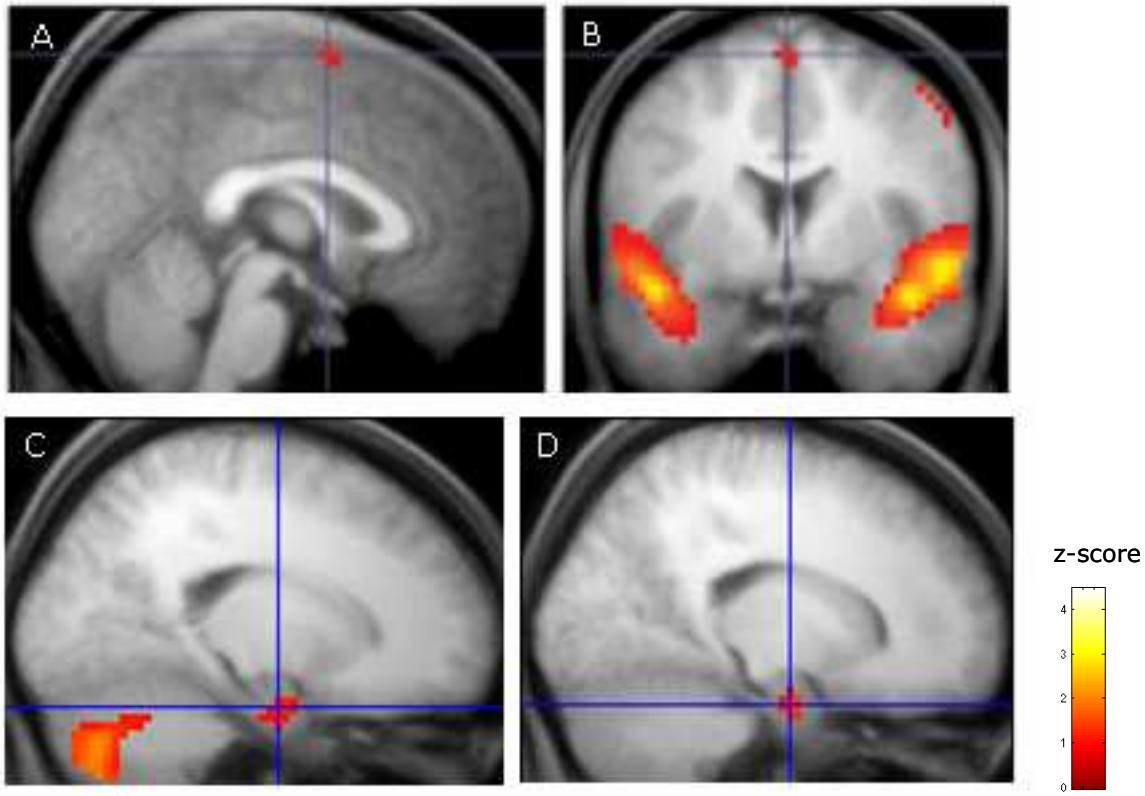

Figure 9: **Brain activation during the perception of piano music**. Subjects demonstrates activity in the supplementary motor area (SMA, 0/0/69). Further, participants demonstrate activity in the left and right amygdala (-18/-6/-18 and 18/-6/-21). The results are superimposed on the sagittal (a, c, d) and coronal (b) section of the mean structural scan of the 18 subjects investigated in the fMRI experiment ($p < 0.05$, FDR corrected).

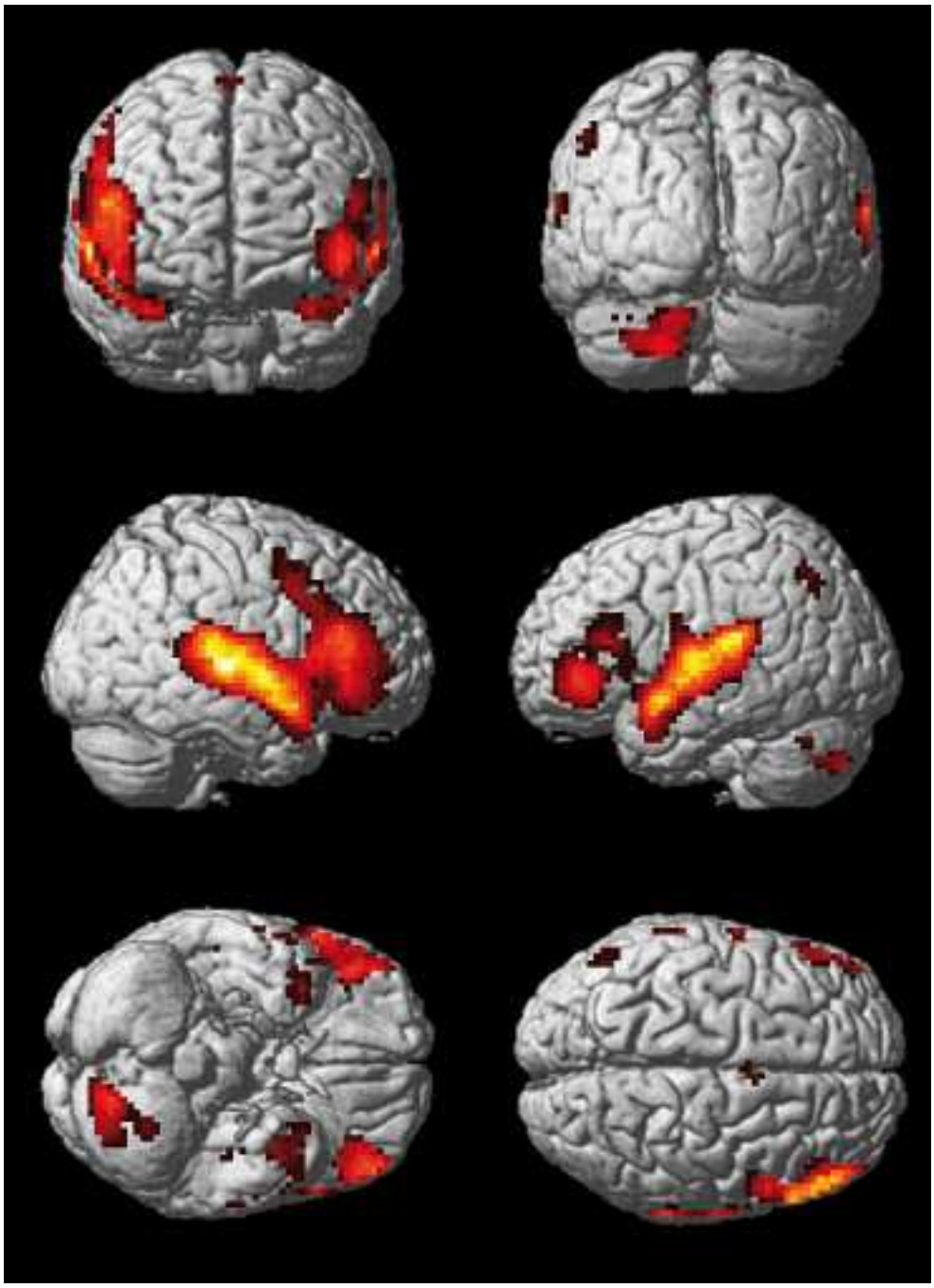

Figure 10: **Brain areas activated in 18 right-handed individuals during the exposure of piano music.** Areas of activation ($p < 0.05$, FDR corrected) are projected onto a 3-D surface taken from SPM5. Subjects demonstrate activity in the left and right auditory cortex, in the left and right inferior frontal cortex (including Broca`s areas), and in the left and right cerebellum (more pronounced on the left side).

MNI-Coordinates (x/y/z)			Z-Score	Brain region	Probability	Assigned to
54	-24	3	6.86	Right Superior Temporal gyrus	TE 1.1: 10 %	-
57	-9	0	6.50	Right Middle Temporal Gyrus	TE 1.2: 50 %	TE 1.2
48	-18	6	6.50	Right Heschls Gyrus	TE 1.0: 90 %	TE 1.0
-39	-30	15	6.03	Left Rolandic Operculum	TE 1.1: 70 %	TE 1.1
-48	3	-12	5.94	Left Superior Temporal Gyrus	TE 1.2: 20 %	-
-54	-27	15	3.73	Left Superior Temporal Gyrus	No map available	No map available
-39	-21	0	5.91	Left Superior Temporal Gyrus	TE 1.1: 10 %	-
-27	-60	-27	4.03	Left Cerebelum	No map available	No map available
42	-72	-42	3.52	Right Cerebelum	No map available	No map available
57	18	6	4.28	Broca	Area 44: 60 %	Area 44
57	27	0	4.15	Broca	Area 45: 60 %	Area 45
-54	33	18	3.72	Broca	Area 45: 80 %	Area 45
0	0	69	4.49	SMA	Area 6: 60 %	Area 6
18	-6	-21	3.06	Amygdala	Amygdala: 70 %	Amygdala
-18	-6	-18	3.50	Amygdala	Amygdala: 100 %	Amygdala

Table 3**:** BOLD signal change for the contrast **listening to piano music > baseline**, peak MNI-coordinates and z-scores are given. The corresponding brain region and the probability and assignment to a probabilistic-anatomical map is displayed as calculated with the SPM Anatomy Toolbox [25]. The table shows peaks activated at the following statistical threshold: $p < 0.05$ (FDR corrected), cluster-size > 10. Area 6 = premotor cortex, TE = primary auditory cortex, and area 44/45 = Broca`s area.

6.2.1 Functional MRI results

Both right and left amygdala showed significant auditory-stimulation-related BOLD effects ($p<0.05$, corrected for multiple comparisons, see table 4 and figure 13, 14). Positive signal changes were predominantly found in LB, negative signal changes were predominantely observed in SF and CM. There were no significant voxelwise differences between consonant and dissonant musical stimuli. The lateralization pattern in LB, SF and CM was investigated by calculating a lateralization index (LI) as a function of the BOLD percentage signal change (PSC, see figure 15). LB and SF showed a similar lateralization pattern with voxels with both the positive- and negative-most PSCs lateralized to the left amygdala. In contrast, CM showed a lateralization pattern with negative PSC predominating in the left and positive PSC in the right amygdala.

To determine whether there were significant differences in mean PSC between the amygdala subregions, a region of interest (ROI) analysis was performed. The ROI was defined as the area with 90% or 100% probability to belong to LB, SF, and CM. The mean PSC for each right and left subregion for each individual subject was determined. Based on this ROI data, differential responses in right and left amygdala subregions were tested. For the mean responses across all four music conditions, left LB showed significant higher PSC than left SF and left CM ($p<0.005$). Separate analysis of consonant/dissonant stimulus class revealed that the same difference between left LB and SF as well as left LB and CM was found for the consonant and for the dissonant stimuli (the results are illustrated in figure 16).

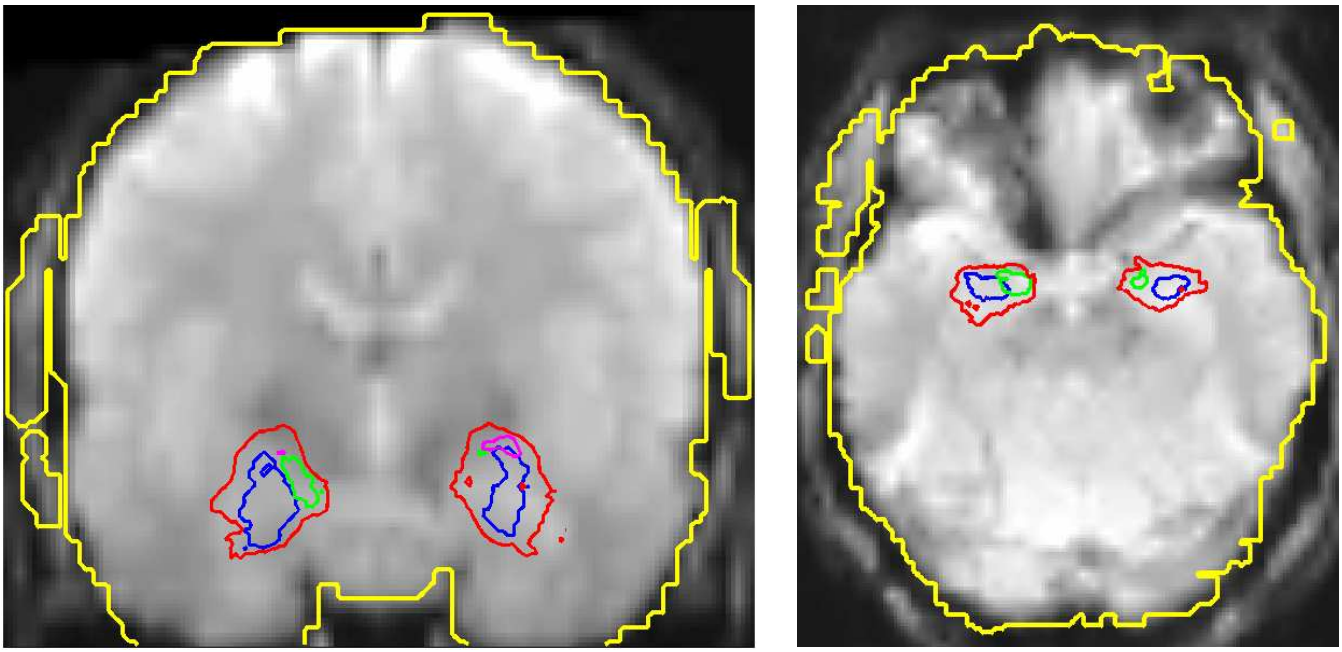

Figure 11: **EPI data quality.** A representative example of raw EPI (echoplanar imaging) data normalized to MNI space is shown in a coronar (MNI y = -7 mm) and axial (MNI z = -20 mm) section. The axial section corresponds approximately to the sections shown in [271]. The example represents the average across all EPI volumes acquired during the experimental session of one subject. The outline of the amygdala is shown (red line), enclosing the area with at least 50% probability of belonging to the amygdala (according to the probabilistic maps from Amunts and co-workers [24]). The extent of the laterobasal (LB) group of the amygdala (LB, >=80% probability) is shown in blue, the superficial group (SF) in green, and the centromedial group (CM) in magenta. In addition, the outline of the segmentation mask enclosing the area with sufficient signal for application of point spread function (PSF) based EPI distortion correction (see reference [106] for further details) is shown in yellow. In all subjects, the whole analyzed extent of the amygdala was within the segmentation mask and therefore distortion correction was possible in this region. Good EPI signal quality in the amygdala region was achieved in all subjects investigated.

		Volume of Left Amygdala Responses (mm^3)		Volume of Right Amygdala Responses (mm^3)	
		Positive	**Negative**	**Positive**	**Negative**
Subregion	LB	60	23	13	-
	SF	25	60	2	-
	CM	-	57	-	-

Table 4: **Significant music-related signal changes in LB, SF, and CM.** Volumes with significant effects (in mm^3) for the right and left amygdala presented separately for positive and negative signal changes. Results are given for the mean effect across all four music conditions ('Mean'). LB: laterobasal group, SF: superficial group, CM: centromedial group.

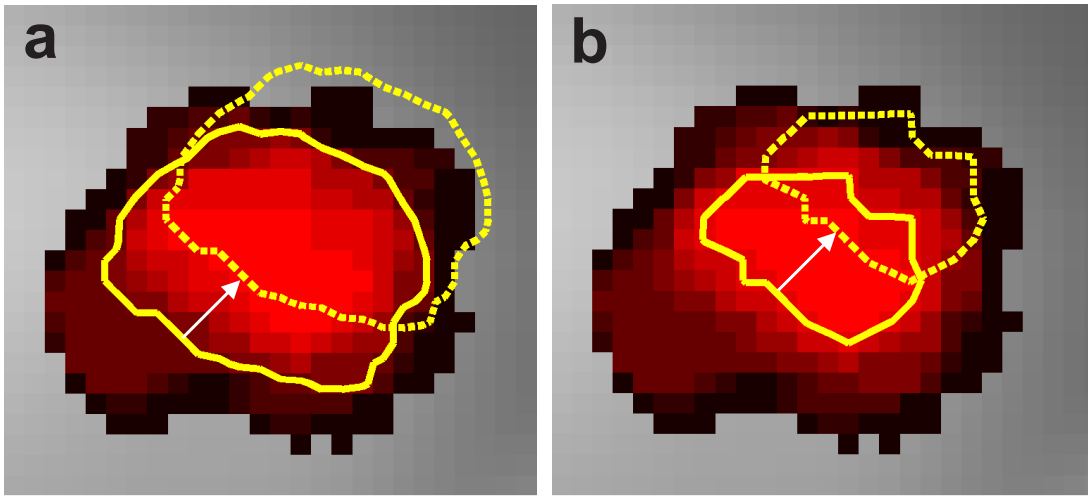

Figure 12: **Simulated effect of probabilistic region of interest (ROI) definition on robustness against localization errors.** In (a) and (b), axial sections through the laterobasal part (LB) of the left amygdala are shown at z = -29 (MNI). Probabilities to belong to LB are color coded with black = 10% and pure red = 100%. In (a), the probabilistic ROI is defined as the area with >= 50% probability to belong to LB (solid yellow line). As a consequence of a simulated localization error which consists of a linear shift of approximately 4 mm (indicated by the white arrow) the true measured volume is localized as indicated by the dashed yellow line, containing voxels with little or no probability to belong to LB. In contrast, when restricting the ROI to voxels with 90% or 100% LB probability (b) and given an equally large localization error, the true measured volume is still entirely located within the area of LB. In this way, the robustness against localization errors could be increased, counteracting potential localization errors.

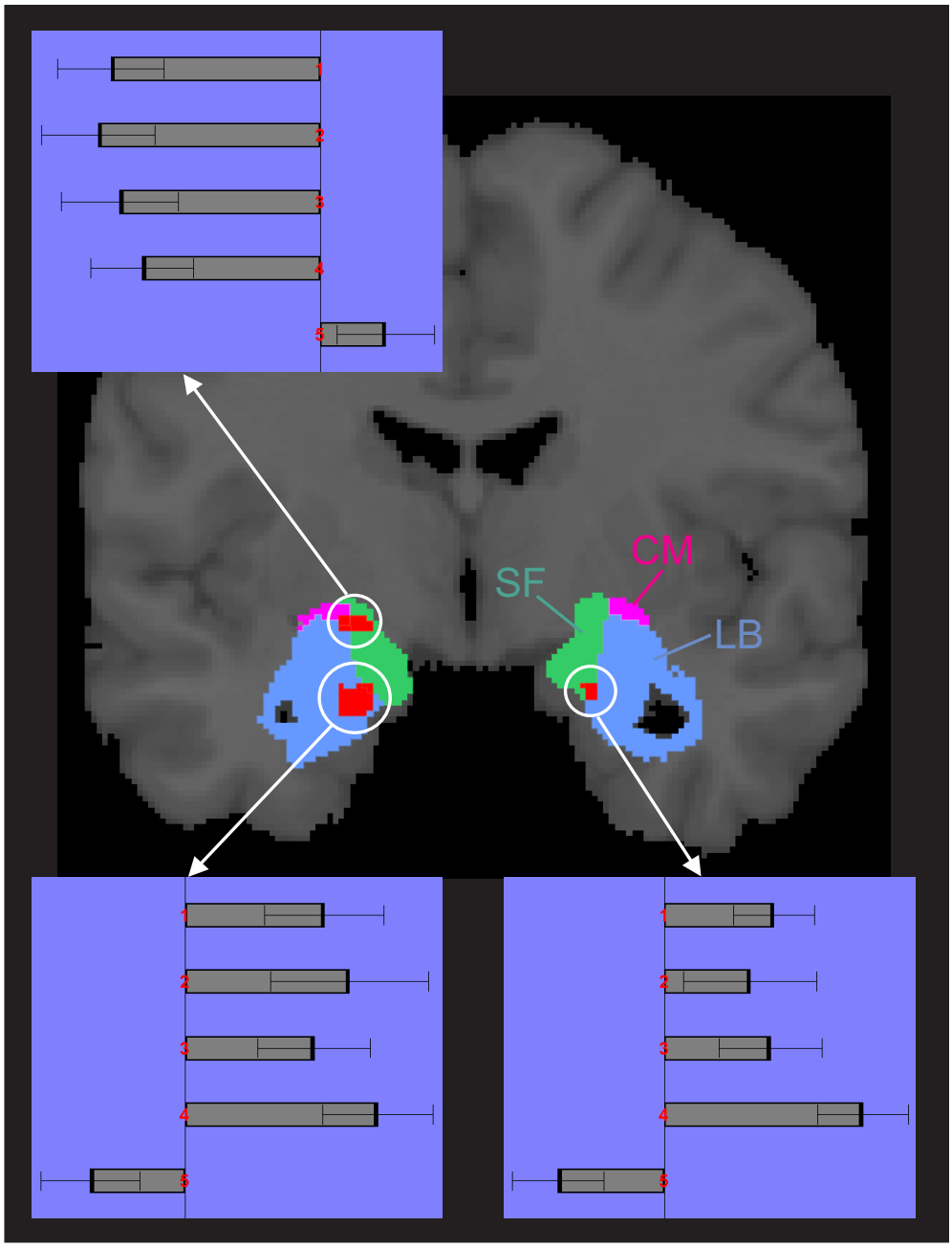

Figure 13: **Auditory stimulation related amygdala responses.** The extent of the amygdala subregions LB (laterobasal group), SF (superficial group), CM (centromedial group) defined by maximum-probability maps (MPMs, [25]) are rendered in blue, green, and magenta, respectively, on a coronal section. Regions with significant ($p<0.05$, corrected for multiple comparisons in the search volume) auditory stimulation related responses are shown in red. The BOLD percentage signal change (PSC) of each of the three activation sites in the four music conditions (1: dissonant slow, 2: consonant slow, 3: dissonant fast, 4: consonant fast) is presented as mean and standard error. The fifth PSC value refers to the time period during which subjects evaluated the emotional effect evoked by the preceding musical piece, compared with rest. In the left amygdala, a cluster with positive responses to all music conditions was mainly located in LB and a cluster with negative responses was mainly found in SF and CM. A smaller cluster with positive responses was also found in the right amygdala approximately in the mirror position to the positively responding left cluster.

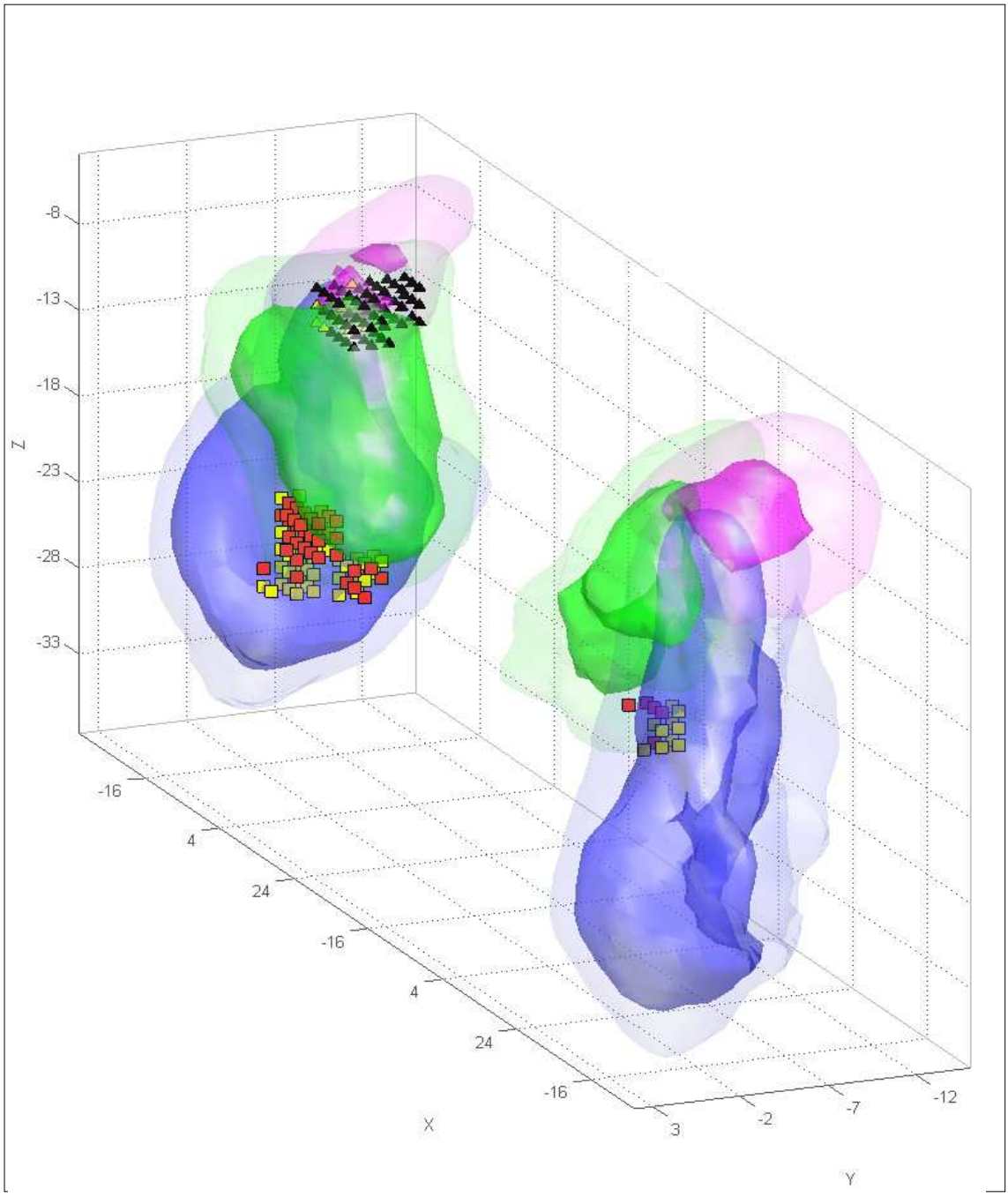

Figure 14: **Human amygdala responses to music in probabilistically defined anatomical regions.** The volumes with at least 50% and 80% probability to belong to the three major amygdala subregions: LB (laterobasal group, blue), SF (superficial group, green), and CM (centromedial group, magenta) are rendered with high (for 50% probability) and low (for 80% probability) transparency. Voxels with a significant increase in BOLD signal to music presentation are displayed as red or yellow squares ($p<0.05$, corrected for multiple comparisons, see material and methods for further details). Voxels with a significant signal decrease are displayed as black or yellow triangles. Anatomical probabilities for red and black responses were 50% to 60%, for yellow responses 70% or above. The majority of significant effects was found in the left amygdala. Positive effects were found in both right and left LB and SF, negative effects were localized in left LB, SF and CM. For visualization, probability maps were smoothed using a spatial filter with a 5 mm isometric Gaussian convolution kernel.

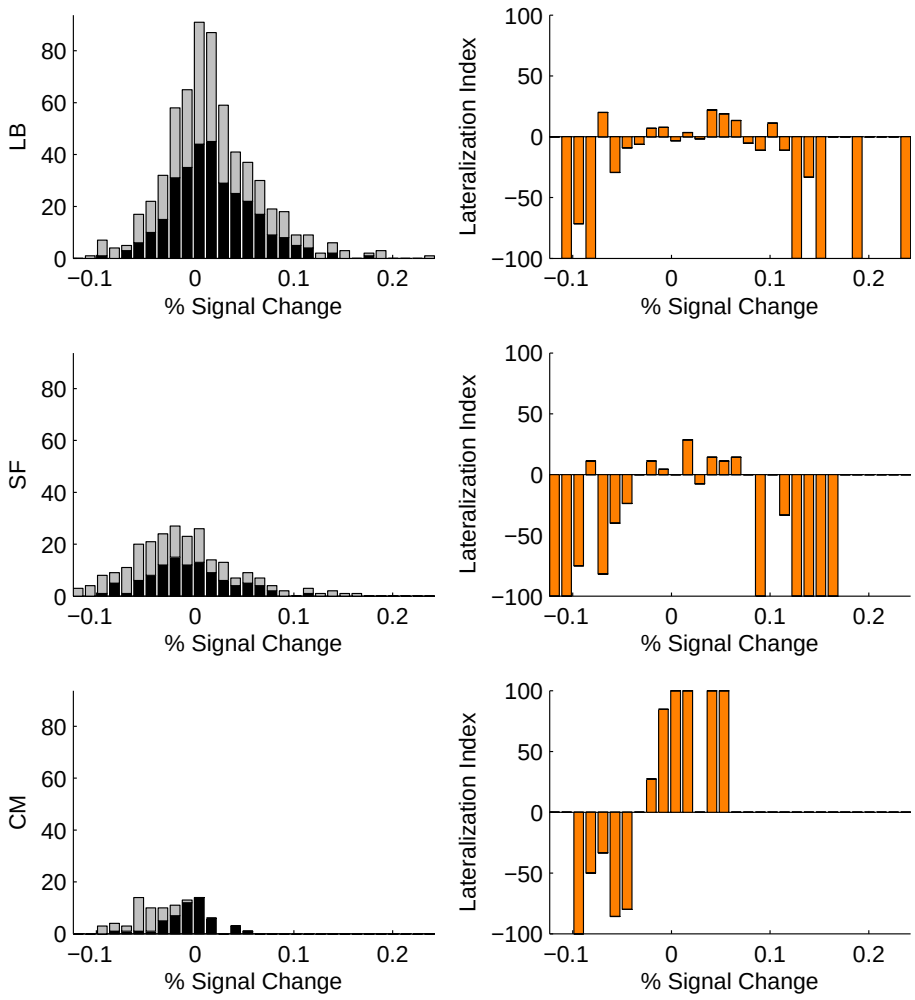

Figure 15: **Lateralization patterns in the major subdivisions of the human amygdala.** Histograms on the left show the distribution of BOLD percentage signal change (PSC) for voxels in: LB (laterobasal group), SF (superficial group), and CM (centromedial group). Values for the right (black) and left (light grey) amygdala are shown in a stacked way. For each PSC bin, a lateralization index (LI) was calculated. LIs of 100, -100, and 0 indicate purely right-sided, purely left-sided, and symmetrically distributed effects, respectively. LB and SF showed a similar lateralization pattern of both extremely positive and negative PSC predominating in the left amygdala. CM showed a different lateralization pattern with negative PSC predominating in the left and positive PSC in the right amygdala.

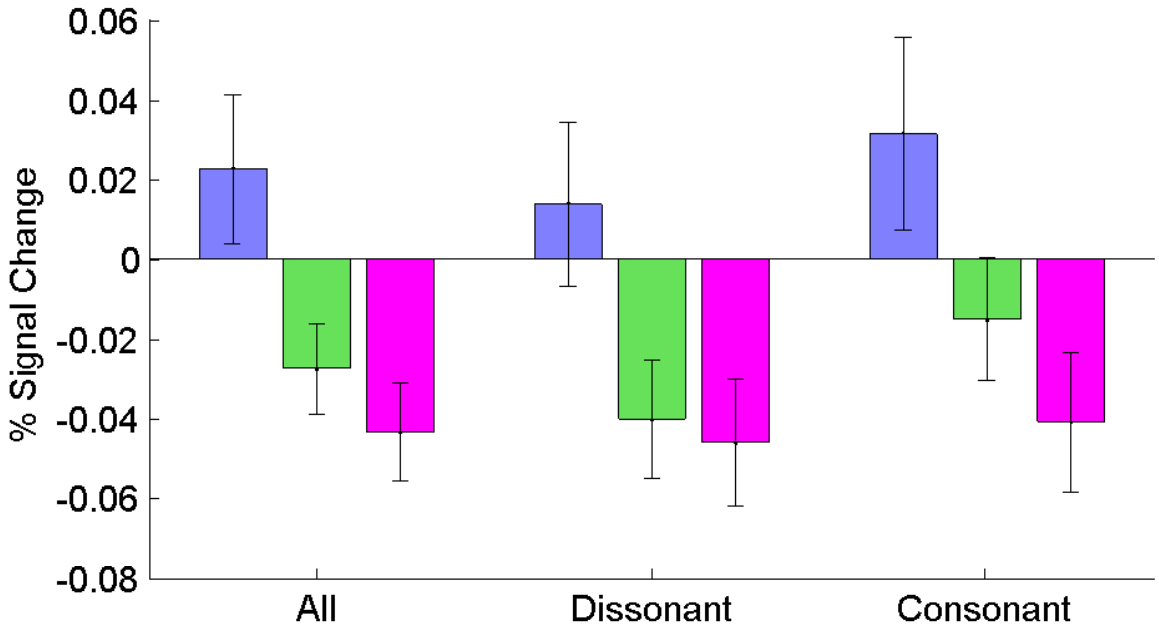

Figure 16: **Response differences between amygdala subregions.** A region of interest (ROI) analysis to statistically evaluate response differences between the core regions (with 90-100% assignment probability) of the three amygdala subregions was performed (see Material and Methods for further details). Bars in the above figure show the result of three averaging steps: first across all voxels of a given area, then either across all four music conditions, the dissonant conditions, or the consonant conditions, and finally across all subjects. Results are given for left LB (laterobasal group, blue), SF (superficial group, green), and CM (centromedial group, magenta). Error bars indicate the standard error of the mean from of the average across subjects. In each case, the differences between left LB and left SF and CM were significant at $p<0.005$. There were no corresponding significant differences in the right amygdala.

6.2.2 Can the amygdala-subregions be distinguished by 3 mm isotropic voxels?

In the fMRI experiment presented in this work as well as many other neuroimaging studies functional images were acquired using a multislice gradient echo planar imaging method (EPI) with a isotropic spatial resolution of 3 mm. A basic methodological issue in neuroimaging studies investigating the human amygdala relates to its small volume and the fact that the amgydala should be distinguished from its neighboring areas. Figure 17 illustrates the size relations between the human amygdala and its subregions and 3 mm isotropic voxels and the amygdala`s neighboring areas are shown on figure 18.

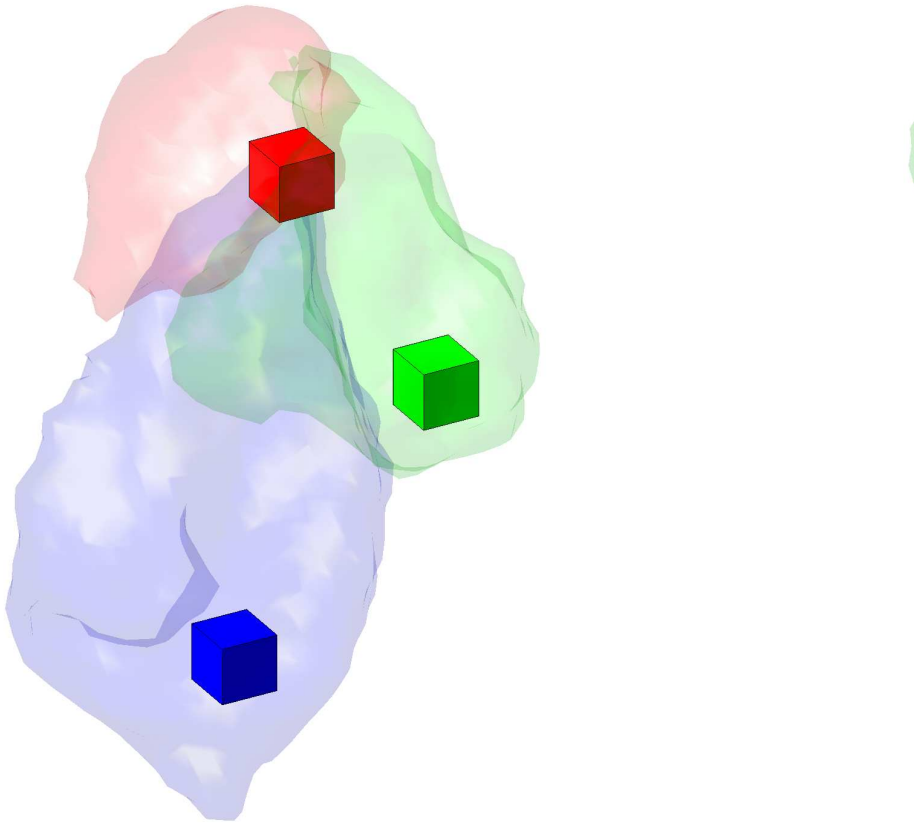

Figure 17: **Size relations** between amygdala-subregions (laterobasal group = blue, superficial group = green, centromedial group = red) and 3 mm isotropic voxels. The approximate size of the human amygdala: x = 27 mm, y = 19 mm, z = 34 mm.

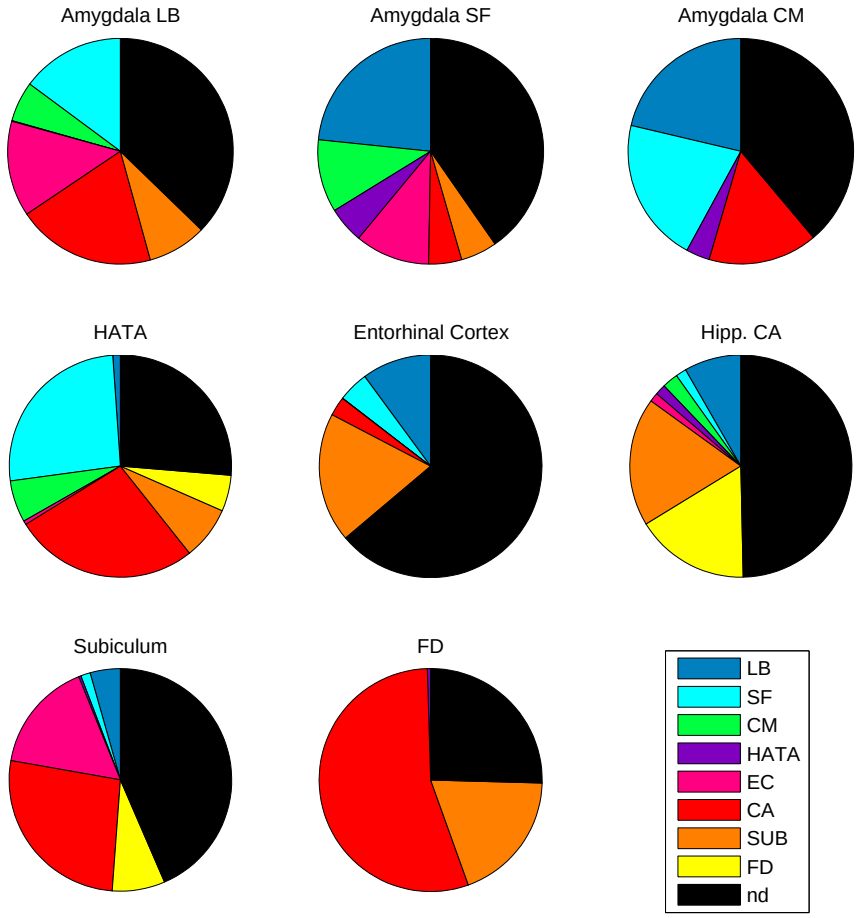

Figure 18: Pie charts representing the **neighboring areas of the amygdala and its subregions** (LB = laterobasal group, SF = superficial group, CM = centromedial group), the hippocampal-amygdaloid transition area (HATA), and the hipocampus-subreagions (EC = entorhinal cortex, CA = cornu ammonis, SUB = subicular complex, FD = fascia dentata) defined by the maximum probabilistic maps (MPMs) [25]. Black space represents brain areas which are not defined yet by MPMs. The charts indicate that, for instance, approximately 15% of the surface of LB is neighbouring SF and approximately 20% of the surface of LB is neighbouring CA (turquoise and red parts of the plot in the upper tight corner, respectively).

In order to examine this question, a simulation analysis based on isotropic voxel sizes ranging from 1- 6 mm was carried out. Figure 19 illustrates the mean probability percentage (see red figures) of voxel-assignments to the amygdala-subregions (LB = laterobasal group, SF = superficial group, CM = centromedial group). The voxels had >= 90 % assignment probability to the probabilistic map of the human amygdala ([24], like in the amygdala-subregion analysis). All voxels were up-sampled to 1 mm isotropic resolution and the mean probability percentage (see red figures) of voxel-assignment to the amygdala-subregions was calculated, because the

probabilistic-anatomical map applied in this analysis had such a spatial resolution. The results show that assignment accuracy was high for LB and for SF (> 87 %), and for CM (> 82 %) for simulated measurement with 3 mm isotropic voxel size. The lesser accuracy for CM might be related to the fact that this subregion has a smaller volume in comparison to LB and SF. These results show that assignments with good anatomical specificity can be made, at 3 mm voxel size, to LB and SF, and with somewhat lesser anatomical specificity also to CM. There was only little dependence of anatomical specificity on voxel size, indicating that the choice of 3 mm voxel size did not result in a markedly reduced anatomical specificity as compared to the anatomical specificity that could have been obtained at higher spatial imaging resolution.

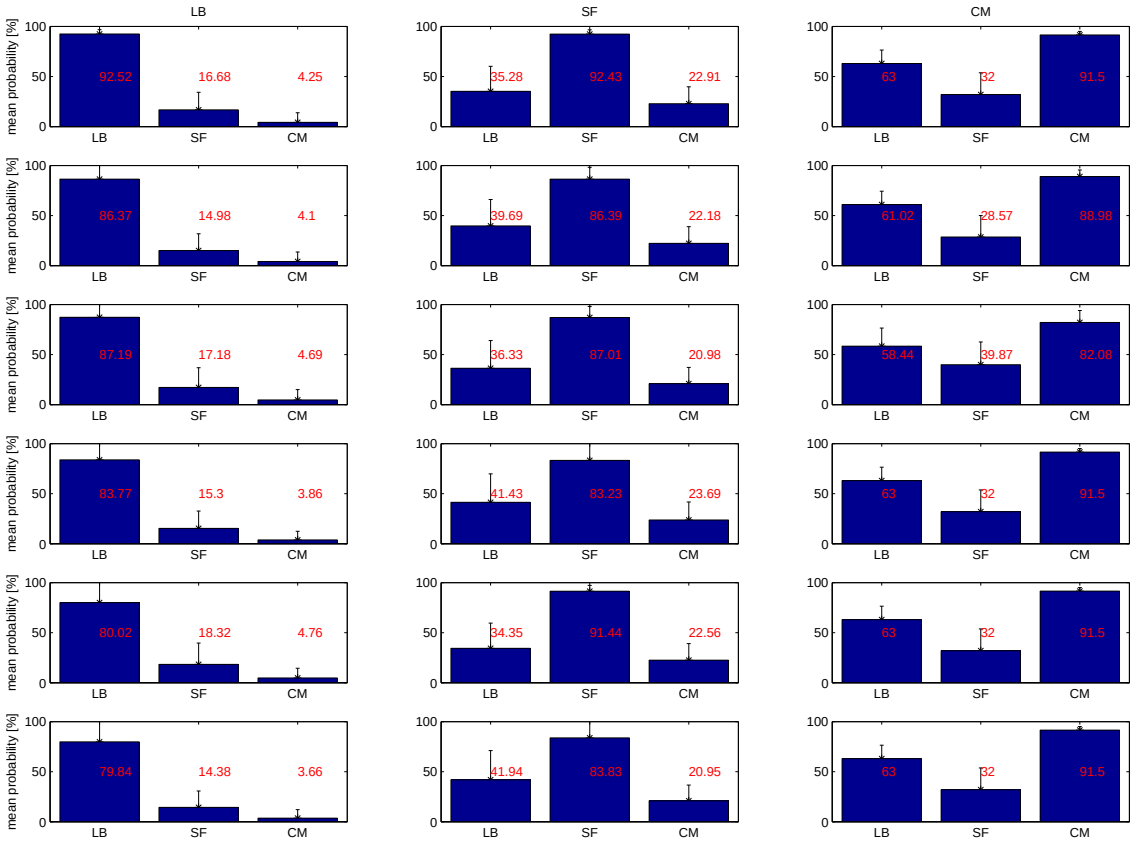

Figure 19 illustrates the **mean probability percentage (see red figures) of voxel-assignment to the amygdala-subregions** (LB = laterobasal group, SF = superficial group, CM = centromedial group). This analysis is simulated for isotropic voxel sizes ranging from 1- 6 mm. The first row (top) of plots refers to 1 mm voxel size, and second row to 2 mm, and so on.

6.3 *Brain areas correlating with affect intensity*

Consistent with the hypothesis the correlation with the individual AIM-scores revealed that subjects with higher scores demonstrated increased activity in the right and left somatosensory cortex and in the right and left supramarginal gyrus. Both activations were more pronounced to the right hemisphere. Moreover, there was also activity in the right insula, and in the left cerebellum. The results are illustrated in table 5 and figure 20 and 21 ($p < 0.005$ uncorrected for multiple comparisons in the a priori regions of interest).

MNI-Coordinates (x/y/z)			Z-Score	Brain region	Probability	Assigned to
- 63	- 27	33	3.04	Left Supramarginal Gyrus	Area 2: 10 %	-
30	- 39	42	3.18	Right Supramarginal Gyrus	Area 2: 50 %	Area 2
-39	- 48	63	3.26	Left Superior Parietal Lobule	Area 2: 20 %	-
-30	- 81	-39	3.10	Left Cerebellum	No map available	No map available
-42	- 75	-36	3.01	Left Cerebellum	No map available	No map available
66	- 21	39	3.20	Right Supramarginal Gyrus	No map available	No map available
60	- 27	21	3.22	Right Supramarginal Gyrus	OP 1: 30 %	-
66	- 24	27	3.06	Right Supramarginal Gyrus	OP 1: 40 %	OP 1
39	12	-15	3.20	Right Insula	No map available	No map available
33	- 42	69	3.20	Right Postcentral Gyrus	Area 1: 80 %	Area 1
42	- 39	66	3.10	Right Postcentral Gyrus	Area 1: 100 %	Area 1

Table 5: BOLD signal change for the **positive correlation with the individual AIM-Scores**, peak MNI-coordinates and z-score are given. The corresponding brain region and the probability and assignment to a probabilistic-anatomical map is displayed as calculated with the SPM Anatomy Toolbox [25]. The table shows peaks activated at the following statistical threshold: $p < 0.005$ (uncorrected), cluster-size > 10 voxel. OP 1 = parietal operculum, Area 1 = primary somatosensory cortex, Area 2 = secondary somatosensory cortex

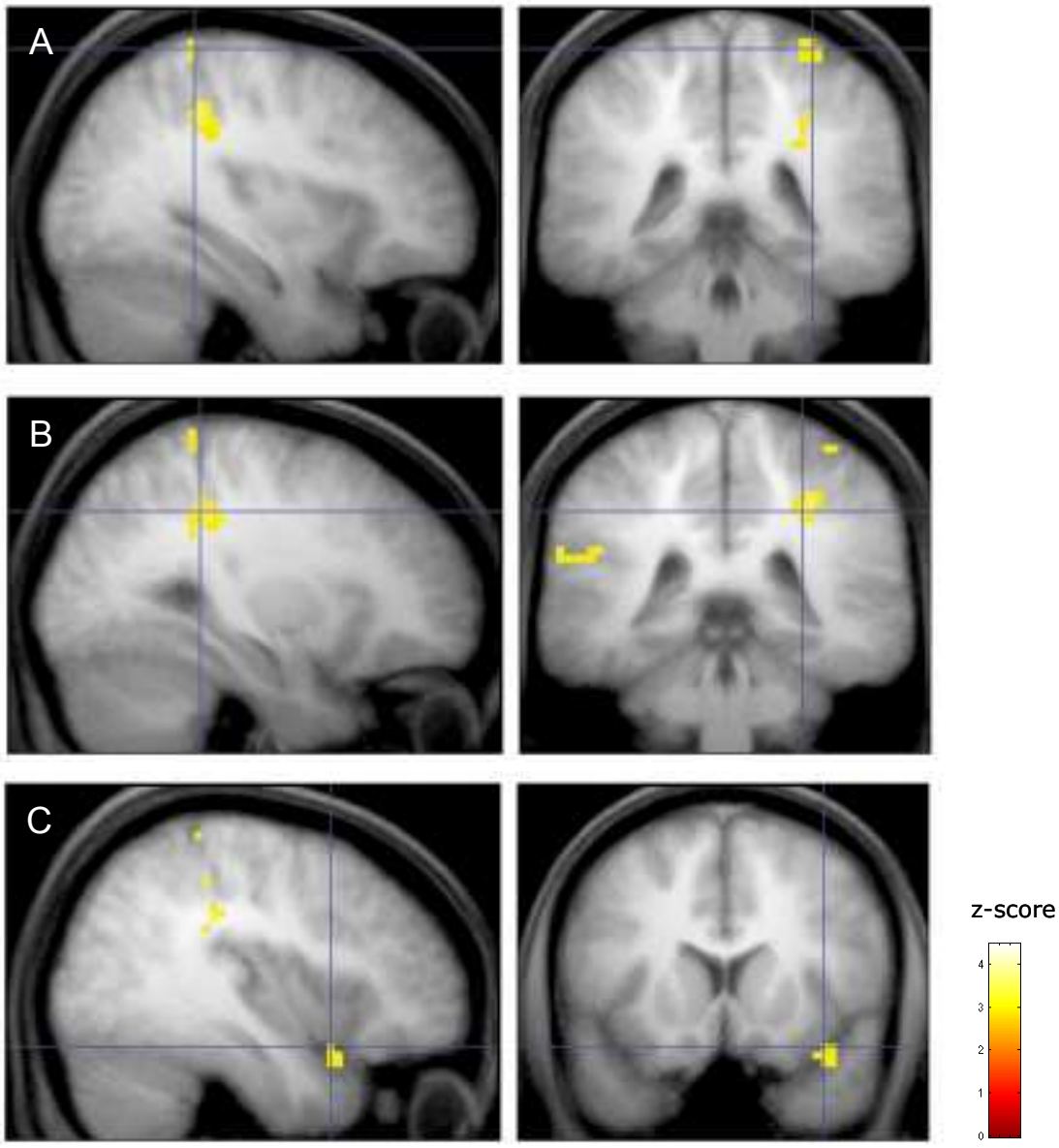

Figure 20: **Brain areas positiv correlating with the affect intensity scores**. Subjects with higher affect intensity scores demonstrate stronger activity a.) in the right somatosensory cortex (33/-42/69), b.) the right supramarginal gyrus (66/-27/21), and c.) in the right insula (39/12/-15). The results are superimposed on the sagittal and coronal section of the mean structural scan of the 18 subjects investigated in the experiment.

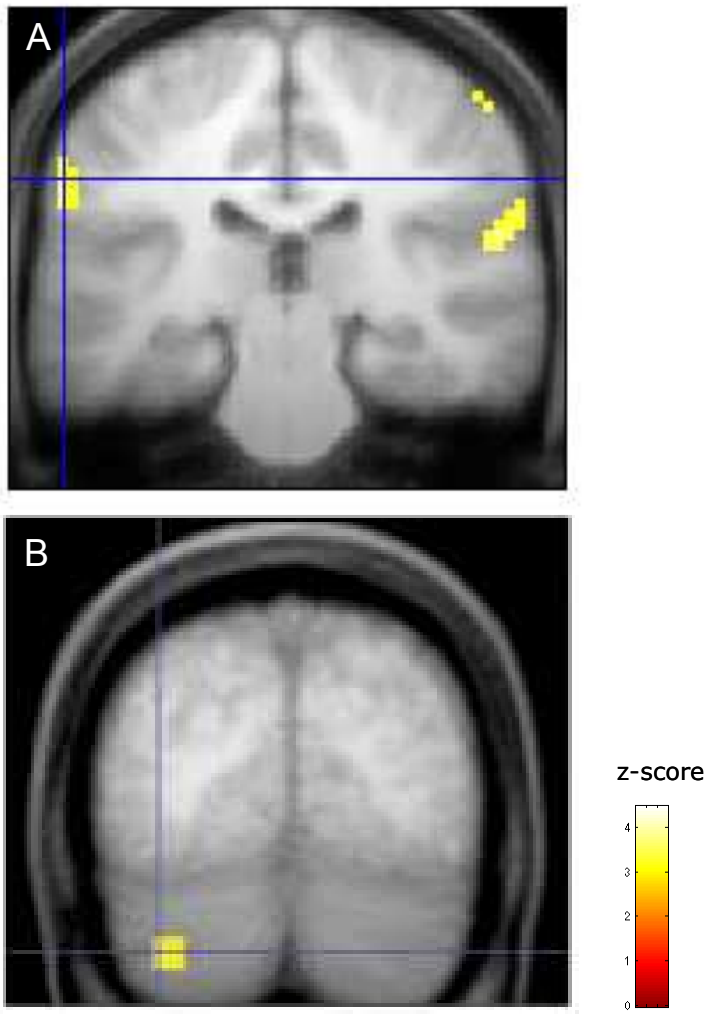

Figure 21: **Brain activation positiv correlating with the affect intensity scores**. Individuals with higher affect intensity scores demonstrate stronger activity a.) in the left cerebellum (-30/-81/-39), b.) and in the left supramarginal gyrus (-63/-27/33). The results are superimposed on the sagittal and coronal section of the mean structural scan of the 18 subjects investigated in the experiment.

6.4 *Functional differentiation within the human insula*

6.4.1 Meta-analysis of insula-studies using functional imaging

A total of 80 articles were identified through the literature search in Medline. After reading the articles, 50 were included according the inclusion criteria outlined in methods. The reasons for exclusion were: a.) in 12 studies the absence insula activation, b.) 8 studies described region of interests analysis and did not report MNI or Talairach coordinates for the insula activation, and c.) in 10 studies the contrasts were not calculated with subjects or healthy controls. 50 articles containing 112 peak coordinates entered into the insula meta-analysis.

Language and auditory processing: A meta-analysis of 20 previous neuroimaging studies investigating language (5 investigating speech perception [232–237], and 5 speech production [238–242], 2 studies exploring perception of vocalization [33,67], and 8 studies investigating music perception [35,68,243–247]) were analyzed. The 45 coordinates demonstrate activation in the anterior insula extending to the fronto-opercular region (figure 22 shows the results). The language studies had 18 stereotaxic coordinates on the left, and 8 on the right hemisphere, whereas the studies investigating different aspects of music perception or the processing of vocalization demonstrate 9 coordinates of the left and 10 on the right hemisphere. Insular cortex activation related to language and activation-peaks related to task sets reported by Dosenbach and co-workers [66] are shown in figure 23.

Sensorimotor processing: 20 studies investigating hand and/or leg sensorimotor-related tasks [248–267] were analysed in the meta-analysis. The 49 coordinates (27 on the left and 22 on the right side) demonstrated repeatedly activation in the mid-anterior insula. The results are shown in figure 24.

Peripheral autonomic change: 10 studies reporting peripheral autonomic change related activity

in the insula were analysed. 2 studies investigated cardiovascular activity [14,15], 2 sympathetic skin responses [12,13], 1 pupil responses [82], and 1 study explored the administration of procaine, a drug evoking peripheral arousal [83]. In total, 22 coordinates (6 on the left and 16 on the right hemisphere) were analysed. The results are shown in figure 25.

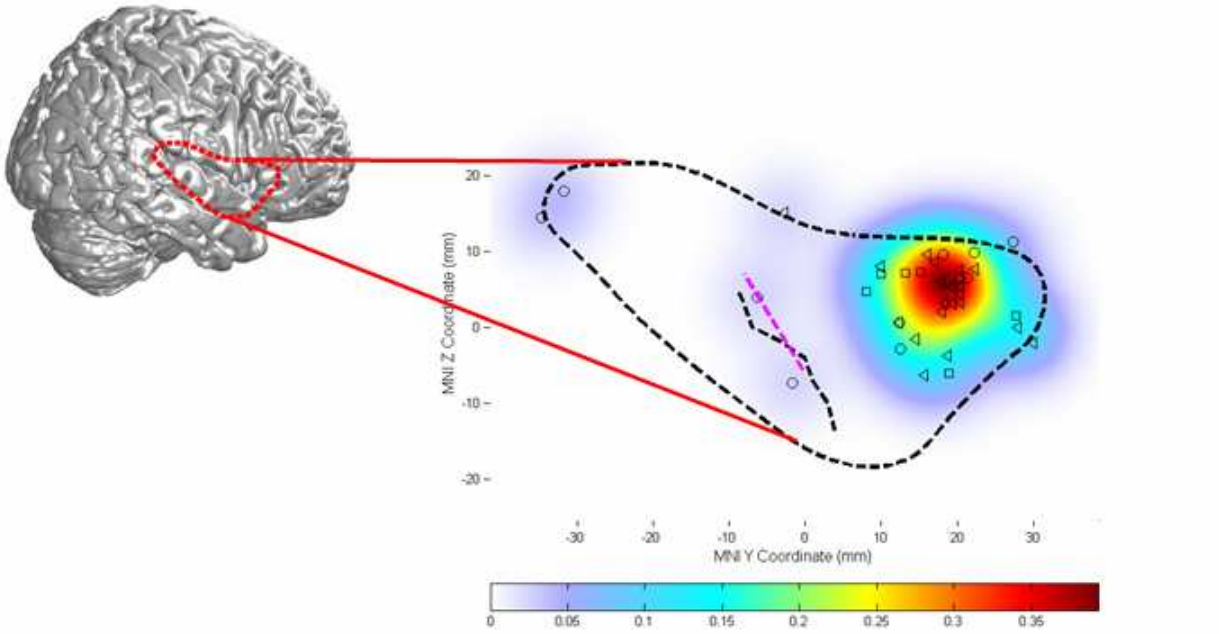

Figure 22: **Insular cortex activation related to language and auditory processing** was determined by a coordinate-based meta-analysis of 20 previous imaging studies. Left, the outline of the left insula is projected on the surface of the Colin-brain template (SPM5). Activation likelihood estimates (ALEs, [21]) are color coded. The highest likelihood for the language and auditory processing related activation is red. The black dashed line indicates the mean outline of the left insula, and the black dashed line inside the insula refers to an individual central insular sulcus which divides the insula in an anterior and posterior part. The Insular cortex is marked according the anatomy visible in the T1 spm-template. The red dashed line refers to the mean central insular sulcus. Peaks of activation from the right and the left sides have been summarized on this representation of the left insula. Each of the 3 symbols indicates different functions: circles = music processing, squares = perception of vocalization, triangles = language.

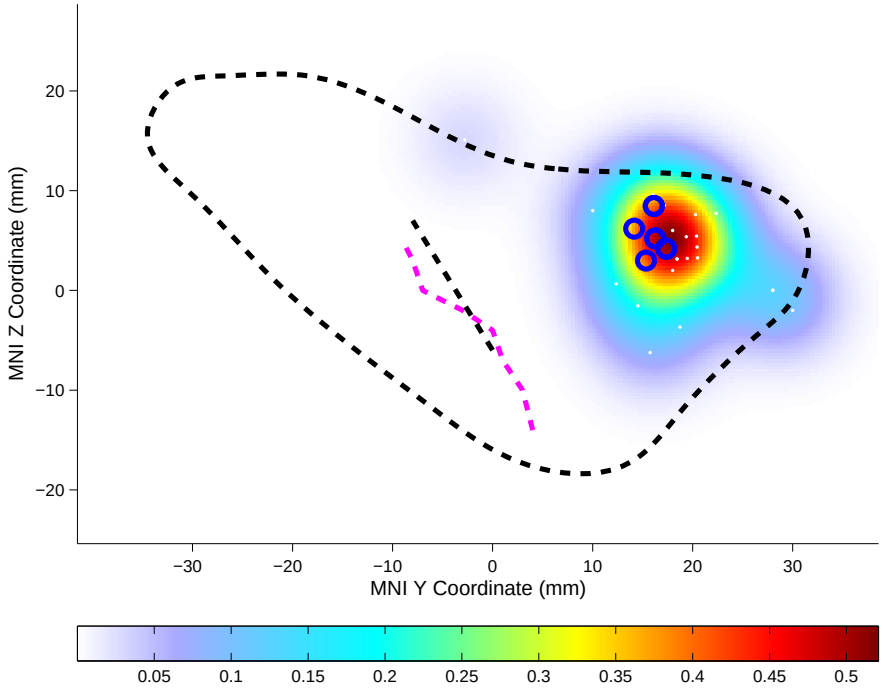

Figure 23: **Insular cortex activation related to language and activation-peaks related to task sets reported by Dosenbach and co-workers [66].** The Blue circles indicate activation-peaks related to task sets [66] and the black dots represent activation-peaks related to language processing taken from figure 22. Conventions like in table 22.

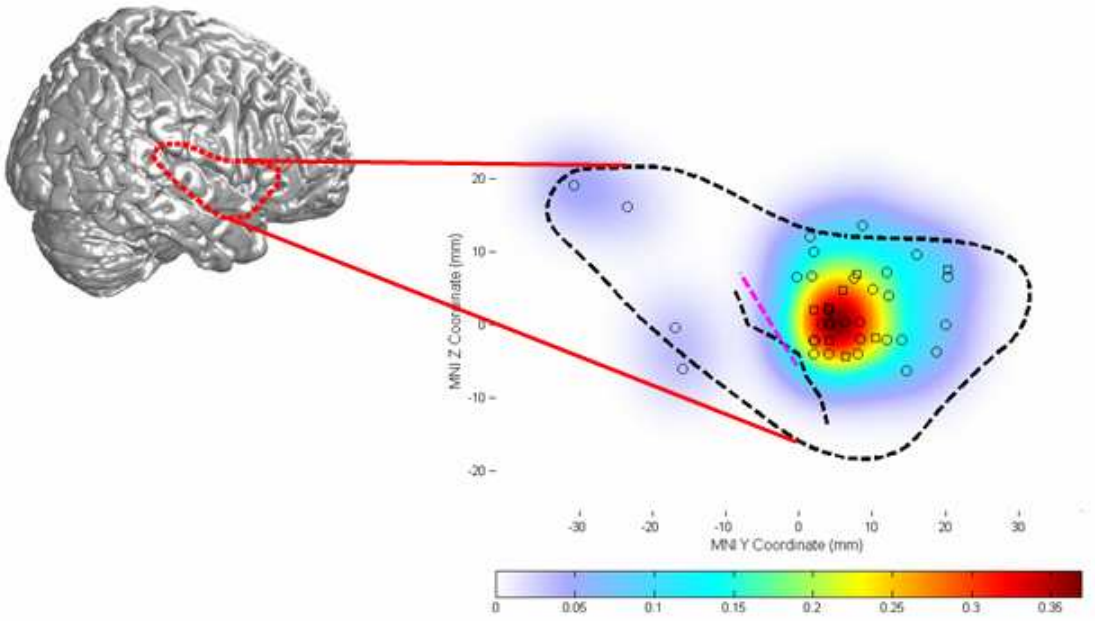

Figure 24: **Insula cortex activation related to sensorimotor tasks** was determined by a meta-analysis or previous neuroimaging studies. Activation likelihood estimates (ALEs, [21]) are color coded. Peaks of activation from the right and the left sides have been summarized on this representation of the left insula. Each of the 3 symbols indicates one function: circles = hand movement, squares = foot movement, triangles = hand and foot movement. Conventions like in figure 22.

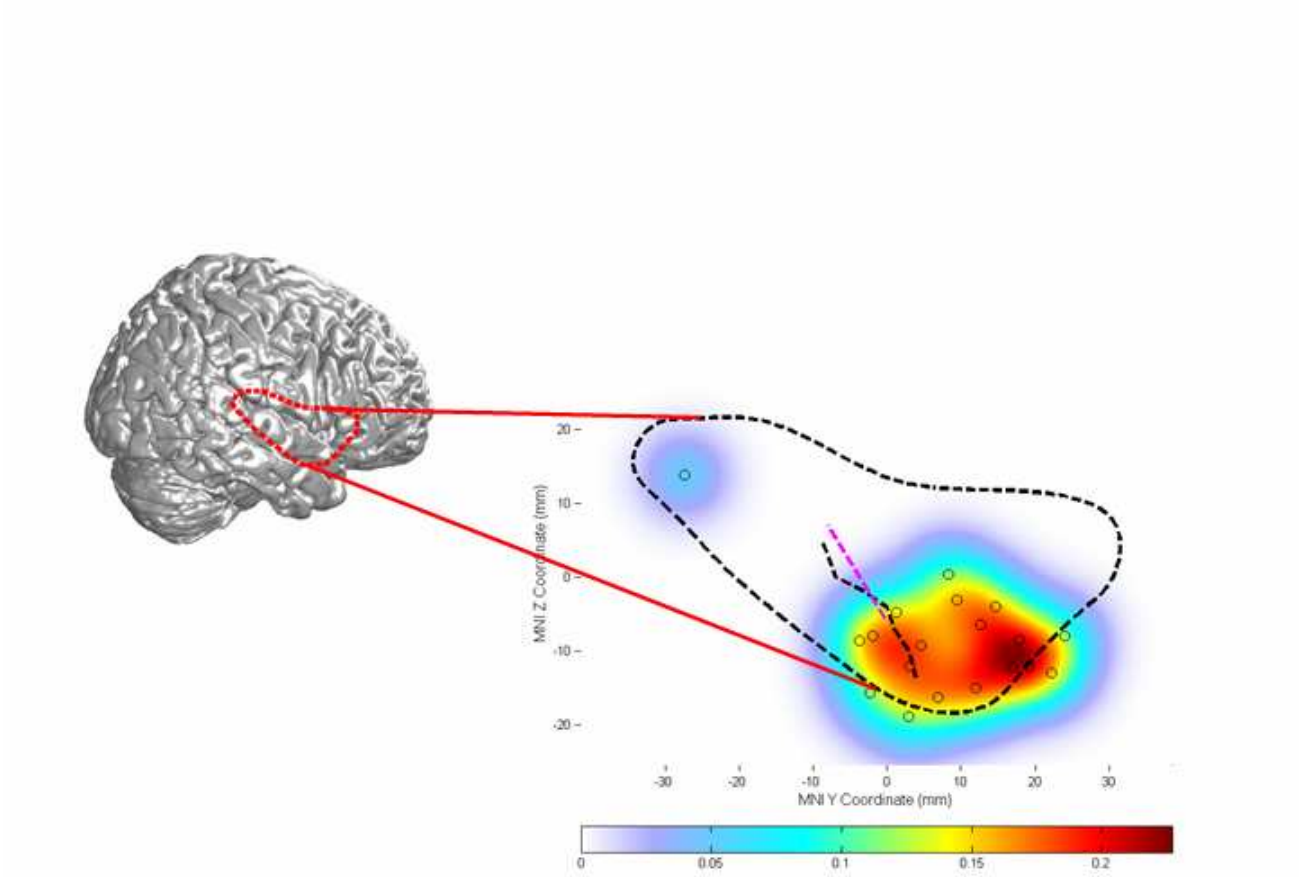

Figure 25: **Anteroventral insula activity presumably related to change in peripheral nervous system** was determined by a meta-analysis or previous neuroimaging studies. Activation likelihood estimates (ALEs, [21]) are color coded. Peaks of activation from the right and the left sides have been summarized on this representation of the left insula. Each of the 4 symbols indicates one function: asterix = cardiovascular change, triangle = skin response, circled = pupil response, squares = procaine. Conventions like in figure 22.

6.4.2 Functional MRI results

Subjects with high affect intensity scores demonstrated stronger activity in the somatosensory cortex and in the supramarginal gyrus (both more pronounced on the right hemisphere). In addition, these subjects also demonstrated stronger activity in the right insular cortex. The insula meta-analysis was used to delineate the exact insula-region. Figure 26 shows that the insula activation-peak (indicated by the square) positive correlating with the affect intensity scores is located in the anteroventral insula region. The insula meta-analysis suggests that activity in the anteroventral insula might be related to change in peripheral nervous system.

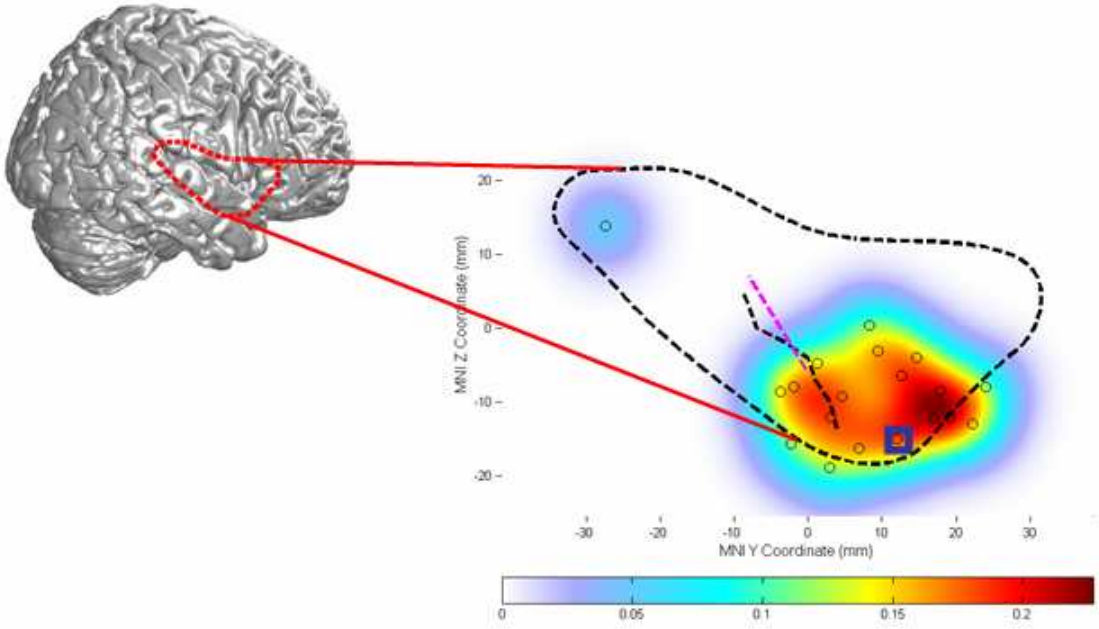

Figure 26: **The insular cortex activation revealed in the positive correlation with the affect intensity scores** was delineated by the coordinate-based meta-analysis of 10 previous imaging studies investigating change in peripheral nervous system. Activation likelihood estimates (ALEs, [21]) are color coded. Black circles = insula activation presumably related to change in peripheral nervous system, square = insula activation positive correlating with affect intensity scores. Conventions like in figure 22.

6.5 *Meta-analysis of amygala-studies using functional imaging*

A coordinate-based meta-analysis of previous fMRI and PET studies investigating emotional processing and reporting amygdala-activation was carried out. A total of 120 articles with 288 amygdala coordinates were included according the inclusion criteria outlined in methods. The principle aim of this amygdala meta-analysis was to determine brain area(s) that are consistently co-activated with the amygdala. To realize this analysis, only published amygdala-coordinates that were probabilistically located in the amygdala entered the (co-)activation likelihood estimation (ALE) [19]. For this step, maximum probability maps (MPMs) [24,25] were used for anatomical assignment. 66.67 % of the peaks were located in the amygdala (in total 192 peaks, 102 in LB, 83 in SF, and 7 in CM). 33.33 % of the peaks were, according to the MPM assignment, located outside of the amygdala, although they were reported as amygdala activation. 12.5 % of the peaks were located in the hippocampus, and 20.8 % were neither in the amygdala nor in the hippocampus. Figure 27 illustrates the peak-distribution in the amygdala and its subregions.

The (co-)activation likelihood estimation (ALE) [19] with the 192 peaks located in the amygdala (66.67 % peaks) revealed a consistent, significant co-activation in the left and in the right insula ($p < 0.05$, permutation-test, FDR corrected). The found co-activation was more pronounced at the right side and extended to the frontal operculum (see figure 28). Figure 29 illustrates the exact position of the insular ALE peak (located in the anteroventral insula) found in the co-activation analysis in relation to the functional map of the insula established in this thesis.

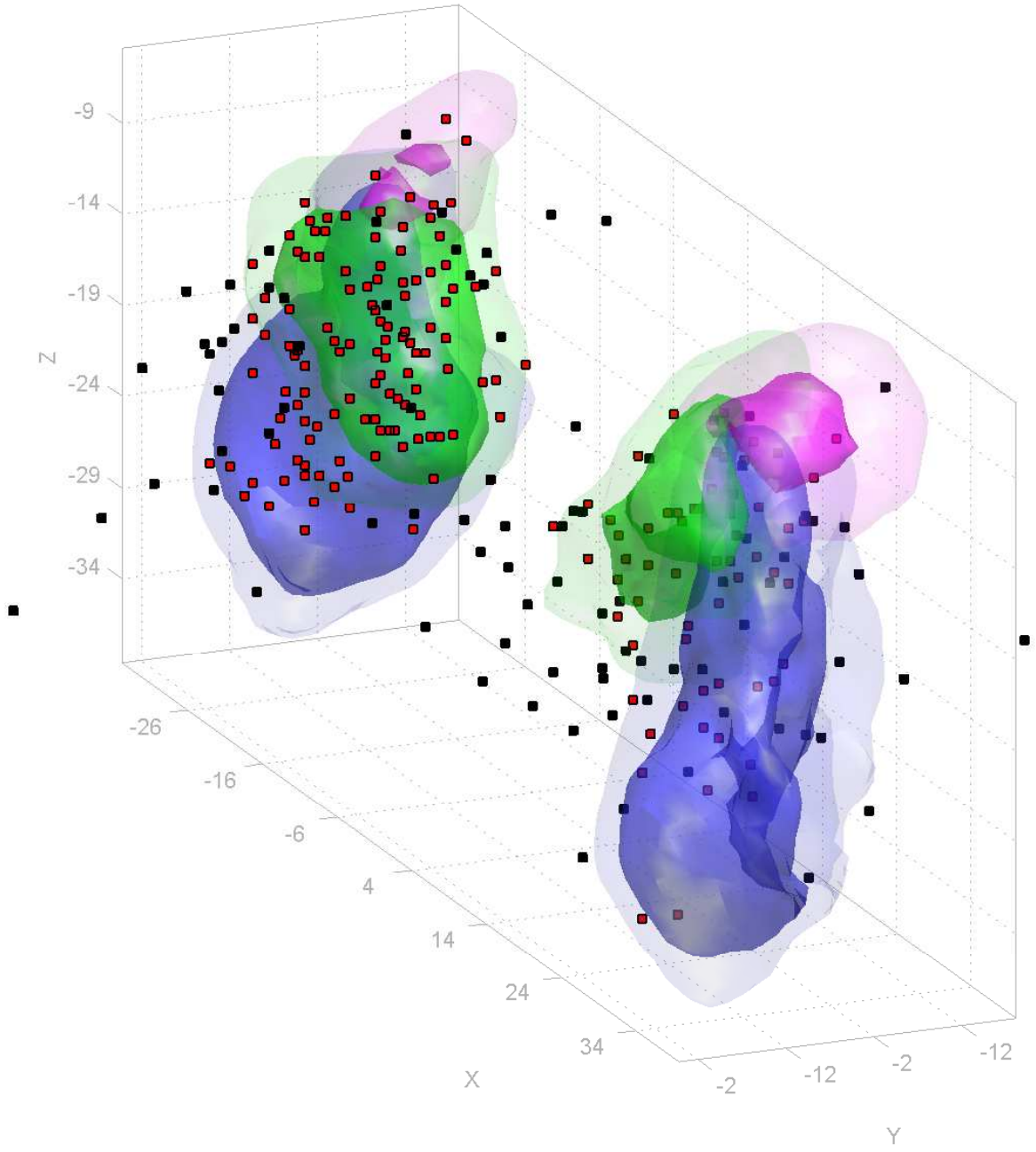

Figure 27 illustrates the **peak-distribution of the amygdala meta-analysis**. According to the maximum probability maps (MPMs) [24,25] 66.67 % of the peaks were located in the amygdala (in total 192 peaks, red dots). 33.33 % of the peaks were not located in the amygdala-region: 12.5 % of the peaks were located in the hippocampus, and 20.8 % were neither in the amygdala nor in the hippocampus.

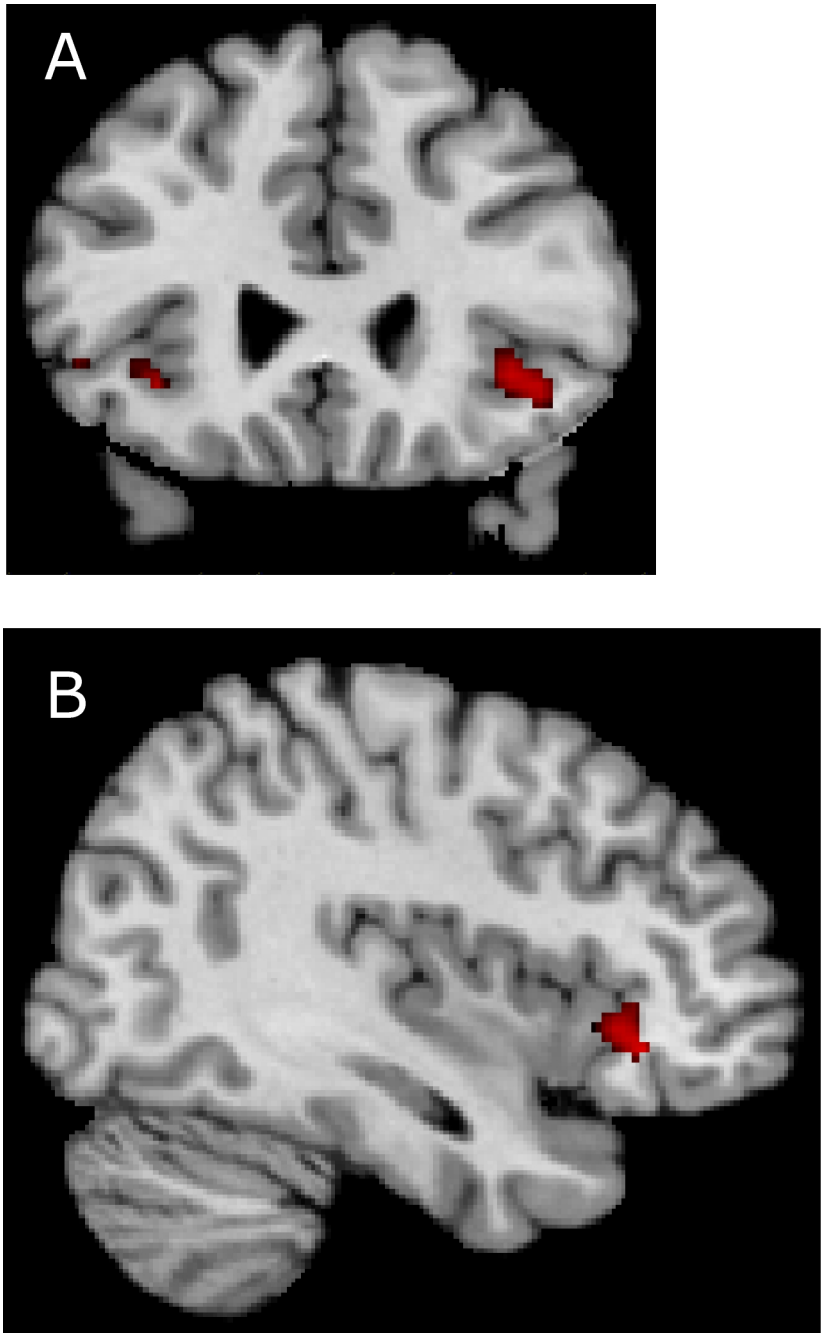

Figure 28: **The amygdala-co-activation analysis revealed significant co-activation in the insular cortex** (more pronounced in the right hemisphere). The co-activation in the insula (x=39/y=25/z=-8) was determined by a meta-analysis of 192 activation peaks which were probabilistically defined being located in the amygdala. The activation peaks were taken from previous imaging studies investigating emotional processing. The results are superimposed on the Colin brain (SPM5) and shown on a.) a coronal (z = -8), and b.) on a sagittal section (x = 39). The results are shown at the flowing statistical treshold: $p < 0.05$, corrected (permutation-test, FDR corrected).

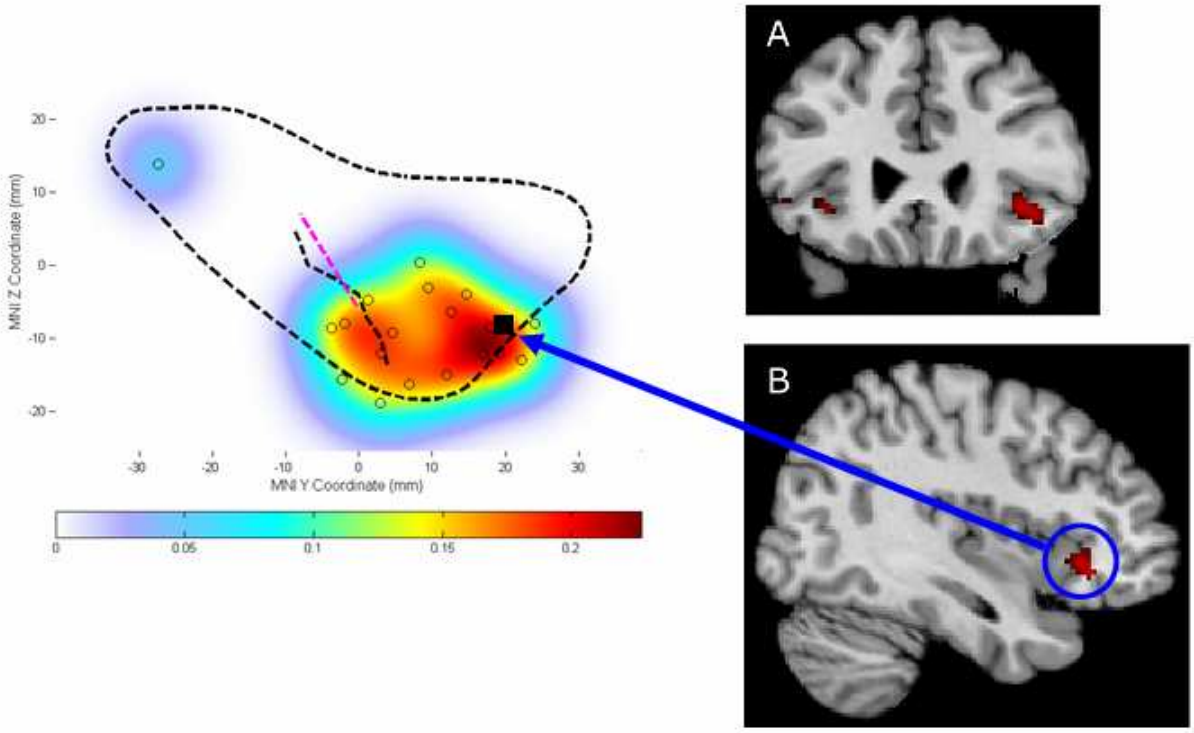

Figure 29: **The insular cortex co-activation revealed in the co-activation likelihood estimation (ALE) of previous neuroimgaing studies reporting amygdala-activation.** The position of the insula co-activation peak **(square)** is shown in relation to the results of the coordinate-based meta-analysis of 10 previous imaging studies investigating change in peripheral nervous system. The outer black dashed line indicates the approximate outline of the left insula (conventions like in figure 22). Black dots = insula activation presumably related to change in peripheral nervous system.

7 Discussion

7.1 *Brain network activated during listening to piano music*

In this study a brain network including the auditory cortices, the left and right inferior frontal cortex including Broca`s area, the cerebellum, the supplementary motor area (SMA), and the left and right amygdala has been identified in individuals without professional music education during the exposure to piano music.

In the present investigation music has been used as stimuli. Several previous functional imaging studies have examined the neural circuitry underlying emotional processing of music in a variety of functional contrasts. Using positron emission tomography (PET) Blood and colleagues investigated responses to melodies of varied degrees of dissonance [272], and Blood and Zatorre compared responses to subject-selected 'favorite' music minus music selected by the other subjects [34]. In another PET-study, Brown and colleagues [244] investigated music presentation versus rest. Based on functional MRI, studies have compared unpleasant and pleasant music [35], music in minor and major mode [273], music and scrambled music [274], or happy, sad and neutral music [245]. The activation in the cerebellum seems to be the most reproducible effect across studies using different imaging methods, different stimuli and contrasts (see table 6). It has been suggested that the cerebellum plays a role in rhythm analysis [275]. Another study report that the cerebellum is involved in both, pitch and duration sequence processing, suggesting that the cerebellum might play a role in sequence analysis in general rather than a specific motor preparation in response to rhythm [276].

Furthermore, activity in the SMA and in the inferior frontal cortex (IFC) including Broca`s area has been observed. Previous studies using fMRI [277] or magnetoencephalography (MEG) [278] suggest that this brain area might be involved in music-syntactic processing.

Alternatively, the inferior frontal cortex including Broca's area and particularly the observed activation in the SMA might be interpreted as motor related. According to this perspective it

could be argued that listening to music might induce the desire to move (e.g. to tap the rhythm) which subjects had to inhibit during the experiment because they received the instruction to avoid any overt movement. Both brain areas have been described being involved in movement execution [279,280], and in observation of movement sequences [281,282]. Further, the present study but also previous studies using music as stimuli reported the involvement of the SMA and/or of the IFC including Broca`s area ([34,35,274], see Table 6). This explanation is in agreement with the fact that both areas, the SMA and the IFC have been described in negative motor control tasks [265,283,284]. Moreover, this and three previous image studies reported effects in the amygdala region which will be discussed in the following chapter [34,35,245].

Study	Method	Inferior frontal cortex	SMA	Amygdala	Cerebellum
Blood & Zatorre, 2001	PET		+	+	+
Brown et al., 2004	PET				+
Menon & Levitin, 2005	PET	+			
Khalfa et al., 2005	fMRI				
Kölsch et al., 2006	fMRI	+	+	+	+
Mitterschiffthaler et al., 2007	fMRI			+	+
This study	fMRI	+ (incl. Broca)	+	+	+

Tabel 6: **List of neuroimaging studies investigating emotional processing of music**

7.1.1 Functional MRI

In the present study fMRI combined with probabilistic anatomical maps has been used to investigate functional response properties of human amygdala subregions [24]. The utility of this approach critically rests on the EPI signal quality in the amygdala region. By application of

a new online correction method for geometric EPI distortions based on the point spread function (PSF) [106] good EPI signal quality at 3 Tesla in the amygdala region was achieved. The results clearly demonstrate the existence of significant fMRI response differences between probabilistically defined human amygdala subregions. In the present study music has been used as stimuli to evoke amygdala responses. Several previous functional imaging studies have probed the neural circuitry underlying music processing in a variety of functional contrasts. Three of these imaging studies reported effects in the amygdala region [34,35,245]. However, the specific response properties of the anatomical amygdala subregions were not assessed in these studies. One of the previous studies reporting amygdala effects for musical stimuli focused on differential activation between pleasant and unpleasant pieces [35]. In contrast, other studies using for example gustatory, olfactory, or visual stimuli have emphasized the similarity of responses to both pleasant and unpleasant stimuli in the human amygdala [26,27,93,94]. In line with these later results, the data of this study support the notion of a basically similar amygdala response pattern both to pleasant and to unpleasant stimuli. In this study, this basic pattern was characterized by increased BOLD responses ('activation') in LB and decreased BOLD responses ('deactivation' [103]) in SF and CM. Beyond this basic pattern, further research is however needed to tease out the finer auditory-induced modulations of human amygdala responses along the valence and arousal dimensions (for a recent study in the olfactory domain, see reference [28]).

Importantly, there were no differences in familiarity ratings for both the pleasant and unpleasant tunes in our study. Subjects' familiarity with the experimental stimuli may shape amygdala responses, as several studies have shown [95–98] that the response of the human amygdala to emotional facial expressions diminishes with repeated presentations, that is, with increasing familiarity. The role of familiarity differences in previous studies of auditory-evoked human amygdala responses is less clear and could explain why amygdala-deactivation was found when subjects listened to highly familiar music in contrast to music selected by the other participants [34].

The basic response pattern within probabilistically defined human amygdala subregions found in this study fits well into general concepts of mammalian amygdala organization [41]. In various animal species LB contains auditory responsive neurons [285] and has been shown to be the main target of sensory, including auditory, afferents to the amygdala in anatomical studies [43–45]. The activation effects in LB that were observed may reflect a similar involvement of the human LB in the processing of auditory inputs. Further, reciprocal changes in firing probability between lateral and central medial amygdala neurons have been reported in cats [286]: Auditory stimulation caused firing probabilities of lateral and central medial neurons to oscillate in phase opposition, with an initial excitation in LB and inhibition in CM. It has been proposed that these reciprocal response patterns result from inhibitory influences of LB on CM, mediated by interposed intra-amygdala nuclei [286]. This reciprocal functional organization parallels the reciprocal auditory-evoked BOLD effects observed in the group mean effects of the current study for LB and CM. Whether BOLD signals in human LB and CM do show reciprocal behavior on a finer temporal scale remains to be investigated. Also in a previous fMRI study, reciprocal signal changes during implicit fear conditioning were reported for two spatially segregated responses in the amygdala region [185], suggesting that this reciprocal behavior may be a more general characteristic of the human amygdala.

The results point also to different lateralization patterns for CM as compared with LB and SF. The general issue of lateralization of emotional functions in the human amygdala has been a matter of much debate [287], but lateralization in the context of subregional differences within the amygdala has not yet been considered. We found a predominance of the positive- and negative-most responses in LB and SF of the left amygdala. In contrast, the positive-most responses in CM predominated on the right and the negative-most responses on the left. This suggests that differentiating between LB, SF, and CM might be important for studies on lateralization of amygdala function. In this study relatively unknown piano melodies of 24 second duration as auditory stimulation were used. Other studies have shown [96,98] that the response-habituation process to emotional facial expressions is more rapid for the right than for the left amygdala. This could explain why, using relatively long stimuli, a predominance of the

positive- and negative responses in the left amygdala (both in LB and SF) were found. One might speculate whether shorter piano melodies evoke more bilateral amygdala activation in LB and SF.

The approach, which has been applied in this study, requires high BOLD imaging localization accuracy. Sources of spatial fMRI localization errors include EPI image distortions [106], draining vein effects [107], and inaccuracies arising from spatial data pre-processing [288]. The problem of spatial EPI distortions has been addressed, which are particularly prominent in the medial temporal lobe [271], by applying a new distortion correction method based on the BOLD point spread function [106]. Making use of the shift and broadening of the point spread function in phase encoding direction, the original signal location and intensity in phase encoding direction is recovered to result in an undistorted image [106]. While image distortions are more severe in the amygdala region as compared with other commonly examined brain regions, the draining vein problem can be assumed to be less pronounced in the amygdala for the following reasons: (1) the draining vein problem is more severe for large areas of activated neuronal tissue [107], but the amygdala, and especially its subnuclei, is/are relatively small. (2) Contamination by apparent activation along a draining vein will be most pronounced if a single vein drains the activated area (see also [107]). The amygdala is however drained by several veins [108], again reducing the draining vein problem; and, (3) these general considerations are confirmed by experimental data from BOLD venography. Venograms indicated that there are no sizable draining vein artifacts in the amygdala region [109].

Furthermore, the main findings of the present study were based on the anatomical core (with 90-100% assignment probabilities) of the amygdala subregions, increasing the robustness of the results against spatial errors and thus counteracting the potential effects as discussed above while still maintaining excellent anatomical specificity. These considerations and the fact that the present results conform to concepts of internal amygdala organization from animal research strengthen the assumption that the responses have been described in this study truly

reflect activation patterns of the major human amygdala subregions. The results imply that treating the human amygdala as a single entity, a predominant approach in current functional imaging studies, may be problematic. Averaging responses over voxels of the whole extent of the amygdala or restricting data interpretation to a single peak value may fail to capture the full complexity of amygdala responses. More importantly, averaging of positive and negative signals emanating from different amygdala subregions may even lead to false negative results as opposite effects may cancel each other out.

The present study is a first step in subdivision-level investigation of the human amygdala using probabilistic maps. To pursue this approach further, not only the spatial accuracy of amygdala fMRI needs to be optimized, but also a precise estimation of the magnitude of residual spatial localization errors in the amygdala region and of their impact on the functional results needs to be developed. In this way, the combination of fMRI with probabilistic anatomical maps may make an important contribution to our understanding of the internal functional organization of the human amygdala and of its neuronal mechanisms.

7.1.2 Meta-analysis of amygdala-studies

The principle aim of the coordinate-based meta-analysis of previous neuroimaging studies reporting amygdala-activation was to determine brain area(s) that are consistently co-activated with the amygdala. To realize this analysis only published amygdala-coordinates which were probabilistically defined located in the amygdala entered the (co-)activation likelihood estimation (ALE) [19]. In this meta-analysis a total of 120 articles reporting 288 amygdala-coordinates were identified through a literature search in Medline. According to the maximum probability maps [24,25] 66,67 % of the peaks were located in the amygdala. These results suggest that applying probabilistic maps improve functional localization, because one third of the peaks were not located in the amygdala or even in the hippocampus.

Further, insula activation has been revealed in the co-activation likelihood estimation (ALE) [19] of previous neuroimgaing studies reporting amygdala-activation. The position of the insula activation-peak was delineated by the coordinate-based meta-analysis of previous neuroimaging studies reporting insula activity. The insula activation-peak was located in the anteroventral insula extending to the frontal operculum. The insula meta-analysis suggests (which will be discussed next chapter more detailed) that this insula region might be related to change in peripheral nervous system, which has been claimed to play an important role in emotion [16,17]. The anteroventral insular cortex is reciprocally connected to brain areas such as the brainstem, hypothalamic nuclei, and the centromedial group (CM) of the amygdala [49,50] known to be involved in autonomic function [51,52]. In the insula meta-analysis most of the neuroimaging studies also report amygdala activation [37,39,83,268–270] which supports the assumption that both, the insular cortex and the amygdala, are involved in a brain network that mediates emotional states.

7.2 *The insular cortex*

Extensive research in humans and nonhumans demonstrate that the insular cortex is involved in various functions including, language, auditory processing, peripheral autonomic change, and sensorimotor processing, [54–60]. A question is however whether these different functions evoke reproducible activation patterns within the human insula.

The results demonstrate that the anterior insular cortex, extending to the adjacent deep frontal operculum is consistently activated by neuroimaging studies involved in language, music processing and perception of vocalization. Several studies claim that the human insula is involved in language [54,55]. This assumption is in agreement to the fact that there are connections between the insula and the frontal operculum and also with superior temporal sulcus [50]. In addition, a lesion study, reported impaired speech in a patient with a left anterior insular infarction, suggesting that the insula is involved in a functional network that mediates speech [71]. In this insula meta-analysis 10 speech processing studies, 5 studies reporting speech perception-induced [232,233,235–237], and 5 studies demonstrating speech production-induced [239,289–292] insula activity were included. 18 stereotaxic coordinates were on the left, and 8 on the right hemisphere, suggesting in mostly right-handed subjects a tendency for dominance in the left hemisphere. The meta-analysis included 11 stereotaxic coordinates from 7 studies investigating different aspects of music processing. 6 coordinates were on the left, and 5 on the right hemisphere, suggesting in comparison to language a more bilateral processing. Regarding hemispheric specialization it has been speculated whether comprehension of speech intonation relies predominantly upon left sided language areas whereas the evaluation of emotional tone is processed more bilateral as proposed by Wildgruber and co-workers [293]. It might be that the studies included in this meta-analysis and investigating music and the perception of vocalization used more emotional material (e.g. infant crying) in relation to the studies investigating speech.

This meta-analysis of previous functional imaging studies demonstrate that studies investigating sensorimotor hand and/or leg movement [248–267] demonstrate activity in the mid anterior insula. This finding is in line with the fact that the anterior insula has connections with various brain areas involved in motor processing such as the basal nuclei (caudate nucleus and ventral striatum) [65], the premotor cortex, and the supplementary motor area (SMA) [50]. Furthermore, the anterior insula has also been found to be active during imagery of standing and walking [294], and has been reported to be involved in the 'sense of agency' of hand movement [295], that is, the experience of oneself being the cause of an action, which is a fundamental aspect of action representation. According to Fink and co-workers the left anterior insula contains a somatotopic motor map that includes representations of finger, shoulder, and leg movement [296]. In this meta-analysis of previous functional imaging studies investigating sensorimotor hand and/or leg movement [248–267] a somatotopic organization was not found which could be also due to the fact that the studies included in the present meta-analysis differ in various aspects such as they used different motor tasks, different subjects, scanner, which could have the consequence that meta-analyses might not have sufficient spatial resolution.

Most recently, a short time training effect in the 'sensorimotor area' of the anterior insula has been demonstrated using functional MRI. In this study passive listening to melodies previously learned by subjects on a piano evoked insular activity in the 'sensorimotor hand area'. This training effect was already evident after 20-30 minutes of training [297], indicating that in the insula training effects are possible already on a short time scale. This finding is also in line with the assumption that the anterior insula might have sensorimotor integration properties [55]. In the meta-analysis of sensorimotor tasks, 27 stereotaxic coordinates were on the left, and 22 on the right hemisphere, suggesting in right-handed subjects mostly performing with their right side, a slight tendency for dominance in the left hemisphere.

Further, this meta-analysis shows that neuroimaging studies investigating peripheral autonomic change, measured by cardiovascular activity [14,15], sympathetic skin or [12,13] pupil responses [82], or after the administration of procaine [83], reproducible activate the

anteroventral insular cortex. Williamson and co-workers reported already in an early neuroimaging studies a functional link between insula-activity and cardiovascular modulation [298]. Birbaumer and co-worker [37] report that skin conductance response increased in a classical condition paradigm in the acquisition phase only in healthy controls and not in psychopaths. In addition, during acquisition only healthy controls showed activity in the fronto-limbic circuit including the anteroventral insula. All these findings together, are in agreement with the fact that the anteroventral insular cortex is reciprocally connected to brain areas such as the brainstem, hypothalamic nuclei, and the centromedial nucleus (CM) of the amygdala [49,50] known to be involved in autonomic function [51,52]. It has been speculated that the insula, especially the anteroventral portion, provides because of its connections a neural relay for conveying sensory information to the limbic system [50]. This association between sensory systems and limbic structures is important because it could enable the transition from perception of events in the external world to relevant motivational states in order being able to act appropriately. Regarding lateralization Christensen and co-workers demonstrated that particularly right sided insular damage was related to abnormalities in electrocardiography in patients with acute stroke [299]. Oppenheimer and colleagues reported that in epileptic patients, electrical stimulation particularly of the right insula elicited changes in heart rate [80]. In this meta-analysis on previous neuroimaging studies 6 coordinates were on the left, and 16 on the right hemisphere, suggesting in mostly right-handed subjects also a tendency for dominance in the right hemisphere.

Taken together, this meta-analysis suggests functional specializations within the anterior insula. Recently, Dossenbach and co-workers suggested based on a cross-studies analysis that the anterior insula and the adjacent frontal operculum is involved in a brain network that forms a more general task-set processing system [66]. The present meta-analysis illustrates, that their published insula activation peaks were located in the anterior insula 'speech processing area' which might be due to the fact that many of their analysed studies were speech related. The present meta-analysis can, however, not reject their assumption since both findings to not exclude each other.

In summary, this meta-analysis suggest functional specialization for speech and auditory processing, sensorimotor functions, and peripheral autonomic change, which may help interpreting insula-activation found in neuroimaging studies as already shown in a previous study for a sensorimotor related task [297].

7.3 *Brain activation correlating with affect intensity*

A growing number of studies demonstrate a strong association between personality traits and brain activation [2–4]. In this study functional MRI has been used to examine brain activation associated with individual differences in affect intensity, a personality dimension that refers to the degree to which individuals experience the strength of their emotion during the exposure of the same affect-evoking stimuli [84]. The results of this study show that, during the exposure of music, participants with high affect intensity scores demonstrate stronger activation in the somatosensory cortex, in the supramarginal gyrus (SMG, both more pronounced on the right hemisphere), in the right insula, and in the cerebellum than participants with low affect intensity scores. The found brain activation in the present fMRI study is unlikely to result from anxiety associated with the scanning-environment or from previous musical education because these scores did not correlate with the AIM-scores.

The network of brain areas with enhanced activation in subjects with high AIM has previously been associated with the (visual) recognition of emotions [91]. In this study, Adolphs and colleagues investigated 108 subjects with focal brain lesions using three different tasks that assessed the recognition and naming of six basic emotions from facial expressions. The authors report that particularly the right somatosensory cortex plays a central role in recognizing emotions from facial expressions. In addition, they also report the involvement of the right SMG, and of the right insula. The interpretation that emotionally sensitive people demonstrate stronger activation in a network of brain areas that has been described being involved in recognition of emotions is in agreement of a recent behavioral study showing that subjects with

high aim-scores demonstrate a better performance in an emotion recognition task than subjects with lower scores [88].

In a previous PET study, 41 subjects had the task to recall and to re-experience personal life episodes characterized by sadness, happiness, anger or fear [300]. The authors report that the process of feeling emotions also activates the somatosensory cortex and the insula. A possible explanation of this finding is that there might be a relationship between the two processes of "feeling an emotion" and "recognition of an emotion" in the way that individuals are receptive to and recognize the emotion expressed in music by internally simulating and "feeling" that emotion. Such a relationship between feeling and recognition of emotion would fit nicely to the observation that high AIM scoring subjects demonstrate better emotion recognition abilities [88].

The insula meta-analysis of previous functional neuroimaging studies was used to delineate the more general function of the region of the insular cortex showing consistently activation in the correlation with the individual aim-scores. This meta-analysis shows that neuroimaging studies investigating peripheral autonomic change, measured by cardiovascular activity [14,15], sympathetic skin or [12,13] pupil responses [82], or after the administration of procaine (a drug that induces physiological arousal) [83], reproducible activate the anteroventral insular cortex. The peak of the insula-activation found in the positive aim-correlation was also located in the anteroventral region of the insula, suggesting that subjects with high AIM scores might have had the tendency to demonstrate a higher peripheral arousal response to the music stimuli than individuals high lower scores on the affect intensity dimension. This interpretation is in agreement with the fact that the anteroventral insular cortex is reciprocally connected to brain areas such as the brainstem, hypothalamic nuclei, and the centromedial nucleus (CM) of the amygdala [49,50] known to be involved in autonomic function [51,52].

In the present study that was exclusively based on right-handed subjects the *right* insula was activated. Regarding lateralization, Christensen and co-workers demonstrated that particularly

right sided insular damage was related to abnormalities in electrocardiography in patients with acute stroke [299]. Oppenheimer and colleagues reported that in epileptic patients, electrical stimulation particularly of the right insula elicited changes in heart rate [80]. In the meta-analysis on previous neuroimaging studies investigating peripheral change (also in mostly right-handed subjects), 6 activation foci were on the left, and 16 on the right hemisphere, suggesting also a tendency for dominance in the right hemisphere in right handed subjects.

As shown in the insula meta-analysis presented in this thesis, the anteroventral insula seems to be involved in decrease and enhancement of peripheral autonomic activity. This finding may contribute to understanding the mechanisms which underlay differences in affect intensity hypothesized by Larsen and co-workers [18]. The present results support the assumption that individuals with high aim-scores have the tendency to react more physiological during the exposure of emotional stimuli. Further research is however necessary to evaluate this assumption further (e.g. by measuring heart rate). In addition, further potential mechanisms, which might contribute to individual differences in affect intensity, should be examined. For example, Larsen and co-workers report that individual differences in affect intensity is related to how subjects interpret emotional stimuli [18].

In conclusion, in the present thesis a relationship between affect intensity and a brain network that has previously been reported being involved in emotion recognition, as well as a potential mechanism underlying these differences has been described by using the functional map of the insula established in this thesis. The insula activation positive correlating with affect intensity could be assigned to the part of the insula consistently showing peripheral autonomic change related activation, suggestion a tendency for stronger physiological response in individuals scoring high in affect intensity as a possible cause for individual differences in affect intensity. However, in further research further mechanisms underlying differences in affect intensity should evaluated and it should be kept in mind that the questionnaires, which are used to assess personality traits such as affect intensity, have a limited validity and reliability. Therefore the results of this fMRI study should be seen as a first approach in investigating the

neural basis for individual differences in emotional responsiveness.

8 Conclusion

In this present work functional MRI and meta-analyses were combined with cyto-architectonically defined probabilistic maps to analyze the response characteristics of brain regions involved in emotional processing. Probabilistic anatomical maps provide a precise concept of localization which accounts for inter-individual anatomical variability and provides information about localization even when current structural brain scans do not enable the differentiation of brain areas based on macro-anatomical landmarks, as was demonstrated in the present thesis in respect to response properties of the major amygdala sub-regions that were investigated during processing of emotionally significant auditory information. In order to be spatially precise, however, functional MRI measurements require high BOLD imaging location accuracy. Sources of spatial location errors include EPI image distortions, draining vein effects, and inaccuracies arising from inaccuracies in spatial data preprocessing such as image normalization. Several of these problems have been addressed and discussed in this work. But a precise estimation of the magnitude of spatial localization errors, particularly in the amygdala-region, needs to be quantified in future research.

Previously, it has been argued that functional measurements have a low reliability [22,23]. The meta-analyses in the present thesis demonstrated that neuroimaging studies investigating similar functions (e.g. emotional processing) show relatively consistent responses across different experiments, different subjects, and different stimuli, as was demonstrated for the anterior insular cortex. The present work suggests that meta-analyses in particular when using probabilistically defined brain-areas combined with (co-)activation likelihood estimation-analysis provide a tool to investigate the reproducibility of activation effects and thus contribute to ruling out false positive effects. In addition, meta-analyses may provide functional maps which can help interpreting functional MRI results as shown in this thesis.

9 Supplement

Tabel I-III show the studies of the insula meta-analysis

Authors (year)	Method	Handed-ness	Spatial filter size	Investigated effect	Coordinates x/y/z Talairach (Tal) or MNI space	
Seifritz et al., 2003	fMRI	-	6 mm	Perception of vocalisation: Infant crying > laughing in Parents > non-parents Mothers > childless women Fathers > childless men	 -40/13/6 (Tal) -40/15/6 -38/13/6	 44/10/6 (Tal) 42/8/4 43/10/6
Lorberbaum et al., 2002	fMRI	right	6 mm	Perception of vocalisation: Mothers listening to infant crying > rest	-	15/18/-6 (Tal) 24/27/0
Mitterschiffthaler et al., 2007	fMRI	right	8 mm	Music perception: Processing of neutral > sad and happy music	-36/-30/18 (Tal)	-
Bengtsson & Ullén, 2006	fMRI	right	10 mm	Music perception: Melody processing Rhythm processing	-39/-33/15 (Tal)	36/27/9 (Tal)
Tillmann et al., 2006	fMRI	right	7 mm	Music perception: Less-related > related	-	40/12/-3 (Tal)
Koelsch et al., 2005	fMRI	right	5.6 mm	Music perception: Pleasant > unpleasant music	-29/18/8 (Tal)	34/21/5 (Tal)
Brown et al., 2004	PET	right	10 mm	Music perception: Music > rest	-46/-6/4 (Tal)	44/-2/-6 (Tal)
Platel et al., 1997	PET	right	20 mm	Music perception: Rhythm > (pitch and timbre)	-36/12/0 (Tal)	-
Zatorre et al., 1994	PET	right	20 mm	Music perception: First/last note judgement > passive melodies	-31/22/8 (Tal)	38/20/5 (Tal)
Beaucousin et al., 2007	fMRI	right	8 mm	Speech perception: Grammatical classification of sentences > beep detection Affective classification of sentences containing or not affective prosody > during grammatical classification	-34/28/0 (MNI -30/28/0 (MNI)	38/30/-2 (MNI)
				Speech perception:		

Dehaene-Lambertz et al., 2006	fMRI	right	5 mm	First sentence First > second presentation	-48/16/8 (Tal) -32/16/8 (Tal)	-
Skipper et al., 2005	fMRI	right	4 mm	Speech perception: Audiovisual > video-alone	-31/-2/14 (Tal)	-
Xiao et al., 2005	fMRI	right	8 mm	Speech perception: Pseudoword > rest Real word > rest	-34/13/-2 (Tal) -33/14/-2 (Tal)	-
Röder et al., 2002	fMRI	right	6 mm	Speech Perception: Syntax effect Semantic effect	-	31/19/2 (Tal) 34/20/4 (Tal)
Meyer et al., 2002	fMRI	right	-	Speech perception: Prosodic speech > normal speech Prosodic speech > syntactic speech	-34/17/7 (Tal) -34/17/7	27/20/3 (Tal) 26/19/4
Brown et al., 2006	PET	right	10 mm	Speech production: Sentence generation task > rest	-42/12/0 (Tal) -34/22/6 -30/15/-6	38/20/6 (Tal)
Riecker et al., 2002	fMRI	right	10 mm	Speech production: Isochronous > perceptual baseline Rhythmic > pereptual baseline	-27/18/2 (Tal) -30/18/2	24/18/2 (Tal) 33/20/2
Blank et al., 2002	fMRI	right	10 mm	Speech production	-36/10/8 (MNI) -36/28/0	-
Hashimoto et al., 2003	fMRI	right	14 mm	Speech production: Fast > nomal	-30/18/6 (MNI)	-
Rieckert et al., 2000	fMRI	right	10 mm	Speech production: Overt speech	-35/18/-4 (Tal)	-

Table I: **20 neuroimaging studies investigating language, music processing or perception of vocalization** (4 studies used PET = positron emission tomography, and 16 used fMRI = functional magnetic resonance tomography). The studies gave their coordinates either in talairach (Tal) or MNI space. The spatial filter size (Gaussian or Hanning) ranged from 4 to 20 mm full width at half-maximum (FWHM).

Authors (year)	Method	Handed-ness	Spatial filter size	Investigated effect (side of movement)	Coordinates x/y/z Talairach (Tal) or MNI space	
Cunnington et al., 2002	fMRI	right	4 mm	Externally-triggered movements self-initiated movements (index, middle finger of the right hand)	-42/4/-4 (MNI) -42/-16/-6 -42/2/-4	-
Ehrsson et al., 2000	fMRI	right	8 mm	Precision-grip task > matching rest condition (right hand)	-	32/20/0 (MNI)
Indovina & Sanes, 2001	fMRI	right	4 mm	Move < No-Move (hand hand)	-	52/18/–4 (Tal)
Jantzen et al., 2002	fMRI	right	4 mm	Pre practice syncopation Pre practice synchronization (right index finger and thumb)	-45/-29/19 -32/20/5 -41/-29/19 (Tal)	-
Johansen-Berg & Matthews, 2002	fMRI	right	5 mm	Main effect for button pressing (left hand)	–42/2/–2	28/–22/16 (Tal)
Kawahima et al., 2000	fMRI	right	12 mm	Visually cued finger movement tasks < Rest (index finger of right hand)	-46/8/-2 (Tal)	-
Kim et al., 2005	fMRI	right	?	finger tapping quantity finger tapping frequency (right thumb)	-	49.5/7.5/5.5 37.5/-16.5/-0.5 (Tal)
Macar et al., 2004	fMRI	right	6 mm	Force task < baseline (left finger)	-39/3/0 (Tal)	-
Martin et al., 2004	fMRI	right	4 mm	finger–thumb opposition task < rest (right hand)	-34/9/12	34/9/12 (Tal)
Saini et al., 2004	fMRI	right	5 mm	Figure writing (right hand)	-	42/14/-6 (MNI)
Toma et al., 2003	fMRI	right	8 mm	Predictive movement to a regularly presented cue Reactive movement to a regularly presented cue Reactive movement to an irregularly presented cue (right index finger)	-40/2/11 -48/2/6 -46/0/6 (Tal)	-
Ward & Frackowiak, 2003	fMRI	right	8 mm	Hand grip task Dominant hand (right) Non-dominant hand (left)	 -38/2/-2 -40/14/-4 -36/12/-2 -38/4/0	 40/8/-4 44/2/10 40/4/2 50/14/-8

						(MNI)
Wiese et al., 2005	fMRI	right	9 mm	Epoche related analysis Combined model (self initiated movement of the right index finger)	-44/6/0 -42/6/0	42/8/0 44/12/3 (Tal)
Jahanshahi et al., 1995	PET	right	20 X 20 X 12 mm	Self-initiated movements Externally triggered movements (right index finger)	-40/10/4 -40/4/0 (Tal)	38/16/8
Larsson et al., 1996	PET	7 right/1 left	4 mm	Self-paced movement task Visually triggered movement (right index finger)	-	33/12/6 30/16/8 (Tal)
Sahyoun et al., 2004	fMRI	right	5 mm	active > rest (right foot movement)	-44/2/2	58/4/2 (MNI)
Rocca et al., 2007	fMRI	right	10 mm	anterior versus posterior position of the right upper limb (hand and foot movements with right limbs)	-46/8/6	34/20/6 (MNI)
Dobkin et al., 2004	fMRI	right	5 mm	voluntary movement of the right ankle passive movement of the right ankle (right foot movement)	-41/4/-2	34/10/-2 48 6 4 (Tal)
Ciccarelli et al., 2005	fMRI	right	8 mm	Right active foot movement (right foot movement)	-48/4/2	46/6/-4 (MNI)
Kew et al., 1994	PET	right	10 mm	During moving a joystick with the right hand in healthy controls	-34/-8/8 -42/8/4	34/12/0 (Tal)

Table II: **20 imaging studies reporting sensorimotor related activation in the anterior insula** (3 studies used PET = positron emission tomography, and 17 used fMRI = functional magnetic resonance tomography). 16 studies investigated hand, 2 studies examined leg, and 1 article reported foot and leg movement-related insula-activation. The studies gave their coordinates either in talairach (Tal) or in MNI space. The spatial filter size (Gaussian or Hanning) ranged from 4 to 20 mm full width at half-maximum (FWHM).

Authors (year)	Method	Handed-ness	Spatial filter size	Investigated effect (side of movement)	Coordinates x/y/z Talairach (Tal) or MNI space	
Fredrikson et al., 1998	PET	-	20 mm	Negative correlation between Cerebral Blood Flow and Electrodermal Activity	-	52/17/-8 (Tal)
Veit et al., 2002	fMRI	right	10 mm	During acquisition phase of conditioning in healthy controls (Skin conductance responses were recorded)	-57/9/-3 (MNI)	57/12/-6 48/21/-12
Birbaumer et al., 2005	fMRI	right	15 mm	During acquisition phase of conditioning in healthy controls (Skin conductance was recorded)	-36/3/-12 (MNI)	36/12/-15 (MNI)
Nagai et al., 2004	fMRI	right	12 mm	Regional brain activity related to change in skin conductance	-	36/24/-8
Servan-Schreiber et al., 1998	PET	-	20 mm	Increased activation associated with Procaine (procaine induces autonomic responses)	-36/4/-8 (Tal)	32/-2/-8
Gianaros et al., 2004	PET	mostly right	10 mm	Regional activity correlated with high-frequency hear period variability	-38/-3/-13 (Tal)	
Critchley et al., 2005	fMRI	right	8 mm	Activity reflecting both error processing and sympathetic arousal (pupil responses)	-34/18/-11	34/16/-11
Critchley et al., 2000	PET	right	12 mm	Greater regional Cerebral Blood Flow at higher Heart rate Greater regional Cerebral Blood Flow at lower Heart rate	-	28/14/6 (Tal) 62/6/-14 40/2/-16 42/-14/4
Critchley et al., 2003	fMRI	right	10 mm	Regional activity related to heart rate variability	-58/8/0	54/14/-4

				(heart rate)		
Deseilles et al., 2006	PET	right	16 mm	The insula covaried with the amygdala more during wakefulness than during rapid eye movement sleep in relation to the variability in heart rate	-	34/-6/-12 (MNI)

Table III: **10 imaging studies reporting anterior insula activity related to peripheral autonomic change** (5 studies used PET = positron emission tomography, and 5 used fMRI = functional magnetic resonance tomography). The studies gave their coordinates either in talairach (Tal) or in MNI space. The spatial filter size (Gaussian or Hanning) ranged from 8 to 20 mm full width at half-maximum (FWHM).

Tabel IV includes studies of the amygdala meta-analysis

Authors (year)	**Method**	**Handed-ness**	**Spatial filter size (mm)**	**Investigated effect (side of movement)**	**Coordinates x/y/z Talairach (Tal) or MNI space**	
Bornhövd et al., 2002	MRI	Left	6	laser(300-600mJ)	-27 0 -27	24 0 -24
Berns et la. 2005	MRI	Right	8	mental rotation		15 -3 -18
Canli et la., 2002	MRI	Right	8	rate emotionality of fearful faces	-23 -6 -18	24 -7 -17
Das et al., 2005	MRI	Right	8	fearful faces	-24 4 -18	22 -6 -12
Etkin et al., 2004	MRI	Right	8	masked fearful faces indicate color of fearful faces		28 10 -22 16 -8 -12
Goldstein et al., 2005	MRI	Right	8	negative pictures negative pict.	-24 -9 -12 -21 -3 -21	24 0 -21
Hamann et al., 2004	MRI	-	8	sexual pictures of couples male subjects viewing sexual pictures of couples male activation as response to sexual pictures of couples	-16 0 -20 -16 0 -24 -20 0 -20 -20 -4 -20 -16 0 -16	16 0 -16 24 -4 -24 16 0 -16
Evans et al., 2002	MRI	Right	6	Air hunger	-20 2 -14	24 4 -14
Kilpatrick et al., 2003	PET	Right	8	rate arousing film		20 -4 -24
Liddell et al., 2004	MRI	predominant Right	8	masked fear faces	-18 2 -20	28 -4 -12
Morris et al., 2001	PET	Right	12	pictures of food;indicate,if they had seen picture before	-14 -4 -20	
Ochsner et al., 2002	MRI	Right	6			16 -12 -20
Ochsner et al., 2004	MRI	-	6	increase negative emotions in response to aversive pictures look at aversive pictures and respond naturally	-18 -10 -14 -30 -2 -20 -28 -4 -14	 20 0 -24
Phan et la., 2003	MRI	Right	8	aversive pict., rate unpleasentness	-21 -6 -15	

				aversive pict. aversive pict.	-9 0 -12 -18 -3 -15	
Phan et al., 2004	MRI	Right	6	rating emotionality of pict.	-27 0 -15 -21 -6 -12	33 -6 -12
Phan et al., 2005	MRI	Right	6	avers. pict.,maintain feelings avers. pict.,maintain feelings increasing neg.emotion	-32 -4 -24 -28 0 -28 -26 6 -26	26 2 -24 16 0 -28
Royet et al. 2000	PET	Right	-	emotional odor; rate pleasentness	-22 0 -12	
Small et al. 2003	MRI	Right	7	intense pleasent/unpleasent taste intense pleasent taste intense unpleasent	 -24 -6 -21 -12 -12 -21	15 -10 -15 27 -9 -12
Sato et al. 2004	MRI	Right	6	angry face angry face towards subject	-20 -6 -10 -22 -11 -16	
Stark et al. 2005	MRI	Right	6	disgust. Pict./SMgroup erotic pict./nonSMgroup erotic pict./SMgroup	-21 -3 -15 -21 -3 -18	 24 6 -18 30 -3 -15
Schendan et al. 2003	MRI	-	-	sequence in SRTT		21 6 -21
Vuilleumier et al. 2001	MRI	-	8	fearful faces attending to fearful faces	-20 -2 -18 -26 -2 -20	
Winston et al. 2002	MRI	Right		untrustworthy faces	-16 -4 -20	-18 0 -24
Wang et al. 2006	MRI	Right	8	sad pict., rate sadness		14 -7 -18
Williams et al. 2005	MRI	Right	6	fearful faces	-28 -2 -24 26 -6 -10	26 -2 -24
Gottfried et al. 2002	MRI	Right	8	appetitive conditioned stimuli(indicate gender)	-20 -14 -12	14 -12 -22 16 -10 -12
Gottfried et al. 2003	MRI	Right	8	odor+picture(UCS+CS+)(indicate presence/abscense of odor)	-21 -6 -24	
Odoherty et al. 2003	MRI	Right	8	reward for choice,imperative(no free choice) reward for choice,imperative+choice	-27 -3 -27 -27 -3 -30	
Odothery et al. 2002	MRI	-	10	Anticipation of glucose (taste)		28 -8 -14
Vuilleumier et al. 2004	MRI	Right	8	fearful faces	-15 -3 -21	24 -3 -21
Singer et al. 2004	MRI	Right	10	cooperative face in intentional task emotional face(indicate gender)	-21 0 -18 -21 0 -21	
Gottfried et al. 2002	MRI	Right	8	neutral face(CS)with any odor(UCS);indicate gender of face neutral face(CS)with unpleasent odor(UCS)	-14 -10 -18	24 -8 -18 24 -12 -16 18 -6 -16
Mcclure et al. 2004	MRI	-	8	angry faces, neutral faces		34 -6 -12 36 -2 -20

						36 0 -14
				angry faces, fearful faces	-28 2 -20	38 2 -18
				angry faces (for female subjects)	-20 -8 -6	
				neutral faces (for male subjects)	-22 -10 -8	
Labar et al. 2003	MRI	Right	8	dynamic emotional pictures(actors)(identify classification)	-19 -8 -23	26 -4 -23
				dynamic fearful pictures(actors)		11 -11 -19
				dynamic fearful pictures(actors)	-15 -15 -11	26 -4 -26
				neutral dynamic pictures	-15 -8 -19	
Hamann et al. 2002	MRI	-	8	positive words	-24 -8 -20	
				negative words	-24 -8 -16	
Bishop et al. 2004	MRI	Right	8	fearful faces(average across attended and unattended)		20 -8 -22
				attended fearful vs attended neutral faces	-18 -10 -20	26 -12 -18
Labar et al. 2001	MRI	Right	7	pictures of food, hungry subjects	-21 -3 -27 -15 -12 24 -33 6 -30	
Morris et al. 2004	MRI	Right	6	acquisition CS+(=neutral face+niose)(indicate sex)	-24 -10 -12	
				acquisition CS+(*time interaction))		30 0 -12
				repeat CS+ and reversal CS+		18 2 -24
				repeat CS+ and reversal CS-		30 2 -26
Ernst et al. 2002	PET	-	10	card games:guessing	-28 2 -26	
Canli et al. 2005	MRI	Right		fearful faces(activation as Function of TPH2 G-703Tgenotype)	-22 0 -18	
				happy faces(activation as function of genotype)	-16 -8 -14	24 -2 -14
				sad faces(activation as function of genotype)	-22 -8 -12	
Ashwin et al. 2006	MRI	Right	-	all faces(high fear, low fear, neutral)(judge degree of emtion)	-24 5 -15 -16 -6 -11	20 -8 -13
				high fear expression	-11 -4 -8	
				neutral expression		34 -4 -8
Wood et al. 2005	MRI	Right	12	sentence with negative attitude inhibition('chris likes murder)(subjects decide about consistency)		28 -9 -26
Taylor et al. 2006	MRI	-	8	crosshair fixation(risky family background)	-20 -8 -18	
Sterpenich et al. 2006	MRI	Right	8	recognized emotional faces		8 -6 -24
Small et al. 2005	MRI	Right	7	summed odorant conditions(pleasent,retronasal ,orthonasal)(rating of pleasentness and intensity afterwards)	-27 0 -21	
Seymour et al. 2005	MRI	Right	6	appetitive predicrion error	-20 2 -26	

Sergerie et al. 2006	MRI	Right	8	remembered fearful faces fearful faces	-24 -8 -20 -20 -4 -12 -14 -8 -24	30 2 -34 30 0 -34
Schienle et al. 2005	MRI	Right	9	viewing disgusting pictures	-18 -6 -18	24 0 -24
Protopopescu et al. 2005	MRI	Right	-	positive words in early half of the study panic words in early half of the study panic words in early half of the study panic vs neutral words, early half of study	-21 0 -24 -27 -3 -24 -21 -6 -12 -27 -3 -27	 18 -3 -24
Ogino et al. 2006	MRI	Right	6*6*10	images evoking fear(subjects imagine own fear)	-20 4 -16	
De_martino et al. 2006	MRI	Right	8	subject choose sure option in the gain frame and gamble option in loss frame	-14 2 -24	12 2 -20
Lewis et al. 2007	MRI	Right	8	increasing arousal in negative words increasing arousal in negative and positive words	-24 -2 -12 -20 -8 -14	
De Ben et al. 2005	MRI	10 Right (of 12)	10	covert recognition of aversive faces	-24 -12 -15	
Coricelli et al. 2005	MRI	Right	8	Influence of cumulative experience of regret on choice-related gamble	-8 -4 -24	
Corden et al. 2006	MRI	-	8	normal fear scorers:direct gaze of neutral face vs averted face; gender judgement both groups: direct gaze of neutral face normal fear scorers only: direct gaze	-27 0 -18 -21 -3 -21 -27 -3 -15	30 -6 -21 21 -5 -15 21 -6 -12
Beaver et al. 2006	MRI	Right	8	pictures of appetizing food	-20 2 -12	
De Araujo et al. 2005	MRI	Right	10	test odor labeled as cheddar cheese (->neutral)+pleasent odor		20 4 -25
Smith et al. 2006	MRI	Right	8	correct source judgments from negative pictures emotional pictures	-24 -3 -18 -24 -6 -15	
Somerville et al. 2006	MRI	Right	6	all recognition trials (recognize faces and remember learned name) faces paired with emotional context	-21 -4 -15	18 -7 -15 15 -9 -12
Winston et al. 2006	MRI	-	8	attractiveness task (judgment)	-24 0 -24	
Stark et al. 2004	MRI	Right	9	disgusting pictures(rating afterwards) fear-inducing pictures changes between first and second session with regard to contrast disgusting/neutral	-18 -3 -27 18 -9 -18 18 6 -24	21 -6 -18
Ruby et al. 2004	PET	-	10	Emotional content of stimuli irrespective of the	-26 14 -32	26 -2 -24

				perspective(subject has to chose 1 of 3 answers to stimuli)		
Wang et al. 2006	MRI	Right	8	sad film clips sad film clips	-22 -8 -15 -19 -8 -15	26 -8 -18 22 -8 -15
Gläscher et al. 2004	MRI	Mostly Right	11	maximal fear facial expression, minimal fear facial expression maximal fear facial expression, neutral facial expression	-15 0 15	 18 0 -18
Wild et al. 2003	MRI	Right	9	stimuli congruent to subjects' movement		30 -9 -9
Gottfried et al. 2003	MRI	Right	6	target conditioned stimulus (CS+) unpaired (no UCS)	-15 -6 -18	
Gottfried et al. 2004	MRI	Right	6	activation during conditioning and extinction (CS+with/without UCS) activation during extinction(unplesant odor=CS; CS+with/without UCS; CS-)	-15 -9 -21 -27 -9 -24	12 -6 -15 33 -3 -27
Kirsch et al. 2005	MRI	Right	10	1 from 2 simultaneously presented angry/afraid faces was matched with an identical target face of identical expression nonsocially relevant threatening stimuli	-24 3 -24 -21 0 -24	
Holstege et al. 2003	PET	Right	10	ejaculation	-18 2 -24	
Hooker et al. 2006	MRI	Right	8	objects on womans neutral face:subjects predicts if woman will react fearful or happy->womans reaction		22 0 -18
Britton et al. 2005	PET	Right	12	emotional processing of traumatic/stressful scripts	-28 2 -26	
Vuilleumier et al. 2003	MRI	Right	8	fearful faces	-20 -10 -30	20 -10 -28
Lotze et al. 2006	MRI	Right	9	filmclip of expressive gesture	-21 -6 -18	21 -6 -18
Tabbert et al. 2006	MRI	-	9	CS+=rhombus(Unaware of conditioning>aware), UCS=electrical stimulation CS+(Unaware of conditioning) CS+ mit UCS (Aware>unaware) CS+ mit UCS (Aware) CS+ mit UCS (Unaware)	 -30 0 -27 -30 0 -27	27 3 -18 27 3 -18 21 0 -15 27 3 -21 33 3 -21
Williams et al. 2005	MRI	Right	8	attend picture of fearful face		32 12 -22
Plailly et al. 2004	MRI	Right	8*8*10	9 familiar+ 9 unfamiliar odorants(judge odor presence)	-24 -6 -12	20 -16 -10
Pessoa et al. 2005	MRI	-	8	face(neutral or fearful)with 2 peripheral bars->subject indicates sex picture with 2 bars and central fixation cross:subject	-21 -5 -19 -26 -5 -27	19 -7 -21 22 -4 -29

				indicates,if bar-orientation is the same		
Royet et al. 2003	MRI	Right (14)	8*8*10	Tar-odor (rate hedonic intensity) Pleasant Apricot & Lemon odor and unpleasant Garlic and Tar odor	-22 -2 -12 -12 -6 -12	
Dresel et al. 2005	MRI	Right	8	subjects whistle	-22 0 -16	26 0 -14
Desseilles et al. 2006	PET	Right	16	rapid eye movement sleep	-30 -2 -18	
Winston et al. 2003	MRI	Right	8	fearful male/female face at low statial frequencies (indicate gender)+ (gesicht verzerrt und vermischt mit einem anderen)	-18 -6 -33	33 -6 -24
Levesque et al. 2003	MRI	Right	12	sad film	-24 3 -18	
Critchley et al. 2000	PET	Right	12	low stress tasks	-30 5 -21	
Eugene et al. 2003	MRI	Right	12	sad film	-30 0 -17	
Anderson et al. 2003	MRI	Right	6	fearful faces(indicate gender)		22 2 -33
Hariri et al. 2003	MRI	-	8	match 1 of 2 threats(visual stimuli) with identical target stimulus match 1 of 2 threats(visual stimuli)with identical target stimulus	-22 -5 -15 -26 -8 -15	26 -5 -15 26 -8 -15
Yang et al. 2003	MRI	Right	4	happy faces(indicate gender)	-20 -8 -16	26 0 -16
Fischer et al. 2004	MRI	Right	12	female faces	-20 -2 -24	
Beauregard et al. 2001	MRI	-	12	erotic film excerpt(rating afterwards)		25 -2 -17
Harenski et al. 2006	MRI	Right	6	watch moral pictures (unpleasant scene, indicating specific moral violation) watch non-moral pictures (unpleasant scene) supress feelings while watching non-moral pictures	-21 -5 -18 -24 1 -32	 18 -2 -32
Hariri et al. 2002	MRI	-	8	Placebo-subjects:match expression angry/afraid to 1 of 2 faces dextroamphetamine-subjects:match expression angry/afraid to 1 of 2 faces	-22 -5 -19 -18 -5 -19	16 -3 -19 16 -3 -19
Williams et al. 2006	MRI	-	8	activation to fearful faces;young and middle aged subjects	-24 -8 -20	
Williams et al. 2006	MRI	-	8	unconscious perception of fearful faces (only shown for 16.7ms)	-16 2 -16	18 2 -16
Winston et al. 2003	MRI	Right	8	highly emotional face expressions(indicate more male/more emotional)	-24 -6 -18	34 0 -26
Killgore et al. 2003	MRI	Right	10	pictures of food pictures of high caloric food	-22 -12 -19 -20 0 -24	22 -4 -21
Elliot et al. 2003	MRI	Right	10	gamble with reward		24 -6 -18
Bishop et al. 2006	MRI	Right	10	fearful faces		18 2 -16
Ethofer et al. 2006	MRI	Right	10	correlation: difference in valence rating of facial	-24 -6 -24	

				expressions in presence of a fearful voice		
Takahashi et al. 2006	MRI	Right	8	sexual/emotional infidelity (reading sentences implying infidelity) sexual/emotional infidelity for men		22 2 -14 22 2 -14
Carter et al. 2006	MRI	Right	8	implicit,CS+ (abstract colored images)	-27 -3 -12	
Habel et al. 2005	MRI	-	10	watch sad face and try to become sad	-34 -10 -16	
Castriota et al. 2005	MRI	Right	6	naive group drinking wine (aftertaste) wine-glucose contrast in naive group	-22 -8 -18 -28 -12 -16	
Hennenlotter et al. 2005	MRI	Right	8	watch smiling face (video) smile (sign on screen)	-24 -8 -22 20 -4 -10	22 -6 -26 -24 -4 -12
Killgore et al. 2004	MRI	Right	10	masked happy faces masked happy faces	-20 -6 -18	22 0 -20 24 0 -24
Hariri et al. 2000	MRI	Right	6	select emotional face whose affect match target face select emotional face whose affect match target face	-24 -9 -27 -22 -7 -29	24 -1 -26 34 -18 -20
Morris et al. 2001	MRI	Right	6	CS+(angry face) with UCS(white noise burst) CS+(alone) CS+ evoked responses in initial stages of learning	-30 -10 -10 -12 -8 -26 -18 2 -14	
Killgore et al. 2000	MRI	Mostly Right	11.25*11.25 *15	View and remember photographs of single faces View and remember photographs of paired faces who were thought to be couples View and remember photographs of single faces	-27 -7 -11 -23 -2 -23 -19 -6 -23	 24 -10 -35 32 -10 -29
Kiehl et al. 2001	MRI	Right	8	Target stimuli (1500Hz-tone) (subjects had to press key) Target stimuli (1500Hz-tone) (subjects had to press key)	-18 -4 -20 -24 -4 -15	20 -2 -20 18 0 -15
Baumgartner et al. 2006	MRI	Right	12	emotional pictures+emotional music excerpt emotional pictures+emotional music excerpt	-20 -4 -24 -17 -4 -20	 24 -8 -24
Berthoz et al. 2006	MRI	Right	8,6	social violation performed by the self and intentional intentional violation of social norms (reading sentences on a monitor)	-10 -2 -24 -16 -6 -22	24 -4 -26
Etkin et al. 2006	MRI	-	8	emotional face with incongruent word over it: low conflict resolution trial high conflict resolution		18 2 -16 16 0 -16
Van der Veen et al. 2006	MRI	-	8	faces with intense emotional expression		28 -5 -27
Cunningham et al. 2004	MRI	-	12	written emotional words: correlation between activation	-20 -4 -16	

				and rated emotion intensity		
Fitzgerald et al. 2006	MRI	Right	8	pictures of faces with different emotions fearful face expression angry face expressions disgusted facial expressions sad facial expressions neutral facial expressions happy facial expressions	-24 -2 -24 -22 -8 -24 -20 -8 -24 -20 -4 -22 -26 -6 -24 -20 -8 -18 -20 -4 -22	
George et al. 2001	MRI	Right	10	faces with direct gaze	-18 6 -24	
Cheng et al. 2006	MRI	Right	6	2.5s movies of a human grasping food double-subtraction: hungry group watching 2.5s movies of a human grasping food vs. 2.5s movies of human grasping pictures	-16 -4 -16 -16 -4 -14	
Bartolo et al. 2006	MRI	Right	9	watching picture and considering it to be funny	-18 -4 -22	
Garrett et al. 2006	MRI	Right	4	watching aversive pictures	-22 4 -20	20 -2 -12
Keightley et al. 2003	MRI	Right	10	direct emotional processing(identify emotion)	-28 -3 -15	16 -3 -24
Eippert et al. 2007	MRI	Right	12	Viewing negative pictures, Viewing neutral pictures (2.5 sec) Viewing negative pictures and decreasing emotional reaction by distancing themselves Viewing negative pictures and increasing emotional reaction Masked viewing negative pictures and increasing emotional reaction, masked by increase-minus-view	-24 -3 -12 -27 -3 -21 -18 0 -12	30 -3 -12 21 3 -18 24 0 -21

10 Acknowledgements

I thank Prof. Dr. Martin Hautzinger and Prof. Dr. Niels Birbaumer from the University of Tübingen for the supervision of this thesis and for making this dissertation possible.

I am very thankful to Dr. Tonio Ball from the Epilepsy Center at the University Hospital Freiburg for the supervision of this research. He inspired and supported this work in a very creative way and he provided the in-house developed software package for the statistical analysis of the amygdala-subregion analysis (MTV).

Looking back, I want to thank Prof. Dr. Jürgen Hennig from the MR-physics at the University Hospital Freiburg for providing the scanner and the equipment for the fMRI experiment. I am very thankful to Prof. Dr. Oliver Speck for the supervision the MR-physics part of this work and for the great technical support.

I thank Prof. Dr. Andreas Schulze-Bonhage from the Epilepsy Center at the University Hospital Freiburg for support and providing optimal working conditions and Prof. Dr. Wilfried Gruhn from the University of Music Freiburg for thoughtful advice on music selection.

Furthermore, I thank Benjamin Rahm, Simon Eickhoff, and Christoph Kaller for their support and helpful discussions. Simon Eickhoff provided the in-house developed software package for the statistical analysis of the amygdala-coactivation analysis.

My warm thanks to Johanna Derix, Tom Breckel, Silvia Willadt, and Johanna Wentlandt for their help in searching the literature for the meta-analyses and/or for support in data analysis.

The MRI-compatible headphones were provided by the University of Freiburg, and the "YAMAHA Stiftung 100 Jahre e. V.", Germany.

11 References

1. Davidson RJ, Irwin W (1999) The functional neuroanatomy of emotion and affective style. Trends Cogn Sci 3: 11-21.

2. Canli T, Sivers H, Whitfield SL, Gotlib IH, Gabrieli JD (2002) Amygdala response to happy faces as a function of extraversion. Science 296: 2191.

3. Leiberg S, Anders S (2006) The multiple facets of empathy: a survey of theory and evidence. Prog Brain Res 156: 419-440.

4. Singer T (2006) The neuronal basis and ontogeny of empathy and mind reading: Review of literature and implications for future research. Neurosci Biobehav Rev

5. Dalgleish T (2004) The emotional brain. Nat Rev Neurosci 5: 583-589.

6. Calder AJ, Lawrence AD, Young AW (2001) Neuropsychology of fear and loathing. Nat Rev Neurosci 2: 352-363.

7. Phelps EA, LeDoux JE (2005) Contributions of the amygdala to emotion processing: from animal models to human behavior. Neuron 48: 175-187.

8. Sander D, Grafman J, Zalla T (2003) The human amygdala: an evolved system for relevance detection. Rev Neurosci 14: 303-316.

9. Vuilleumier P (2005) How brains beware: neural mechanisms of emotional attention. Trends Cogn Sci 9: 585-594.

10. Zald DH (2003) The human amygdala and the emotional evaluation of sensory stimuli. Brain Res Brain Res Rev 41: 88-123.

11. Critchley HD, Wiens S, Rotshtein P, Ohman A, Dolan RJ (2004) Neural systems supporting interoceptive awareness. Nat Neurosci 7: 189-195.

12. Fredrikson M, Furmark T, Olsson MT, Fischer H, Andersson J, Langstrom B (1998) Functional neuroanatomical correlates of electrodermal activity: a positron emission tomographic study. Psychophysiology 35: 179-185.

13. Nagai Y, Critchley HD, Featherstone E, Trimble MR, Dolan RJ (2004) Activity in ventromedial prefrontal cortex covaries with sympathetic skin conductance level: a physiological account of a "default mode" of brain function. Neuroimage 22: 243-251.

14. Critchley HD, Corfield DR, Chandler MP, Mathias CJ, Dolan RJ (2000) Cerebral correlates of autonomic cardiovascular arousal: a functional neuroimaging investigation in humans. J Physiol 523 Pt 1: 259-270.

15. Critchley HD, Daly EM, Bullmore ET, Williams SC, Van Amelsvoort T, Robertson DM, Rowe A, Phillips M, McAlonan G, Howlin P, Murphy DG (2000) The functional neuroanatomy of social behaviour: changes in cerebral blood flow when people with

autistic disorder process facial expressions. Brain 123 (Pt 11): 2203-2212.

16. James W (1894) Physical basis of emotion. Psychological Review 101: 207-230.

17. Niedenthal PM (2007) Embodying emotion. Science 316: 1002-1005.

18. Larsen RJ, Billings DW, Cutler SE (1996) Affect intensity and individual differences in informational style. J Pers 64: 185-207.

19. Eickhoff SB, Laird A, Lancaster JL, Fox PT, Zilles K (2007) Improved activation likelihood estimation meta-analysis of functional imaging data. Submitted

20. Laird AR, Fox PM, Price CJ, Glahn DC, Uecker AM, Lancaster JL, Turkeltaub PE, Kochunov P, Fox PT (2005) ALE meta-analysis: controlling the false discovery rate and performing statistical contrasts. Hum Brain Mapp 25: 155-164.

21. Turkeltaub PE, Eden GF, Jones KM, Zeffiro TA (2002) Meta-analysis of the functional neuroanatomy of single-word reading: method and validation. Neuroimage 16: 765-780.

22. Feredoes E, Postle BR (2007) Localization of load sensitivity of working memory storage: quantitatively and qualitatively discrepant results yielded by single-subject and group-averaged approaches to fMRI group analysis. Neuroimage 35: 881-903.

23. Raemaekers M, Vink M, Zandbelt B, van Wezel RJ, Kahn RS, Ramsey NF (2007) Test-retest reliability of fMRI activation during prosaccades and antisaccades. Neuroimage

24. Amunts K, Kedo O, Kindler M, Pieperhoff P, Mohlberg H, Shah NJ, Habel U, Schneider F, Zilles K (2005) Cytoarchitectonic mapping of the human amygdala, hippocampal region and entorhinal cortex: intersubject variability and probability maps. Anat Embryol (Berl) 210: 343-352.

25. Eickhoff SB, Stephan KE, Mohlberg H, Grefkes C, Fink GR, Amunts K, Zilles K (2005) A new SPM toolbox for combining probabilistic cytoarchitectonic maps and functional imaging data. Neuroimage 25: 1325-1335.

26. Anderson AK, Christoff K, Stappen I, Panitz D, Ghahremani DG, Glover G, Gabrieli JD, Sobel N (2003) Dissociated neural representations of intensity and valence in human olfaction. Nat Neurosci 6: 196-202.

27. Small DM, Gregory MD, Mak YE, Gitelman D, Mesulam MM, Parrish T (2003) Dissociation of neural representation of intensity and affective valuation in human gustation. Neuron 39: 701-711.

28. Winston JS, Gottfried JA, Kilner JM, Dolan RJ (2005) Integrated neural representations of odor intensity and affective valence in human amygdala. J Neurosci 25: 8903-8907.

29. Kim H, Somerville LH, Johnstone T, Alexander AL, Whalen PJ (2003) Inverse amygdala and medial prefrontal cortex responses to surprised faces. Neuroreport 14: 2317-2322.

30. Kim H, Somerville LH, Johnstone T, Polis S, Alexander AL, Shin LM, Whalen PJ (2004) Contextual modulation of amygdala responsivity to surprised faces. J Cogn Neurosci 16: 1730-1745.

31. Whalen PJ, Shin LM, McInerney SC, Fischer H, Wright CI, Rauch SL (2001) A functional MRI study of human amygdala responses to facial expressions of fear versus anger. Emotion 1: 70-83.

32. Sander K, Scheich H (2005) Left auditory cortex and amygdala, but right insula dominance for human laughing and crying. J Cogn Neurosci 17: 1519-1531.

33. Seifritz E, Esposito F, Neuhoff JG, Luthi A, Mustovic H, Dammann G, von Bardeleben U, Radue EW, Cirillo S, Tedeschi G, Di Salle F (2003) Differential sex-independent amygdala response to infant crying and laughing in parents versus nonparents. Biol Psychiatry 54: 1367-1375.

34. Blood AJ, Zatorre RJ (2001) Intensely pleasurable responses to music correlate with activity in brain regions implicated in reward and emotion. Proc Natl Acad Sci U S A 98: 11818-11823.

35. Koelsch S, Fritz T, DY VC, Muller K, Friederici AD (2006) Investigating emotion with music: an fMRI study. Hum Brain Mapp 27: 239-250.

36. Birbaumer N, Grodd W, Diedrich O, Klose U, Erb M, Lotze M, Schneider F, Weiss U, Flor H (1998) fMRI reveals amygdala activation to human faces in social phobics. Neuroreport 9: 1223-1226.

37. Birbaumer N, Veit R, Lotze M, Erb M, Hermann C, Grodd W, Flor H (2005) Deficient fear conditioning in psychopathy: a functional magnetic resonance imaging study. Arch Gen Psychiatry 62: 799-805.

38. Phillips ML, Drevets WC, Rauch SL, Lane R (2003) Neurobiology of emotion perception II: Implications for major psychiatric disorders. Biol Psychiatry 54: 515-528.

39. Veit R, Flor H, Erb M, Hermann C, Lotze M, Grodd W, Birbaumer N (2002) Brain circuits involved in emotional learning in antisocial behavior and social phobia in humans. Neurosci Lett 328: 233-236.

40. Emery N.J., Amaral D.G. (2000) The role of the amygdala in primate social cognition. In: Lane R.D., Nadel L., editors. Cognitive Neuroscience of Emotion. New York: Oxford University Press. pp. 156-191.

41. LeDoux JE (2000) Emotion circuits in the brain. Annu Rev Neurosci 23: 155-184.

42. LeDoux JE (2000) Cognitive-emotional interactions: listen to the brain. In: Lane R.D., Nadel L., editors. Cognitive Neuroscience of Emotion. New York: Oxford University press. pp. 129-155.

43. McDonald AJ (1998) Cortical pathways to the mammalian amygdala. Prog Neurobiol 55: 257-332.

44. McDonald AJ (2003) Is there an amygdala and how far does it extend? An anatomical perspective. Ann N Y Acad Sci 985: 1-21.

45. Price JL (2003) Comparative aspects of amygdala connectivity. Ann N Y Acad Sci 985: 50-58.

46. Pitkanen A, Savander V, LeDoux JE (1997) Organization of intra-amygdaloid circuitries in the rat: an emerging framework for understanding functions of the amygdala. Trends Neurosci 20: 517-523.

47. Sah P, Faber ES, Lopez DA, Power J (2003) The amygdaloid complex: anatomy and physiology. Physiol Rev 83: 803-834.

48. Gonzalez-Lima F, Scheich H (1986) Classical conditioning of tone-signaled bradycardia modifies 2-deoxyglucose uptake patterns in cortex, thalamus, habenula, caudate-putamen and hippocampal formation. Brain Res 363: 239-256.

49. Barbas H, Saha S, Rempel-Clower N, Ghashghaei T (2003) Serial pathways from primate prefrontal cortex to autonomic areas may influence emotional expression. BMC Neurosci 4: 25.

50. Shelley BP, Trimble MR (2004) The insular lobe of Reil--its anatamico-functional, behavioural and neuropsychiatric attributes in humans--a review. World J Biol Psychiatry 5: 176-200.

51. Loewy AD, Spyer KM (1990) Central regulation of autonomic function. Oxford University Press.

52. Mesulam MM, Mufson EJ (1982) Insula of the old world monkey. III: Efferent cortical output and comments on function. J Comp Neurol 212: 38-52.

53. Heimer L, de Olmos JS, Alheid GF, Pearson J, Sakamoto N (1999) The human basal forebrain.

54. Ackermann H, Riecker A (2004) The contribution of the insula to motor aspects of speech production: a review and a hypothesis. Brain Lang 89: 320-328.

55. Augustine JR (1996) Circuitry and functional aspects of the insular lobe in primates including humans. Brain Res Brain Res Rev 22: 229-244.

56. Bamiou DE, Musiek FE, Luxon LM (2003) The insula (Island of Reil) and its role in auditory processing. Literature review. Brain Res Brain Res Rev 42: 143-154.

57. Craig AD (2002) How do you feel? Interoception: the sense of the physiological condition of the body. Nat Rev Neurosci 3: 655-666.

58. Fink GR, Frackowiak RS, Pietrzyk U, Passingham RE (1997) Multiple nonprimary motor areas in the human cortex. J Neurophysiol 77: 2164-2174.

59. Fudge JL, Breitbart MA, Danish M, Pannoni V (2005) Insular and gustatory inputs to the caudal ventral striatum in primates. J Comp Neurol 490: 101-118.

60. Price CJ (2000) The anatomy of language: contributions from functional neuroimaging. J Anat 197 Pt 3: 335-359.

61. Paulus MP, Stein MB (2006) An insular view of anxiety. Biol Psychiatry 60: 383-387.

62. Naqvi NH, Rudrauf D, Damasio H, Bechara A (2007) Damage to the insula disrupts addiction to cigarette smoking. Science 315: 531-534.

63. Thayer JF, Lane RD (2000) A model of neurovisceral integration in emotion regulation and dysregulation. J Affect Disord 61: 201-216.

64. Ture U, Yasargil DC, Al Mefty O, Yasargil MG (1999) Topographic anatomy of the insular region. J Neurosurg 90: 720-733.

65. Chikama M, McFarland NR, Amaral DG, Haber SN (1997) Insular cortical projections to functional regions of the striatum correlate with cortical cytoarchitectonic organization in the primate. J Neurosci 17: 9686-9705.

66. Dosenbach NU, Visscher KM, Palmer ED, Miezin FM, Wenger KK, Kang HC, Burgund ED, Grimes AL, Schlaggar BL, Petersen SE (2006) A core system for the implementation of task sets. Neuron 50: 799-812.

67. Lorberbaum JP, Newman JD, Horwitz AR, Dubno JR, Lydiard RB, Hamner MB, Bohning DE, George MS (2002) A potential role for thalamocingulate circuitry in human maternal behavior. Biol Psychiatry 51: 431-445.

68. Zatorre RJ, Evans AC, Meyer E (1994) Neural mechanisms underlying melodic perception and memory for pitch. J Neurosci 14: 1908-1919.

69. Habib M, Daquin G, Milandre L, Royere ML, Rey M, Lanteri A, Salamon G, Khalil R (1995) Mutism and auditory agnosia due to bilateral insular damage--role of the insula in human communication. Neuropsychologia 33: 327-339.

70. Bamiou DE, Musiek FE, Stow I, Stevens J, Cipolotti L, Brown MM, Luxon LM (2006) Auditory temporal processing deficits in patients with insular stroke. Neurology 67: 614-619.

71. Shuren J (1993) Insula and aphasia. J Neurol 240: 216-218.

72. Zatorre RJ, Meyer E, Gjedde A, Evans AC (1996) PET studies of phonetic processing of speech: review, replication, and reanalysis. Cereb Cortex 6: 21-30.

73. Hickok G, Poeppel D (2007) The cortical organization of speech processing. Nat Rev Neurosci 8: 393-402.

74. Price CJ (2000) The anatomy of language: contributions from functional neuroimaging. J Anat 197 Pt 3: 335-359.

75. Penfield WFME (1955) The insula; further observations on its function. Brain 78: 445-470.

76. Colebatch JG, Deiber MP, Passingham RE, Friston KJ, Frackowiak RS (1991) Regional cerebral blood flow during voluntary arm and hand movements in human subjects. J Neurophysiol 65: 1392-1401.

77. Karnath HO, Baier B, Nagele T (2005) Awareness of the functioning of one's own limbs mediated by the insular cortex? J Neurosci 25: 7134-7138.

78. Hoffman BL, Rasmussen T (1952) Stimulation Studies of Insular Cortex of Macaca Mulatta. Journal of Neurophysiology 16: 343-351.

79. Wall PD, Davis GD (1951) Three cerebral cortical systems affecting autonomic function.

Journal of Neurophysiology 14: 507-517.

80. Oppenheimer SM, Gelb A, Girvin JP, Hachinski VC (1992) Cardiovascular effects of human insular cortex stimulation. Neurology 42: 1727-1732.

81. Yasui Y, Breder CD, Saper CB, Cechetto DF (1991) Autonomic responses and efferent pathways from the insular cortex in the rat. J Comp Neurol 303: 355-374.

82. Critchley HD, Tang J, Glaser D, Butterworth B, Dolan RJ (2005) Anterior cingulate activity during error and autonomic response. Neuroimage 27: 885-895.

83. Servan-Schreiber D, Perlstein WM, Cohen JD, Mintun M (1998) Selective pharmacological activation of limbic structures in human volunteers: a positron emission tomography study. J Neuropsychiatry Clin Neurosci 10: 148-159.

84. Larsen RJ, Diener E (1987) Affect intensity as an individual difference characteristic: A review. Journal of research in personality 21: 1-39.

85. Flett G.L.Boase P.McAndrews M.P.Pliner P.Blankstein K.R. (1986) Affect intensity and the appraisal of emotion. Journal of research in personality 20: 447-459.

86. Thompson CP (1985) Memory for unique personal events: effects of pleasantness. Motivation and Emotion 9: 277-289.

87. Haddock G., Zanna M.P., Esses V.M. (1994) Mood and the expression of intergroup attitudes: The moderating role of affect intensity. European Journal of Social Psychology 24: 189-205.

88. Mutschler I., Schulze-Bonhage A, Rotter S, Ball T. (2007) The impact of affect intensity on recognition of the emotional content of music.

89. Ritz T (1994) Alexithymic characteristics and affective intensity: adaption and relationship between two self-report instruments. Zeitschrift für Differentielle und Diagnostische Psychologie 15: 23-39.

90. Juslin PN (2000) Cue utilization in communication of emotion in music performance: relating performance to perception. J Exp Psychol Hum Percept Perform 26: 1797-1813.

91. Adolphs R, Damasio H, Tranel D, Cooper G, Damasio AR (2000) A role for somatosensory cortices in the visual recognition of emotion as revealed by three-dimensional lesion mapping. J Neurosci 20: 2683-2690.

92. Oldfield RC (1971) The assessment and analysis of handedness: the Edinburgh inventory. Neuropsychologia 9: 97-113.

93. Wicker B, Keysers C, Plailly J, Royet JP, Gallese V, Rizzolatti G (2003) Both of us disgusted in My insula: the common neural basis of seeing and feeling disgust. Neuron 40: 655-664.

94. Liberzon I, Phan KL, Decker LR, Taylor SF (2003) Extended amygdala and emotional salience: a PET activation study of positive and negative affect. Neuropsychopharmacology 28: 726-733.

95. Breiter HC, Etcoff NL, Whalen PJ, Kennedy WA, Rauch SL, Buckner RL, Strauss MM, Hyman SE, Rosen BR (1996) Response and habituation of the human amygdala during visual processing of facial expression. Neuron 17: 875-887.

96. Wright CI, Fischer H, Whalen PJ, McInerney SC, Shin LM, Rauch SL (2001) Differential prefrontal cortex and amygdala habituation to repeatedly presented emotional stimuli. Neuroreport 12: 379-383.

97. Fischer H, Wright CI, Whalen PJ, McInerney SC, Shin LM, Rauch SL (2003) Brain habituation during repeated exposure to fearful and neutral faces: a functional MRI study. Brain Res Bull 59: 387-392.

98. Phillips ML, Medford N, Young AW, Williams L, Williams SC, Bullmore ET, Gray JA, Brammer MJ (2001) Time courses of left and right amygdalar responses to fearful facial expressions. Hum Brain Mapp 12: 193-202.

99. Laux L, Glanzmann P, Schaffner P, Spielberger C.D. (1981) Das State-Trait-Angsinventar (STAI). Weinheim: Beltz Verlag.

100. Litle P, Zuckerman M (1985) Sensation seeking and music performance. Personality and Individual Differences 7: 575-577.

101. Ogawa S, Lee TM, Kay AR, Tank DW (1990) Brain magnetic resonance imaging with contrast dependent on blood oxygenation. Proc Natl Acad Sci U S A 87: 9868-9872.

102. Logothetis NK, Pauls J, Augath M, Trinath T, Oeltermann A (2001) Neurophysiological investigation of the basis of the fMRI signal. Nature 412: 150-157.

103. Shmuel A, Augath M, Oeltermann A, Logothetis NK (2006) Negative functional MRI response correlates with decreases in neuronal activity in monkey visual area V1. Nat Neurosci 9: 569-577.

104. Mukamel R, Gelbard H, Arieli A, Hasson U, Fried I, Malach R (2005) Coupling between neuronal firing, field potentials, and FMRI in human auditory cortex. Science 309: 951-954.

105. Cordes D, Turski PA, Sorenson JA (2000) Compensation of susceptibility-induced signal loss in echo-planar imaging for functional applications. Magn Reson Imaging 18: 1055-1068.

106. Zaitsev M, Hennig J, Speck O (2004) Point spread function mapping with parallel imaging techniques and high acceleration factors: fast, robust, and flexible method for echo-planar imaging distortion correction. Magn Reson Med 52: 1156-1166.

107. Turner R (2002) How much cortex can a vein drain? Downstream dilution of activation-related cerebral blood oxygenation changes. Neuroimage 16: 1062-1067.

108. Merksz M, Ambach G, Palkovits M (1978) Blood supply of the rat amygdala. Acta Morphol Acad Sci Hung 26: 139-171.

109. Robinson S, Windischberger C, Rauscher A, Moser E (2004) Optimized 3 T EPI of the amygdalae. Neuroimage 22: 203-210.

110. Brett M, Johnsrude IS, Owen AM (2002) The problem of functional localization in the human brain. Nat Rev Neurosci 3: 243-249.

111. Brodmann K (1909) Vergleichende Lokalisationslehre der Grosshirnrinde. Leipzig: Barth.

112. Amunts K, Zilles K (2001) Advances in cytoarchitectonic mapping of the human cerebral cortex. Neuroimaging Clin N Am 11: 151-69, vii.

113. Zilles K, Schleicher A, Palomero-Gallather N, Amunts K (2002) Quantitative analysis of cyto- and receptor architecture of the human brain. In: Mazziotta J, Toga A, editors. Brain mapping, the methods. Elsevier. pp. 573-602.

114. Talairach J, Tournoux P. (1988) Coplanar stereotactic atlas of the human brain. Thieme, Stuttgart.

115. Anderson AK, Christoff K, Panitz D, De Rosa E, Gabrieli JD (2003) Neural correlates of the automatic processing of threat facial signals. J Neurosci 23: 5627-5633.

116. Ashwin C, Baron-Cohen S, Wheelwright S, O'Riordan M, Bullmore ET (2007) Differential activation of the amygdala and the 'social brain' during fearful face-processing in Asperger Syndrome. Neuropsychologia 45: 2-14.

117. Bartolo A, Benuzzi F, Nocetti L, Baraldi P, Nichelli P (2006) Humor comprehension and appreciation: an FMRI study. J Cogn Neurosci 18: 1789-1798.

118. Baumgartner T, Lutz K, Schmidt CF, Jancke L (2006) The emotional power of music: how music enhances the feeling of affective pictures. Brain Res 1075: 151-164.

119. Beauregard M, Levesque J, Bourgouin P (2001) Neural correlates of conscious self-regulation of emotion. J Neurosci 21: RC165.

120. Beaver JD, Lawrence AD, van Ditzhuijzen J, Davis MH, Woods A, Calder AJ (2006) Individual differences in reward drive predict neural responses to images of food. J Neurosci 26: 5160-5166.

121. Berns GS, Chappelow J, Zink CF, Pagnoni G, Martin-Skurski ME, Richards J (2005) Neurobiological correlates of social conformity and independence during mental rotation. Biol Psychiatry 58: 245-253.

122. Berthoz S, Grezes J, Armony JL, Passingham RE, Dolan RJ (2006) Affective response to one's own moral violations. Neuroimage 31: 945-950.

123. Bishop SJ, Duncan J, Lawrence AD (2004) State anxiety modulation of the amygdala response to unattended threat-related stimuli. J Neurosci 24: 10364-10368.

124. Bishop SJ, Jenkins R, Lawrence AD (2006) Neural Processing of Fearful Faces: Effects of Anxiety are Gated by Perceptual Capacity Limitations. Cereb Cortex

125. Bornhovd K, Quante M, Glauche V, Bromm B, Weiller C, Buchel C (2002) Painful stimuli evoke different stimulus-response functions in the amygdala, prefrontal, insula and somatosensory cortex: a single-trial fMRI study. Brain 125: 1326-1336.

126. Britton JC, Phan KL, Taylor SF, Fig LM, Liberzon I (2005) Corticolimbic blood flow in

posttraumatic stress disorder during script-driven imagery. Biol Psychiatry 57: 832-840.

127. Canli T, Sivers H, Whitfield SL, Gotlib IH, Gabrieli JD (2002) Amygdala response to happy faces as a function of extraversion. Science 296: 2191.

128. Canli T, Congdon E, Gutknecht L, Constable RT, Lesch KP (2005) Amygdala responsiveness is modulated by tryptophan hydroxylase-2 gene variation. J Neural Transm 112: 1479-1485.

129. Carter RM, O'Doherty JP, Seymour B, Koch C, Dolan RJ (2006) Contingency awareness in human aversive conditioning involves the middle frontal gyrus. Neuroimage 29: 1007-1012.

130. Castriota-Scanderbeg A, Hagberg GE, Cerasa A, Committeri G, Galati G, Patria F, Pitzalis S, Caltagirone C, Frackowiak R (2005) The appreciation of wine by sommeliers: a functional magnetic resonance study of sensory integration. Neuroimage 25: 570-578.

131. Cheng Y, Meltzoff AN, Decety J (2006) Motivation Modulates the Activity of the Human Mirror-Neuron System. Cereb Cortex

132. Corden B, Critchley HD, Skuse D, Dolan RJ (2006) Fear recognition ability predicts differences in social cognitive and neural functioning in men. J Cogn Neurosci 18: 889-897.

133. Coricelli G, Critchley HD, Joffily M, O'Doherty JP, Sirigu A, Dolan RJ (2005) Regret and its avoidance: a neuroimaging study of choice behavior. Nat Neurosci 8: 1255-1262.

134. Critchley HD, Corfield DR, Chandler MP, Mathias CJ, Dolan RJ (2000) Cerebral correlates of autonomic cardiovascular arousal: a functional neuroimaging investigation in humans. J Physiol 523 Pt 1: 259-270.

135. Cunningham WA, Raye CL, Johnson MK (2004) Implicit and explicit evaluation: FMRI correlates of valence, emotional intensity, and control in the processing of attitudes. J Cogn Neurosci 16: 1717-1729.

136. Das P, Kemp AH, Liddell BJ, Brown KJ, Olivieri G, Peduto A, Gordon E, Williams LM (2005) Pathways for fear perception: modulation of amygdala activity by thalamo-cortical systems. Neuroimage 26: 141-148.

137. de Araujo IE, Rolls ET, Velazco MI, Margot C, Cayeux I (2005) Cognitive modulation of olfactory processing. Neuron 46: 671-679.

138. De Martino B, Kumaran D, Seymour B, Dolan RJ (2006) Frames, biases, and rational decision-making in the human brain. Science 313: 684-687.

139. Del Ben CM, Deakin JF, McKie S, Delvai NA, Williams SR, Elliott R, Dolan M, Anderson IM (2005) The effect of citalopram pretreatment on neuronal responses to neuropsychological tasks in normal volunteers: an FMRI study. Neuropsychopharmacology 30: 1724-1734.

140. Desseilles M, Vu TD, Laureys S, Peigneux P, Degueldre C, Phillips C, Maquet P (2006) A prominent role for amygdaloid complexes in the Variability in Heart Rate (VHR)

during Rapid Eye Movement (REM) sleep relative to wakefulness. Neuroimage 32: 1008-1015.

141. Dresel C, Castrop F, Haslinger B, Wohlschlaeger AM, Hennenlotter A, Ceballos-Baumann AO (2005) The functional neuroanatomy of coordinated orofacial movements: sparse sampling fMRI of whistling. Neuroimage 28: 588-597.

142. Eippert F, Veit R, Weiskopf N, Erb M, Birbaumer N, Anders S (2007) Regulation of emotional responses elicited by threat-related stimuli. Hum Brain Mapp 28: 409-423.

143. Elliott R, Newman JL, Longe OA, Deakin JF (2003) Differential response patterns in the striatum and orbitofrontal cortex to financial reward in humans: a parametric functional magnetic resonance imaging study. J Neurosci 23: 303-307.

144. Ernst M, Bolla K, Mouratidis M, Contoreggi C, Matochik JA, Kurian V, Cadet JL, Kimes AS, London ED (2002) Decision-making in a risk-taking task: a PET study. Neuropsychopharmacology 26: 682-691.

145. Ethofer T, Anders S, Erb M, Droll C, Royen L, Saur R, Reiterer S, Grodd W, Wildgruber D (2006) Impact of voice on emotional judgment of faces: an event-related fMRI study. Hum Brain Mapp 27: 707-714.

146. Etkin A, Klemenhagen KC, Dudman JT, Rogan MT, Hen R, Kandel ER, Hirsch J (2004) Individual differences in trait anxiety predict the response of the basolateral amygdala to unconsciously processed fearful faces. Neuron 44: 1043-1055.

147. Etkin A, Egner T, Peraza DM, Kandel ER, Hirsch J (2006) Resolving emotional conflict: a role for the rostral anterior cingulate cortex in modulating activity in the amygdala. Neuron 51: 871-882.

148. Eugene F, Levesque J, Mensour B, Leroux JM, Beaudoin G, Bourgouin P, Beauregard M (2003) The impact of individual differences on the neural circuitry underlying sadness. Neuroimage 19: 354-364.

149. Evans KC, Banzett RB, Adams L, McKay L, Frackowiak RS, Corfield DR (2002) BOLD fMRI identifies limbic, paralimbic, and cerebellar activation during air hunger. J Neurophysiol 88: 1500-1511.

150. Fischer H, Sandblom J, Herlitz A, Fransson P, Wright CI, Backman L (2004) Sex-differential brain activation during exposure to female and male faces. Neuroreport 15: 235-238.

151. Fitzgerald DA, Angstadt M, Jelsone LM, Nathan PJ, Phan KL (2006) Beyond threat: amygdala reactivity across multiple expressions of facial affect. Neuroimage 30: 1441-1448.

152. Garrett AS, Maddock RJ (2006) Separating subjective emotion from the perception of emotion-inducing stimuli: an fMRI study. Neuroimage 33: 263-274.

153. George N, Driver J, Dolan RJ (2001) Seen gaze-direction modulates fusiform activity and its coupling with other brain areas during face processing. Neuroimage 13: 1102-1112.

154. Glascher J, Tuscher O, Weiller C, Buchel C (2004) Elevated responses to constant facial emotions in different faces in the human amygdala: an fMRI study of facial identity

and expression. BMC Neurosci 5: 45.

155. Goldstein JM, Jerram M, Poldrack R, Ahern T, Kennedy DN, Seidman LJ, Makris N (2005) Hormonal cycle modulates arousal circuitry in women using functional magnetic resonance imaging. J Neurosci 25: 9309-9316.

156. Gottfried JA, O'Doherty J, Dolan RJ (2002) Appetitive and aversive olfactory learning in humans studied using event-related functional magnetic resonance imaging. J Neurosci 22: 10829-10837.

157. Gottfried JA, Deichmann R, Winston JS, Dolan RJ (2002) Functional heterogeneity in human olfactory cortex: an event-related functional magnetic resonance imaging study. J Neurosci 22: 10819-10828.

158. Gottfried JA, Dolan RJ (2003) The nose smells what the eye sees: crossmodal visual facilitation of human olfactory perception. Neuron 39: 375-386.

159. Gottfried JA, O'Doherty J, Dolan RJ (2003) Encoding predictive reward value in human amygdala and orbitofrontal cortex. Science 301: 1104-1107.

160. Gottfried JA, Dolan RJ (2004) Human orbitofrontal cortex mediates extinction learning while accessing conditioned representations of value. Nat Neurosci 7: 1144-1152.

161. Habel U, Klein M, Kellermann T, Shah NJ, Schneider F (2005) Same or different? Neural correlates of happy and sad mood in healthy males. Neuroimage 26: 206-214.

162. Hamann S, Mao H (2002) Positive and negative emotional verbal stimuli elicit activity in the left amygdala. Neuroreport 13: 15-19.

163. Hamann S, Herman RA, Nolan CL, Wallen K (2004) Men and women differ in amygdala response to visual sexual stimuli. Nat Neurosci 7: 411-416.

164. Harenski CL, Hamann S (2006) Neural correlates of regulating negative emotions related to moral violations. Neuroimage 30: 313-324.

165. Hariri AR, Bookheimer SY, Mazziotta JC (2000) Modulating emotional responses: effects of a neocortical network on the limbic system. Neuroreport 11: 43-48.

166. Hariri AR, Mattay VS, Tessitore A, Fera F, Smith WG, Weinberger DR (2002) Dextroamphetamine modulates the response of the human amygdala. Neuropsychopharmacology 27: 1036-1040.

167. Hariri AR, Mattay VS, Tessitore A, Fera F, Weinberger DR (2003) Neocortical modulation of the amygdala response to fearful stimuli. Biol Psychiatry 53: 494-501.

168. Hennenlotter A, Schroeder U, Erhard P, Castrop F, Haslinger B, Stoecker D, Lange KW, Ceballos-Baumann AO (2005) A common neural basis for receptive and expressive communication of pleasant facial affect. Neuroimage 26: 581-591.

169. Holstege G, Georgiadis JR, Paans AM, Meiners LC, van der Graaf FH, Reinders AA (2003) Brain activation during human male ejaculation. J Neurosci 23: 9185-9193.

170. Hooker CI, Germine LT, Knight RT, D'Esposito M (2006) Amygdala response to facial

expressions reflects emotional learning. J Neurosci 26: 8915-8922.

171. Keightley ML, Winocur G, Graham SJ, Mayberg HS, Hevenor SJ, Grady CL (2003) An fMRI study investigating cognitive modulation of brain regions associated with emotional processing of visual stimuli. Neuropsychologia 41: 585-596.

172. Kiehl KA, Laurens KR, Duty TL, Forster BB, Liddle PF (2001) Neural sources involved in auditory target detection and novelty processing: an event-related fMRI study. Psychophysiology 38: 133-142.

173. Killgore WD, Casasanto DJ, Yurgelun-Todd DA, Maldjian JA, Detre JA (2000) Functional activation of the left amygdala and hippocampus during associative encoding. Neuroreport 11: 2259-2263.

174. Killgore WD, Young AD, Femia LA, Bogorodzki P, Rogowska J, Yurgelun-Todd DA (2003) Cortical and limbic activation during viewing of high- versus low-calorie foods. Neuroimage 19: 1381-1394.

175. Killgore WD, Yurgelun-Todd DA (2004) Activation of the amygdala and anterior cingulate during nonconscious processing of sad versus happy faces. Neuroimage 21: 1215-1223.

176. Kilpatrick L, Cahill L (2003) Amygdala modulation of parahippocampal and frontal regions during emotionally influenced memory storage. Neuroimage 20: 2091-2099.

177. Kirsch P, Esslinger C, Chen Q, Mier D, Lis S, Siddhanti S, Gruppe H, Mattay VS, Gallhofer B, Meyer-Lindenberg A (2005) Oxytocin modulates neural circuitry for social cognition and fear in humans. J Neurosci 25: 11489-11493.

178. LaBar KS, Gitelman DR, Parrish TB, Kim YH, Nobre AC, Mesulam MM (2001) Hunger selectively modulates corticolimbic activation to food stimuli in humans. Behav Neurosci 115: 493-500.

179. LaBar KS, Crupain MJ, Voyvodic JT, McCarthy G (2003) Dynamic perception of facial affect and identity in the human brain. Cereb Cortex 13: 1023-1033.

180. Levesque J, Eugene F, Joanette Y, Paquette V, Mensour B, Beaudoin G, Leroux JM, Bourgouin P, Beauregard M (2003) Neural circuitry underlying voluntary suppression of sadness. Biol Psychiatry 53: 502-510.

181. Lewis PA, Critchley HD, Rotshtein P, Dolan RJ (2007) Neural correlates of processing valence and arousal in affective words. Cereb Cortex 17: 742-748.

182. Liddell BJ, Brown KJ, Kemp AH, Barton MJ, Das P, Peduto A, Gordon E, Williams LM (2005) A direct brainstem-amygdala-cortical 'alarm' system for subliminal signals of fear. Neuroimage 24: 235-243.

183. Lotze M, Heymans U, Birbaumer N, Veit R, Erb M, Flor H, Halsband U (2006) Differential cerebral activation during observation of expressive gestures and motor acts. Neuropsychologia 44: 1787-1795.

184. McClure EB, Monk CS, Nelson EE, Zarahn E, Leibenluft E, Bilder RM, Charney DS, Ernst M, Pine DS (2004) A developmental examination of gender differences in brain

engagement during evaluation of threat. Biol Psychiatry 55: 1047-1055.

185. Morris JS, Buchel C, Dolan RJ (2001) Parallel neural responses in amygdala subregions and sensory cortex during implicit fear conditioning. Neuroimage 13: 1044-1052.

186. Morris JS, Dolan RJ (2004) Dissociable amygdala and orbitofrontal responses during reversal fear conditioning. Neuroimage 22: 372-380.

187. O'Doherty J, Critchley H, Deichmann R, Dolan RJ (2003) Dissociating valence of outcome from behavioral control in human orbital and ventral prefrontal cortices. J Neurosci 23: 7931-7939.

188. O'Doherty JP, Deichmann R, Critchley HD, Dolan RJ (2002) Neural responses during anticipation of a primary taste reward. Neuron 33: 815-826.

189. Ochsner KN, Bunge SA, Gross JJ, Gabrieli JD (2002) Rethinking feelings: an FMRI study of the cognitive regulation of emotion. J Cogn Neurosci 14: 1215-1229.

190. Ochsner KN, Ray RD, Cooper JC, Robertson ER, Chopra S, Gabrieli JD, Gross JJ (2004) For better or for worse: neural systems supporting the cognitive down- and up-regulation of negative emotion. Neuroimage 23: 483-499.

191. Ogino Y, Nemoto H, Inui K, Saito S, Kakigi R, Goto F (2007) Inner experience of pain: imagination of pain while viewing images showing painful events forms subjective pain representation in human brain. Cereb Cortex 17: 1139-1146.

192. Pessoa L, Padmala S, Morland T (2005) Fate of unattended fearful faces in the amygdala is determined by both attentional resources and cognitive modulation. Neuroimage 28: 249-255.

193. Phan KL, Liberzon I, Welsh RC, Britton JC, Taylor SF (2003) Habituation of rostral anterior cingulate cortex to repeated emotionally salient pictures. Neuropsychopharmacology 28: 1344-1350.

194. Phan KL, Taylor SF, Welsh RC, Ho SH, Britton JC, Liberzon I (2004) Neural correlates of individual ratings of emotional salience: a trial-related fMRI study. Neuroimage 21: 768-780.

195. Phan KL, Fitzgerald DA, Nathan PJ, Moore GJ, Uhde TW, Tancer ME (2005) Neural substrates for voluntary suppression of negative affect: a functional magnetic resonance imaging study. Biol Psychiatry 57: 210-219.

196. Plailly J, Bensafi M, Pachot-Clouard M, Delon-Martin C, Kareken DA, Rouby C, Segebarth C, Royet JP (2005) Involvement of right piriform cortex in olfactory familiarity judgments. Neuroimage 24: 1032-1041.

197. Protopopescu X, Pan H, Tuescher O, Cloitre M, Goldstein M, Engelien W, Epstein J, Yang Y, Gorman J, LeDoux J, Silbersweig D, Stern E (2005) Differential time courses and specificity of amygdala activity in posttraumatic stress disorder subjects and normal control subjects. Biol Psychiatry 57: 464-473.

198. Royet JP, Zald D, Versace R, Costes N, Lavenne F, Koenig O, Gervais R (2000) Emotional responses to pleasant and unpleasant olfactory, visual, and auditory stimuli: a positron

emission tomography study. J Neurosci 20: 7752-7759.

199. Royet JP, Plailly J, Delon-Martin C, Kareken DA, Segebarth C (2003) fMRI of emotional responses to odors: influence of hedonic valence and judgment, handedness, and gender. Neuroimage 20: 713-728.

200. Ruby P, Decety J (2004) How would you feel versus how do you think she would feel? A neuroimaging study of perspective-taking with social emotions. J Cogn Neurosci 16: 988-999.

201. Sato W, Yoshikawa S, Kochiyama T, Matsumura M (2004) The amygdala processes the emotional significance of facial expressions: an fMRI investigation using the interaction between expression and face direction. Neuroimage 22: 1006-1013.

202. Schendan HE, Searl MM, Melrose RJ, Stern CE (2003) An FMRI study of the role of the medial temporal lobe in implicit and explicit sequence learning. Neuron 37: 1013-1025.

203. Schienle A, Schafer A, Stark R, Walter B, Vaitl D (2005) Relationship between disgust sensitivity, trait anxiety and brain activity during disgust induction. Neuropsychobiology 51: 86-92.

204. Sergerie K, Lepage M, Armony JL (2006) A process-specific functional dissociation of the amygdala in emotional memory. J Cogn Neurosci 18: 1359-1367.

205. Seymour B, O'Doherty JP, Koltzenburg M, Wiech K, Frackowiak R, Friston K, Dolan R (2005) Opponent appetitive-aversive neural processes underlie predictive learning of pain relief. Nat Neurosci 8: 1234-1240.

206. Singer T, Kiebel SJ, Winston JS, Dolan RJ, Frith CD (2004) Brain responses to the acquired moral status of faces. Neuron 41: 653-662.

207. Small DM, Gerber JC, Mak YE, Hummel T (2005) Differential neural responses evoked by orthonasal versus retronasal odorant perception in humans. Neuron 47: 593-605.

208. Somerville LH, Wig GS, Whalen PJ, Kelley WM (2006) Dissociable medial temporal lobe contributions to social memory. J Cogn Neurosci 18: 1253-1265.

209. Stark R, Schienle A, Walter B, Kirsch P, Blecker C, Ott U, Schafer A, Sammer G, Zimmermann M, Vaitl D (2004) Hemodynamic effects of negative emotional pictures - a test-retest analysis. Neuropsychobiology 50: 108-118.

210. Stark R, Schienle A, Girod C, Walter B, Kirsch P, Blecker C, Ott U, Schafer A, Sammer G, Zimmermann M, Vaitl D (2005) Erotic and disgust-inducing pictures--differences in the hemodynamic responses of the brain. Biol Psychol 70: 19-29.

211. Sterpenich V, D'Argembeau A, Desseilles M, Balteau E, Albouy G, Vandewalle G, Degueldre C, Luxen A, Collette F, Maquet P (2006) The locus ceruleus is involved in the successful retrieval of emotional memories in humans. J Neurosci 26: 7416-7423.

212. Tabbert K, Stark R, Kirsch P, Vaitl D (2006) Dissociation of neural responses and skin conductance reactions during fear conditioning with and without awareness of stimulus contingencies. Neuroimage 32: 761-770.

213. Takahashi H, Matsuura M, Yahata N, Koeda M, Suhara T, Okubo Y (2006) Men and women show distinct brain activations during imagery of sexual and emotional infidelity. Neuroimage 32: 1299-1307.

214. Taylor SE, Eisenberger NI, Saxbe D, Lehman BJ, Lieberman MD (2006) Neural responses to emotional stimuli are associated with childhood family stress. Biol Psychiatry 60: 296-301.

215. Van Der Veen FM, Evers EA, Deutz NE, Schmitt JA (2007) Effects of acute tryptophan depletion on mood and facial emotion perception related brain activation and performance in healthy women with and without a family history of depression. Neuropsychopharmacology 32: 216-224.

216. Vuilleumier P, Armony JL, Driver J, Dolan RJ (2001) Effects of attention and emotion on face processing in the human brain: an event-related fMRI study. Neuron 30: 829-841.

217. Vuilleumier P, Armony JL, Driver J, Dolan RJ (2003) Distinct spatial frequency sensitivities for processing faces and emotional expressions. Nat Neurosci 6: 624-631.

218. Vuilleumier P, Richardson MP, Armony JL, Driver J, Dolan RJ (2004) Distant influences of amygdala lesion on visual cortical activation during emotional face processing. Nat Neurosci 7: 1271-1278.

219. Wang L, LaBar KS, McCarthy G (2006) Mood alters amygdala activation to sad distractors during an attentional task. Biol Psychiatry 60: 1139-1146.

220. Wild B, Erb M, Eyb M, Bartels M, Grodd W (2003) Why are smiles contagious? An fMRI study of the interaction between perception of facial affect and facial movements. Psychiatry Res 123: 17-36.

221. Williams LM, Barton MJ, Kemp AH, Liddell BJ, Peduto A, Gordon E, Bryant RA (2005) Distinct amygdala-autonomic arousal profiles in response to fear signals in healthy males and females. Neuroimage 28: 618-626.

222. Williams LM, Das P, Liddell BJ, Kemp AH, Rennie CJ, Gordon E (2006) Mode of functional connectivity in amygdala pathways dissociates level of awareness for signals of fear. J Neurosci 26: 9264-9271.

223. Williams LM, Brown KJ, Palmer D, Liddell BJ, Kemp AH, Olivieri G, Peduto A, Gordon E (2006) The mellow years?: neural basis of improving emotional stability over age. J Neurosci 26: 6422-6430.

224. Williams MA, Morris AP, McGlone F, Abbott DF, Mattingley JB (2004) Amygdala responses to fearful and happy facial expressions under conditions of binocular suppression. J Neurosci 24: 2898-2904.

225. Winston JS, Strange BA, O'Doherty J, Dolan RJ (2002) Automatic and intentional brain responses during evaluation of trustworthiness of faces. Nat Neurosci 5: 277-283.

226. Winston JS, Vuilleumier P, Dolan RJ (2003) Effects of low-spatial frequency components of fearful faces on fusiform cortex activity. Curr Biol 13: 1824-1829.

227. Winston JS, O'Doherty J, Dolan RJ (2003) Common and distinct neural responses during direct and incidental processing of multiple facial emotions. Neuroimage 20: 84-97.

228. Winston JS, O'Doherty J, Kilner JM, Perrett DI, Dolan RJ (2007) Brain systems for assessing facial attractiveness. Neuropsychologia 45: 195-206.

229. Wood JN, Romero SG, Knutson KM, Grafman J (2005) Representation of attitudinal knowledge: role of prefrontal cortex, amygdala and parahippocampal gyrus. Neuropsychologia 43: 249-259.

230. Yang TT, Menon V, Eliez S, Blasey C, White CD, Reid AJ, Gotlib IH, Reiss AL (2002) Amygdalar activation associated with positive and negative facial expressions. Neuroreport 13: 1737-1741.

231. Smith AP, Stephan KE, Rugg MD, Dolan RJ (2006) Task and content modulate amygdala-hippocampal connectivity in emotional retrieval. Neuron 49: 631-638.

232. Beaucousin V, Lacheret A, Turbelin MR, Morel M, Mazoyer B, Tzourio-Mazoyer N (2007) FMRI study of emotional speech comprehension. Cereb Cortex 17: 339-352.

233. Dehaene-Lambertz G, Dehaene S, Anton JL, Campagne A, Ciuciu P, Dehaene GP, Denghien I, Jobert A, Lebihan D, Sigman M, Pallier C, Poline JB (2006) Functional segregation of cortical language areas by sentence repetition. Hum Brain Mapp 27: 360-371.

234. Meyer M, Alter K, Friederici AD, Lohmann G, von Cramon DY (2002) FMRI reveals brain regions mediating slow prosodic modulations in spoken sentences. Hum Brain Mapp 17: 73-88.

235. Roder B, Stock O, Neville H, Bien S, Rosler F (2002) Brain activation modulated by the comprehension of normal and pseudo-word sentences of different processing demands: a functional magnetic resonance imaging study. Neuroimage 15: 1003-1014.

236. Skipper JI, Nusbaum HC, Small SL (2005) Listening to talking faces: motor cortical activation during speech perception. Neuroimage 25: 76-89.

237. Xiao Z, Zhang JX, Wang X, Wu R, Hu X, Weng X, Tan LH (2005) Differential activity in left inferior frontal gyrus for pseudowords and real words: an event-related fMRI study on auditory lexical decision. Hum Brain Mapp 25: 212-221.

238. Blank SC, Scott SK, Murphy K, Warburton E, Wise RJ (2002) Speech production: Wernicke, Broca and beyond. Brain 125: 1829-1838.

239. Brown S, Martinez MJ, Parsons LM (2006) Music and language side by side in the brain: a PET study of the generation of melodies and sentences. Eur J Neurosci 23: 2791-2803.

240. Hashimoto Y, Sakai KL (2003) Brain activations during conscious self-monitoring of speech production with delayed auditory feedback: an fMRI study. Hum Brain Mapp 20: 22-28.

241. Riecker A, Ackermann H, Wildgruber D, Dogil G, Grodd W (2000) Opposite hemispheric lateralization effects during speaking and singing at motor cortex, insula and

cerebellum. Neuroreport 11: 1997-2000.

242. Riecker A, Wildgruber D, Dogil G, Grodd W, Ackermann H (2002) Hemispheric lateralization effects of rhythm implementation during syllable repetitions: an fMRI study. Neuroimage 16: 169-176.

243. Bengtsson SL, Ullen F (2006) Dissociation between melodic and rhythmic processing during piano performance from musical scores. Neuroimage 30: 272-284.

244. Brown S, Martinez MJ, Parsons LM (2004) Passive music listening spontaneously engages limbic and paralimbic systems. Neuroreport 15: 2033-2037.

245. Mitterschiffthaler MT, Fu CH, Dalton JA, Andrew CM, Williams SC (2007) A functional MRI study of happy and sad affective states induced by classical music. Hum Brain Mapp

246. Platel H, Price C, Baron JC, Wise R, Lambert J, Frackowiak RS, Lechevalier B, Eustache F (1997) The structural components of music perception. A functional anatomical study. Brain 120 (Pt 2): 229-243.

247. Tillmann B, Koelsch S, Escoffier N, Bigand E, Lalitte P, Friederici AD, von Cramon DY (2006) Cognitive priming in sung and instrumental music: activation of inferior frontal cortex. Neuroimage 31: 1771-1782.

248. Ciccarelli O, Toosy AT, Marsden JF, Wheeler-Kingshott CM, Sahyoun C, Matthews PM, Miller DH, Thompson AJ (2005) Identifying brain regions for integrative sensorimotor processing with ankle movements. Exp Brain Res 166: 31-42.

249. Cunnington R, Windischberger C, Deecke L, Moser E (2002) The preparation and execution of self-initiated and externally-triggered movement: a study of event-related fMRI. Neuroimage 15: 373-385.

250. Dobkin BH, Firestine A, West M, Saremi K, Woods R (2004) Ankle dorsiflexion as an fMRI paradigm to assay motor control for walking during rehabilitation. Neuroimage 23: 370-381.

251. Ehrsson HH, Fagergren A, Jonsson T, Westling G, Johansson RS, Forssberg H (2000) Cortical activity in precision- versus power-grip tasks: an fMRI study. J Neurophysiol 83: 528-536.

252. Indovina I, Sanes JN (2001) Combined visual attention and finger movement effects on human brain representations. Exp Brain Res 140: 265-279.

253. Jahanshahi M, Jenkins IH, Brown RG, Marsden CD, Passingham RE, Brooks DJ (1995) Self-initiated versus externally triggered movements. I. An investigation using measurement of regional cerebral blood flow with PET and movement-related potentials in normal and Parkinson's disease subjects. Brain 118 (Pt 4): 913-933.

254. Jantzen KJ, Steinberg FL, Kelso JA (2002) Practice-dependent modulation of neural activity during human sensorimotor coordination: a functional Magnetic Resonance Imaging study. Neurosci Lett 332: 205-209.

255. Johansen-Berg H, Matthews PM (2002) Attention to movement modulates activity in

sensori-motor areas, including primary motor cortex. Exp Brain Res 142: 13-24.

256. Kawashima R, Okuda J, Umetsu A, Sugiura M, Inoue K, Suzuki K, Tabuchi M, Tsukiura T, Narayan SL, Nagasaka T, Yanagawa I, Fujii T, Takahashi S, Fukuda H, Yamadori A (2000) Human cerebellum plays an important role in memory-timed finger movement: an fMRI study. J Neurophysiol 83: 1079-1087.

257. Kew JJ, Brooks DJ, Passingham RE, Rothwell JC, Frackowiak RS, Leigh PN (1994) Cortical function in progressive lower motor neuron disorders and amyotrophic lateral sclerosis: a comparative PET study. Neurology 44: 1101-1110.

258. Kim JA, Eliassen JC, Sanes JN (2005) Movement quantity and frequency coding in human motor areas. J Neurophysiol 94: 2504-2511.

259. Larsson J, Gulyas B, Roland PE (1996) Cortical representation of self-paced finger movement. Neuroreport 7: 463-468.

260. Macar F, Anton JL, Bonnet M, Vidal F (2004) Timing functions of the supplementary motor area: an event-related fMRI study. Brain Res Cogn Brain Res 21: 206-215.

261. Martin RE, MacIntosh BJ, Smith RC, Barr AM, Stevens TK, Gati JS, Menon RS (2004) Cerebral areas processing swallowing and tongue movement are overlapping but distinct: a functional magnetic resonance imaging study. J Neurophysiol 92: 2428-2443.

262. Rocca MA, Gatti R, Agosta F, Tortorella P, Riboldi E, Broglia P, Filippi M (2007) Influence of body segment position during in-phase and antiphase hand and foot movements: a kinematic and functional MRI study. Hum Brain Mapp 28: 218-227.

263. Sahyoun C, Floyer-Lea A, Johansen-Berg H, Matthews PM (2004) Towards an understanding of gait control: brain activation during the anticipation, preparation and execution of foot movements. Neuroimage 21: 568-575.

264. Saini S, DeStefano N, Smith S, Guidi L, Amato MP, Federico A, Matthews PM (2004) Altered cerebellar functional connectivity mediates potential adaptive plasticity in patients with multiple sclerosis. J Neurol Neurosurg Psychiatry 75: 840-846.

265. Toma K, Ozawa M, Matsuo K, Nakai T, Fukuyama H, Sato S (2003) The role of the human supplementary motor area in reactive motor operation. Neurosci Lett 344: 177-180.

266. Ward NS, Frackowiak RS (2003) Age-related changes in the neural correlates of motor performance. Brain 126: 873-888.

267. Wiese H, Stude P, Nebel K, Forsting M, de Greiff A (2005) Prefrontal cortex activity in self-initiated movements is condition-specific, but not movement-related. Neuroimage 28: 691-697.

268. Critchley HD, Mathias CJ, Josephs O, O'Doherty J, Zanini S, Dewar BK, Cipolotti L, Shallice T, Dolan RJ (2003) Human cingulate cortex and autonomic control: converging neuroimaging and clinical evidence. Brain 126: 2139-2152.

269. Desseilles M, Vu TD, Laureys S, Peigneux P, Degueldre C, Phillips C, Maquet P (2006) A prominent role for amygdaloid complexes in the Variability in Heart Rate (VHR)

during Rapid Eye Movement (REM) sleep relative to wakefulness. Neuroimage 32: 1008-1015.

270. Gianaros PJ, Van Der Veen FM, Jennings JR (2004) Regional cerebral blood flow correlates with heart period and high-frequency heart period variability during working-memory tasks: Implications for the cortical and subcortical regulation of cardiac autonomic activity. Psychophysiology 41: 521-530.

271. Merboldt KD, Fransson P, Bruhn H, Frahm J (2001) Functional MRI of the human amygdala? Neuroimage 14: 253-257.

272. Blood AJ, Zatorre RJ, Bermudez P, Evans AC (1999) Emotional responses to pleasant and unpleasant music correlate with activity in paralimbic brain regions. Nat Neurosci 2: 382-387.

273. Khalfa S, Schon D, Anton JL, Liegeois-Chauvel C (2005) Brain regions involved in the recognition of happiness and sadness in music. Neuroreport 16: 1981-1984.

274. Menon V, Levitin DJ (2005) The rewards of music listening: response and physiological connectivity of the mesolimbic system. Neuroimage 28: 175-184.

275. Penhune VB, Zattore RJ, Evans AC (1998) Cerebellar contributions to motor timing: a PET study of auditory and visual rhythm reproduction. J Cogn Neurosci 10: 752-765.

276. Griffiths TD, Johnsrude I, Dean JL, Green GG (1999) A common neural substrate for the analysis of pitch and duration pattern in segmented sound? Neuroreport 10: 3825-3830.

277. Koelsch S, Fritz T, Schulze K, Alsop D, Schlaug G (2005) Adults and children processing music: an fMRI study. Neuroimage 25: 1068-1076.

278. Maess B, Koelsch S, Gunter TC, Friederici AD (2001) Musical syntax is processed in Broca's area: an MEG study. Nat Neurosci 4: 540-545.

279. Ball T, Schreiber A, Feige B, Wagner M, Lucking CH, Kristeva-Feige R (1999) The role of higher-order motor areas in voluntary movement as revealed by high-resolution EEG and fMRI. Neuroimage 10: 682-694.

280. Makuuchi M (2005) Is Broca's area crucial for imitation? Cereb Cortex 15: 563-570.

281. Rizzolatti G, Craighero L (2004) The mirror-neuron system. Annu Rev Neurosci 27: 169-192.

282. Zentgraf K, Stark R, Reiser M, Kunzell S, Schienle A, Kirsch P, Walter B, Vaitl D, Munzert J (2005) Differential activation of pre-SMA and SMA proper during action observation: effects of instructions. Neuroimage 26: 662-672.

283. Ikeda A, Luders HO, Burgess RC, Shibasaki H (1993) Movement-related potentials associated with single and repetitive movements recorded from human supplementary motor area. Electroencephalogr Clin Neurophysiol 89: 269-277.

284. Lüders H, Lesser RP, Dinner DS, Morris HH, Wyllie E, Godoy J (1988) Localization of cortical function: new information from extraoperative monitoring of patients with

epilepsy. Epilepsia 29: 56-65.

285. Bordi F, LeDoux J (1992) Sensory tuning beyond the sensory system: an initial analysis of auditory response properties of neurons in the lateral amygdaloid nucleus and overlying areas of the striatum. J Neurosci 12: 2493-2503.

286. Collins DR, Pare D (1999) Reciprocal changes in the firing probability of lateral and central medial amygdala neurons. J Neurosci 19: 836-844.

287. Baas D, Aleman A, Kahn RS (2004) Lateralization of amygdala activation: a systematic review of functional neuroimaging studies. Brain Res Brain Res Rev 45: 96-103.

288. Krishnan S, Slavin MJ, Tran TT, Doraiswamy PM, Petrella JR (2006) Accuracy of spatial normalization of the hippocampus: implications for fMRI research in memory disorders. Neuroimage 31: 560-571.

289. Riecker A, Wildgruber D, Dogil G, Grodd W, Ackermann H (2002) Hemispheric lateralization effects of rhythm implementation during syllable repetitions: an fMRI study. Neuroimage 16: 169-176.

290. Blank SC, Scott SK, Murphy K, Warburton E, Wise RJ (2002) Speech production: Wernicke, Broca and beyond. Brain 125: 1829-1838.

291. Hashimoto Y, Sakai KL (2003) Brain activations during conscious self-monitoring of speech production with delayed auditory feedback: an fMRI study. Hum Brain Mapp 20: 22-28.

292. Riecker A, Ackermann H, Wildgruber D, Dogil G, Grodd W (2000) Opposite hemispheric lateralization effects during speaking and singing at motor cortex, insula and cerebellum. Neuroreport 11: 1997-2000.

293. Wildgruber D, Hertrich I, Riecker A, Erb M, Anders S, Grodd W, Ackermann H (2004) Distinct frontal regions subserve evaluation of linguistic and emotional aspects of speech intonation. Cereb Cortex 14: 1384-1389.

294. Jahn K, Deutschlander A, Stephan T, Strupp M, Wiesmann M, Brandt T (2004) Brain activation patterns during imagined stance and locomotion in functional magnetic resonance imaging. Neuroimage 22: 1722-1731.

295. Farrer C, Frith CD (2002) Experiencing oneself vs another person as being the cause of an action: the neural correlates of the experience of agency. Neuroimage 15: 596-603.

296. Fink GR, Frackowiak RS, Pietrzyk U, Passingham RE (1997) Multiple nonprimary motor areas in the human cortex. J Neurophysiol 77: 2164-2174.

297. Mutschler I, Schulze-Bonhage A, Glauche V, Demandt E, Speck O, Ball T (2007) A rapid sound-action association effect in human insular cortex. PLoS ONE 2: e259.

298. Williamson JW, Nobrega AC, McColl R, Mathews D, Winchester P, Friberg L, Mitchell JH (1997) Activation of the insular cortex during dynamic exercise in humans. J Physiol 503 (Pt 2): 277-283.

299. Christensen H, Boysen G, Christensen AF, Johannesen HH (2005) Insular lesions, ECG

abnormalities, and outcome in acute stroke. J Neurol Neurosurg Psychiatry 76: 269-271.

300. Damasio AR, Grabowski TJ, Bechara A, Damasio H, Ponto LL, Parvizi J, Hichwa RD (2000) Subcortical and cortical brain activity during the feeling of self-generated emotions. Nat Neurosci 3: 1049-1056.